STATUS OF THESIS

Title of thesis	Wavelet-Neural Network Based Image Compression System for Colour Images

I ETIK IRIJANTI

hereby allow my thesis to be placed at the Information Resource Centre (IRC) of Universiti Teknologi PETRONAS (UTP) with the following conditions:

1. The thesis becomes the properties of UTP.
2. The IRC of UTP may make copies of the thesis for academic purposes only.
3. This thesis is classified as

☐ Confidential

☑ Non-confidential

If this thesis is confidential, please state the reason:

-

The contents of the thesis will remain confidential for -- years.

Remarks on disclosure:

-

Endorsed by

_____	_____
Signature of Author	Signature of Supervisor
Perum Sedan Asri No. C3, Yogyakarta, Indonesia	Universiti Teknologi PETRONAS
Date :	Date:

APPROVAL PAGE

UNIVERSITI TEKNOLOGI PETRONAS

Approval by Supervisor (s)

The undersigned certify that they have read, and recommend to The Postgraduate Studies Programme for acceptance, a thesis entitled **"Wavelet-Neural Network Based Image Compression System for Colour Images"** submitted by (**Etik Irijanti**) for the fulfillment of the requirements for the degree of Master of Science in Electrical and Electronics Engineering.

_____

Date

Signature : _____

Main supervisor : Assoc. Prof. Dr. Yap Vooi Voon

Date : _____

Signature : _____

Co-Supervisor : _____

Date : _____

TITLE PAGE

UNIVERSITI TEKNOLOGI PETRONAS

Wavelet-Neural Network Based Image Compression System
for Colour Images

By
Etik Irijanti

A THESIS
SUBMITTED TO THE POSTGRADUATE STUDIES PROGRAMME
AS A REQUIREMENT FOR
THE DEGREE OF MASTER OF SCIENCE
ELECTRICAL AND ELECTRONIC ENGINEERING

BANDAR SERI ISKANDAR,
PERAK

OCTOBER 2009

DECLARATION

I hereby declare that the thesis is based on my original work except for quotations and citations which have been duly acknowledged. I also declare that it has not been previously or concurrently submitted for any other degree at UTP or other institutions.

Signature : _____

Name : _____ETIK IRIJANTI_____

Date : _____

ACKNOWLEDGEMENT

First and foremost, all praises and thanks are due to Allah, the almighty God, the source of my life and hope for giving me the strength and wisdom to succeed in life.

I am most grateful to my supervisor Assoc. Prof. Dr. Yap Vooi Voon for giving me an opportunity to pursue a master degree. Many times, his patience and constant encouragement has steered me to be a better person.

I would like also express my gratitude to Dr. M. Yunus Nayan, as my co supervisor that gives me support to conduct my study.

At last and most importantly, I would like to thank my family for their open-mindedness and endless support. They are always close to my heart.

This thesis is dedicated to my beloved parents Mr Paiman and Mrs Wardani, my beloved husband Noor Akhmad Setiawan and my beloved children Ali, Ubai and Atika.

ABSTRACT

There are many images used by human being, such as medical, satellite, telescope, painting, and graphic or animation generated by computer images. In order to use these images practically, image compression method has an essential role for transmission and storage purposes. In this research, a wavelet based image compression technique is used. There are various wavelet filters available. The selection of filters has considerable impact on the compression performance. The filter which is suitable for one image may not be the best for another. The image characteristics are expected to be parameters that can be used to select the available wavelet filter.

The main objective of this research is to develop an automatic wavelet-based colour image compression system using neural network. The system should select the appropriate wavelet for the image compression based on the image features. In order to reach the main goal, this study observes the cause-effect relation of image features on the wavelet codec (compression-decompression) performance. The images are compressed by applying different families of wavelets. Statistical hypothesis testing by non parametric test is used to establish the cause-effect relation between image features and the wavelet codec performance measurements. The image features used are image gradient, namely image activity measurement (IAM) and spatial frequency (SF) values of each colour component.

This research is also carried out to select the most appropriate wavelet for colour image compression, based on certain image features using artificial neural network (ANN) as a tool. The IAM and SF values are used as the input; therefore, the wavelet filters are used as the output or target in the network training.

This research has asserted that there are the cause-effect relations between image features and the wavelet codec performance measurements. Furthermore, the study reveals that the parameters in this investigation can be used for the selection of

appropriate wavelet filters. An automatic wavelet-based colour image compression system using neural network is developed. The system can give considerably good results.

ABSTRAK

Terdapat banyak imej digunakan dalam kehidupan manusia, seperti dalam perubatan, satelit, teleskop, lukisan, atau grafik animasi yang dijana oleh imej-imej komputer. Untuk menggunakan imej-imej secara praktikal, cara pemampatan imej mempunyai peranan penting untuk kegunaan transmisi dan storan. Dalam penyelidikan ini, teknik pemampatan imej berbasis wavelet digunakan. Terdapat pelbagai penapis wavelet yang boleh didapati pada keluarga yang berlainan. Bagaimanapun, pemilihan penapis telah berkesan banyak pada prestasi mampatan. Penapis yang sesuai untuk satu imej mungkin bukan terbaik untuk imej yang berbeza. Ciri-ciri imej diharap boleh digunakan sebagai parameter yang dapat digunakan untuk memilih wavelet yang didapati.

Objektif utama penyelidikan ini adalah bagi membangunkan satu sistem pemampatan imej warna automatik berbasis wavelet menggunakan jaringan saraf. Sistem itu harus memilih wavelet yang sesuai untuk mampatan imej berdasarkan ciri-ciri imej. Dengan tujuan mencapai matlamat utama, kajian ini memerhati hubungan sebab-akibat daripada ciri-ciri imej terhadap prestasi wavelet codec. Imej-imej itu dimampatkan dengan menggunakan wavelet-wavelet daripada keluarga yang berbeza. Pengujian hipotesis statistik digunakan untuk mengetahui hubungan sebab-akibat antara ciri-ciri imej dan ukuran-ukuran prestasi daripada wavelet codec. Ciri imej yang digunakan adalah nilai-nilai kecerunan imej (*image gradient/*IAM) dan frekuensi ruang (*spatial frequency*/SF) untuk setiap komponen warna.

Penyelidikan ini turut dijalankan untuk memilih wavelet yang paling sesuai, berdasarkan ciri-ciri imej menggunakan jaringan saraf tiruan (*artificial neural network*/ANN) sebagai suatu alat bantu. Nilai-nlai IAM dan SF sebagai input; oleh itu, penapis wavelet digunakan sebagai output atau sasaran dalam rangkaian latihan.

Penyelidikan ini telah menyatakan bahawa terdapat hubungan sebab-akibat antara ciri-ciri imej dan ukuran-ukuran prestasi wavelet codec. Lebih jauh, kajian ini

mendedahkan bahawa parameter-parameter dalam siasatan ini dapat digunakan untuk pemilihan penapis wavelet yang sesuai. Satu sistem pemampatan imej warna automatik berbasis wavelet menggunakan jaringan saraf telah dibangunkan. Sistem ini boleh memberikan keputusan yang cukup baik.

TABLE OF CONTENTS

LIST OF TABLES

LIST OF FIGURES

LIST OF ABBREVIATIONS

AI : Artificial Intelligent

ANN : Artificial Neural Network

bpp : bit per pixel

Codec : Compression-Decompression

CR : Compression Ratio

CRT : Cathode Ray Tube

CT : Computerized Tomography

CYM : Cyan Magenta Yellow

DCT : Discrete Cosine Transform

DWT : Discrete Wavelet Transform

EZW : Embedded Zerotrees of Wavelet Transform

HIS : Hue Saturation Intensity

IAM : Image Activity Measurement

JPEG : Joint Photographic Experts Group

LZW : Lempel Ziv Welch

MRI : Magnetic Resonance Imaging

NTSC : National Television System Committee

PAL : Phase Alternation Line

PSNR : Peak Signal to Noise Ratio

RGB : Red Green Blue

RLC : Run Length Coding

SF : Spatial Frequency

SFM : Spectral Flatness Measure

SPIHT : Set Partitioning in Hierarchical trees (SPIHT)

CHAPTER 1

INTRODUCTION

1.1 Background

An image can express more than just words, moreover it is said that an image is more worth than a thousand words. Images have various and important roles in our daily lives. In the medical field, a number of diagnoses are made based on biomedical images derived from physiological signals, MRI, X-ray, ultrasound images, computerized tomography (CT), and other imaging models. Satellite images are useful for environmental scientists, military, and geoscientists. Movies and television bring imaginary information with advent of the internet.

It would not be practical to send images without data compression algorithm because uncompressed image, especially colour image, takes up large storage space and it takes larger time to transmit. Transmission and storage are the key words in the communication. The problem of digital signals transmission through limited bandwidth communication channels is big challenge. Even though the storage cost has reduced severely over the past decade due to large advancement in microelectronics and storage technology, the requirement of data storage and data processing applications is also growing rapidly outpacing the improvement made. The redundancies in data representation can be exploited by data compression methods.

The literature has revealed that the wavelet transform is a very powerful tool for image coding. Wavelets are now widely used in lossy and lossless image compression [1-4]. Unlike many other transforms, a large number of wavelet filters are available

under different families. Also, filters with different characteristics are evolving at regular intervals. It will be shown in this thesis that in wavelet based image compression techniques, the selection of filters has considerable impact the compression performance. The suitable filter for one image may not be the best for another.

Previous researchers investigated and evaluated several wavelet filters for still image compression. These researchers tried to find the most appropriate wavelet for image compression[1][4-6]. Some of these researchers recommended wavelet filter for all types of images without considering the image characteristics. This is not appropriate; because the suitable filter for one image will give different performance for another image with different characteristics. This research proposes a method that can select the most appropriate wavelet for various image types adaptively. The artificial neural network will be used in the selection stage by considering the image features[7].

The study on relationship of image features and wavelet-based codec performances has been investigated by Saha and Vemuri for gray scale images[8-11]. The strong correlation of the features against the wavelet-based codec performance is shown in the results. Other researchers evaluated image quality measures like spatial frequency and their performance for gray scale images[12]. N. Sprljan,S. Grgic and M Grgic, investigated spectral flatness measure in images[13]. However, their works concentrate in using gray scale images and can be extended to explore colour images. Therefore, this research will discuss the characteristics of colour images affect the performance of a wavelet-based codec.

This research will investigate the cause-effect relationship as the logical direction. It is envisage that the cause-effect study using hypothesis statistical test could help better recognition which image characteristics influence the coding performance of a wavelet-based image compression system. This thesis hypothesizes that an adaptive wavelet-based compression system would be feasible based on the image characteristics. The adaptive wavelet-based compression system can use a neural-

network, which would select the most appropriate wavelet based on image characteristics.

Artificial Neural Networks are recent development tools that are modeled from biological neural networks. The advantage of this tool is its ability to solve problems that are difficult to be solved by traditional computing methods.

The study about relationship of image features; image gradient and spatial frequency (IAM and SF) against the wavelet-based image codec performance (PSNR, CR and bpp) will provide useful information that will aid the study of cause effect relation between them. Based on the study, the IAM and SF values can be used as the input and the wavelet can be used as the output of neural network [7].

1.2 Objective

The main objective of this research is to develop an automatic wavelet-based colour image compression system using neural network. The system should select the appropriate wavelet for the image compression based on the image features. In order to reach the main goal, the following objectives should be achieved.

i. To evaluate the correlation of statistical and spatial image characteristics against the wavelet-based codec measurements.

ii. To investigate the effect of image features, especially the image gradient and spatial frequency to the wavelet-based colour image codec.

iii. To select the most appropriate wavelet, based on certain image features using artificial neural network (ANN) as a tool.

iv. To solve the problem automatically instead of manual selection as in a conventional wavelet-based codec.

1.3 Thesis Organization

Chapter 2 discusses the fundamental of colour image, its representation, colour space and human perception. Image feature analysis is also introduced. Some image compression algorithms including both lossless and lossy methods are included in this chapter. The basic of wavelet transform is also discussed. The mathematical properties of wavelet and the theoretical foundation of the discrete wavelet transform (DWT) is discussed in this chapter. The multiresolution analysis features of the wavelet transform that make it appropriate for image compression application are also explained. This chapter also explores the some wavelet-based colour image compression schemes. Preferred image compression algorithms like embedded zero-tree wavelet scheme (EZW) and set partitioning in hierarchical trees (SPIHT) are popular algorithms in wavelet-based image compression. These are discussed in this chapter.

The relationship of wavelet based codec and the image features are also cited here. Also included in this chapter is the discussion of wavelet selection by the MLP neural network.

Chapter 3 will show the methodology of this research to develop adaptive wavelet based colour image compression using neural network. Coefficient correlations between image features and the codec performance measurements are evaluated. The statistical tests are used to establish the cause-effect of image gradient (IAM) and spatial frequency (SF) to the PSNR, CR and bpp values. Kruskal-Wallis test and Friedman test are used to establish the causal effect relation of IAM and SF to PSNR, CR and bpp. These features are used as the input into a neural network system.

Chapter 4 analyzes the results from the proposed algorithm. These include the image features analysis, compressed images measurement evaluation; investigate the coefficient correlation between image features against image codec performance and

determine their fitting evaluation. Statistical test is also conducted to establish the cause-effect. The accuracies of several MLP topologies tried in the experiments are also evaluated.

Chapter 5 summarizes the experiment results, the research contributions and suggestions for future work.

CHAPTER 2

LITERATURE REVIEW

In this chapter, the literature review of this research is described. Image representation, colour space and human perception are described here. The image features that are evaluated in this study, that is statistical image features and spatial characteristics, are presented in this chapter. Included in this chapter is a discussion of the fundamental of image compression and wavelet transform. Furthermore, the basic wavelet transform is introduced.

2.1. Image Representation

The digital image can be represented as a two-dimensional array of data, where I*(m,n)* is associated the image brightness of a pixel at the point *(m,n)*. In linear algebra, that image model is a *matrix*, where one row or column is called a *vector*. This basic image model is for monochrome (one-colour, referred to as gray-scale) image data. Usually, it also can be modeled by I*(m,n)* function related to each part band of brightness information, for multi-band image such as colour image.

The simplest image type is *binary image* that can take two values, usually "0" for black and "1" for white. Gray-scale images are referred to as monochrome. The brightness stage relate to the number of bits used in each pixel. The common images contain 8-bit per pixel data that give 256 (0-255) different brightness (gray) levels[14].

The image type that used in this research is the colour image. The details of this type are described in following section.

2.2. Colour Space and Human Perception

A digital colour image can be viewed as a three-band monochrome image data I*(m,n)*, where each band of data corresponds to a different colour component. Its numerical representation is obtained through an N by M by 3 matrix *A*. Thus, an intensity value at discrete location *(m,n)* with a precision *p* (for instance, one bit for each channel) is expressed by each entry of *A* is a three element integer vector (pixel color). Furthermore, each image component or layer can be viewed as a single channel image, which, under particular conditions, can be analyzed separately from the others. This is not the case for RGB space, because, if two channels are fixed, human visual perception is very sensitive to small changes of value of the remaining channel. Thus, even though RGB is the most common storage format for images, other formats may be improved for compression.

Computer display CRTs (Cathode Ray Tube), normally have three electron guns that illuminate three different types of phosphor dots on the screen. Those phosphor dots, when illuminated, glow with the red, green, and blue primary colors of light. From these primary colors, all other shades are generated.

A combination of real world physical characteristics determines what the human vision system perceives as color. A color space is a mathematical representation of these characteristics. Color Spaces are always three-dimensional. There are many possible color space definitions:

1 Digital imagery often uses the red/green/blue color space, known simply as RGB.
2 The cyan/yellow/magenta space, known as CYM, is used in printing.
3 Hue, saturation, and intensity, (or HSI) is the color space typically used by artists.
4 Intensity-chromaticity color spaces, YUV and YIQ, are used for television broadcast.

Though most work in digital imagery is performed in RGB, which is native to computer displays, many digital image processing applications require transformation

to the other color spaces. Usually utility programs are provided to perform these color space transformations

In lossy data compression, there is the quantization stage. With quantization data cannot be recovered exactly which exploits a data reduction based on their low information content. Nevertheless, for three layers, this can lead to the elimination of some low coefficients in the others layers are not eliminates because they carry high information content. When reconstructing the image at that location, a high visual distortion is introduced. The assumption of analyzing the three layers separately is valid only if they are not correlated with respect the visual appearance[15].

All colour spaces are three-dimensional orthogonal coordinate systems, meaning that there are three axes (in this case the red, green, and blue color intensities) that are perpendicular to one another. This color space is illustrated below. The red intensity starts at zero at the origin and increases along one of the axes. Similarly, green and blue intensities start at the origin and increase along their axes. Because each color can only have values between zero and some maximum intensity (255 for 8-bit depth), the resulting structure is the cube. We can define any color simply by giving its red, green, and blue values, or coordinates, within the color cube. These coordinates are usually represented as an ordered triplet - the red, green, and blue intensity values enclosed within parentheses as shown below.

RGB Space

The simplest and most commonly used colour space is perhaps RGB (see Figure 2.1). Most colors in the visible spectrum can be recreated, although not completely. This scheme is based on the additive properties of color[15].

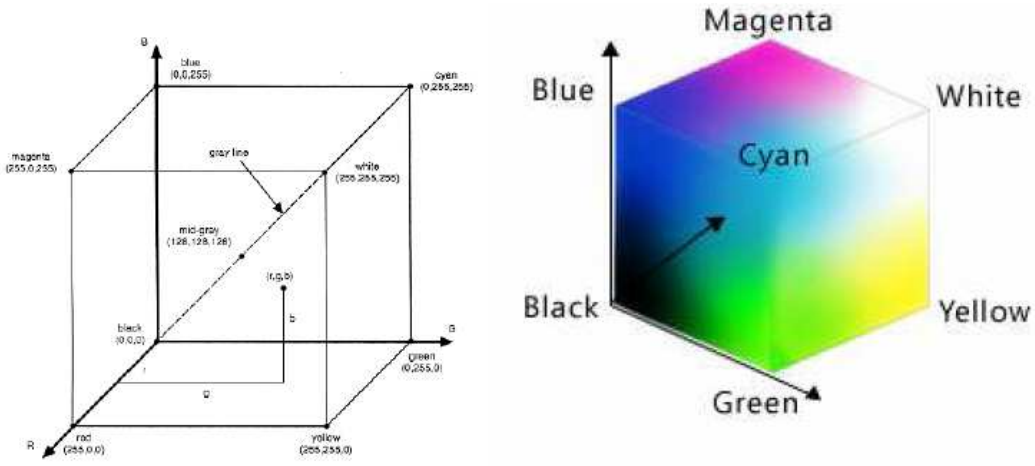

(a)cube diagram (b) colour cube diagram

Figure 2.2 RGB Space [16]

Several colors are shown mapped into their locations in the RGB cube, or color space. Black has zero intensities in red, green, or blue, so it has the coordinates (0,0,0). At the opposite corner of the color cube, white has maximum intensities of each color, or (255,255,255). Full intensity red, having zero green or blue components, also is positioned at a corner of the cube at location (255, 0, 0). Yellow, which is combination of red and green, is positioned at (255, 255, 0). Cyan and magenta, which are combinations of green and blue and red and blue, respectively, are at (0,255,255) and (255, 0, 255). Finally, note that a middle gray is at the exact center of the cube at location (128, 128, 128). All other colors can be described by specifying their coordinates within this cube.

The RGB color space is an additive color space. Its origin starts at black, and all other colors are derived by adding various amounts of the primary colors. It is a natural choice for computer displays where black, or no light intensity, is the starting point, and the increasing intensity of the red, green, and blue electron guns provides the range of colors.

YUV Space

YUV was originally used for PAL (European standard) analog video (see Figure 2.2). To convert from RGB to YUV spaces, the following equations can be used:

$$
\begin{aligned}
Y &= 0.299R + 0.587G + 0.114B \\
U &= 0.492(B - Y) \\
V &= 0.877(R - Y)
\end{aligned}
\qquad (2.1)
$$

Any errors in the resolution of the luminance (Y) are more important than the error in the chrominance (U, V) values. The luminance information can be coded using higher bandwith than the chrominance information[15].

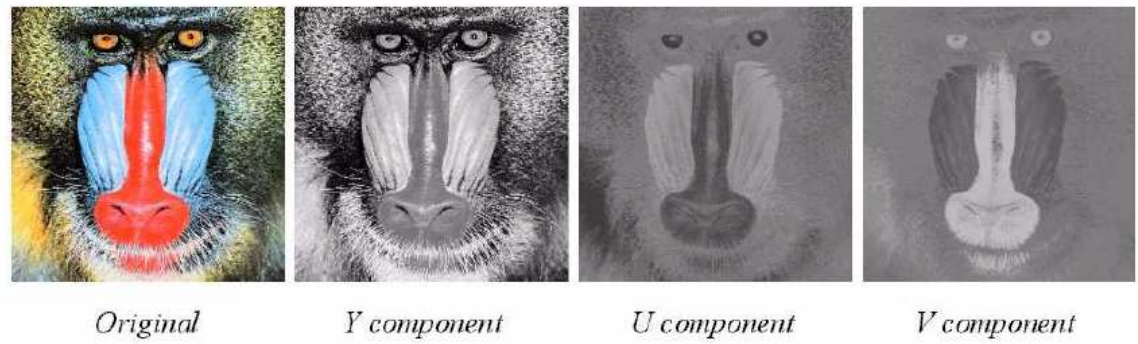

Figure 2.3 Example of YUV Space

YIQ Space

YIQ is used in the U. S. television standard, NTSC (National Television System Committee). It is similar to YUV, except that its color space is rotated 33 degree clockwise, so that I is the orange-blue axis, and Q is the purple-green axis. The equations to convert from RGB to YIQ are[15]:

$$
\begin{aligned}
Y &= 0.299R + 0.587G + 0.114B \\
I &= 0.74(R - Y) - 0.27(B - Y) = 0.596R - 0.275G - 0.321B \\
Q &= 0.48(R - Y) + 0.41(B - Y) = 0.212R - 0.523G + 0.311B
\end{aligned}
\qquad (2.2)
$$

YCrCb Space

YCrCb is a subset of YUV that scales and shifts the chrominance values into the range of 0 to 1. The linear transform from RGB to YCrCb generates one luminance space Y and two chrominance (Cr and Cb) space[15].

$$
\begin{aligned}
Y &= 0.299R + 0.587G + 0.114B \\
Cr &= ((B - Y)/2) + 0.5 \\
Cb &= ((R - Y)/1.6) + 0.5
\end{aligned} \tag{2.3}
$$

Comparison of Colour Spaces

Among these three colour spaces, only YCrCb is the one used in the digital image processing because

1. There is no correlation among the spaces of YCrCb, so each space can be analyzed separately.
2. Human eyes are more sensitive to the change of brightless than of color, so Cr and Cb spaces can be compressed more heavily than Y space to get better compression ratio.

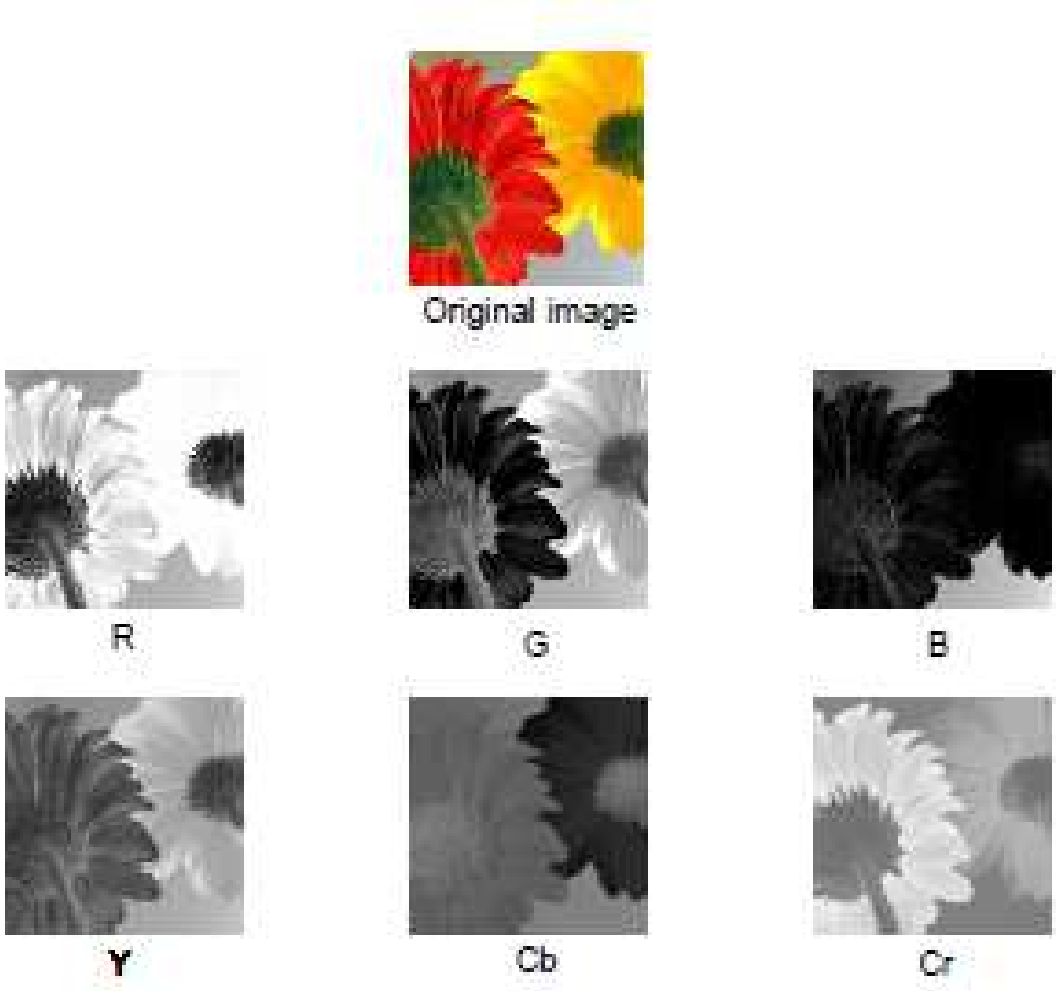

Figure 2.4 Comparisons of the RGB and the YCb Cr Spaces.

2.3. Image Features Analysis

Feature analysis involves examining the features extraction from the images and determining if and how they can be used to solve an imaging problem. A process that begins with feature selection is called as feature extraction. The selected features will be the major factor that determines the complexity and success of the analysis and pattern classification process. Some common features that can be analyzed are shape features, histogram/statistical features and colour features. The feature extraction and feature analysis illustration can be seen in Figure 2.4[14]. A good robust feature can provide consistent results.

The histogram features is a plot of gray level values versus the number of pixels at that value, so that can tell about the brightness and contrast information. The histogram features are also known as statistical features. The features include range, mean, median, different (mean-median), standard deviation, variance, coefficient variance, skewness, kurtosis, brightness energy[10][14][17], gray/color energy, zero-order entropy, first-order entropy, and second-order entropy.

Other features explored in this thesis include image gradient[9], spatial frequency (SF) [12]and spectral flatness measure (SFM)[13].

Figure 2.5 Feature extraction and feature analysis.

Colour images consist of three bands, one each for red, green and blue or commonly called as RGB. All features can be calculated separately for each colour band.

2.4. Image Compression

Image compression involves reducing the size of image data files, while retaining the essential information. This area is continuing to grow due to demands from various different applications such as internet, high-definition television, satellite imaging, and medical imaging increases[14].

The uncompressed image is the original image before compression, the file produced by the compression process is the compressed file, and the image recreated from the compressed file is decompressed image. The compression ratio (CR) is the size of the uncompressed file to the size of the compressed file, and can also be measured in bits per pixel (bpp)[14].

2.4.1. Lossless Compression

There is no data loss in lossless compression; it is suitable for several applications such as medical images. If the data is losslessly compressed, then the original data can be recovered exactly from the compressed data. This is generally used for applications that do not allow any difference between the original and reconstructed data.

Huffman Coding

Huffman coding is developed by D. A. Huffman in 1952[18]. It is a classical data compression method that has been used in various compression applications, including image compression. It is a minimum length code. This means that given the statistical distribution of the gray levels (the histogram), the Huffman algorithm will produce a code that is as close as possible to the minimum bound, the entropy. This

technique results in an unequal (or variable) length code, where the size of the code words can vary[14].

The Huffman algorithm can be described as follow:

i. Determine the gray level probabilities for image by finding the histogram.
ii. Arrange the input probabilities (histogram magnitudes) from smallest to largest.
iii. Combine the smallest two by addition.
iv. GOTO Step 2, until only two probabilities are left.
v. By working backward along the tree, generate code by alternating assignment of 0 and 1.

The histogram is the essential evaluation in the Huffman coding, so any preprocessing to simplify the histogram will help improve the compression ratio[17].

Run-Length-Coding

Run length coding, sometimes called recurrence coding, is one of the simplest data compression algorithms. *Run-Length-Coding* (RLC) is an image compression method that works by counting the number of adjacent pixels with the same gray level value. This count, called the *run-length,* is then encoded and stored. There are several methods of *run-length*.

Basic RLC is used primarily for binary images, but it can use to evaluate complex images that have been preprocessed by thresholding to reduce the number of gray levels to two. There are various ways to execute basic RLC, either use horizontal RLC, counting along the rows, or vertical RLC, counting along the columns.

RLC works best with binary (two value) images. Gray or color images can use RLC by storing the run length and the gray values. Alternately, extension to gray or color images is bitplane RLC, which applies RLC to each bitplane separately. Preprocessing with a gray code can improve compression by bitplane RLC by typically 10% to 15%[14].

Lempel-Ziv-Welch Coding

Lempel-Ziv-Welch (LZW) methods work by encoding strings of data. For images, these strings of data correspond to sequences of pixel values. It works by creating a string table that contains the strings and their corresponding codes. The string table is updated as the file is read, with new codes being put in whenever a new string is encountered. If a string is encountered tat is already in table, the corresponding code for the string is put into the compressed file.

During compression it creates a string table containing strings and the corresponding codes. The string table is not stored but extracted from the compressed data itself. It uses code words with more bits than the original data, extra bits used as index for string entries in the string table.

This algorithm and its variations are used in many image files formats such as GIF and TIFF.

Arithmetic Coding

Arithmetic coding is also a type of statistical coding algorithm similar to Huffman coding. It is better than Huffman coding in compression ratio but requires more computational power and memory. Huffman coding is more attractive than arithmetic coding when simplicity is the major concern[18].

Arithmetic coding transforms input data into a single floating point number between 0 and 1. As each input symbol (in image case, pixel value) is read, the precision required for this number became greater. Because images are very large and the

digital computers' precision finite, an entire image must be divided into small *subimages* to be encoded.

Arithmetic coding uses the histogram as a probability model, so can theoretically achieve the maximum compression specified by the entropy. It works by successively subdividing the interval between 0 and 1, based on the placement of the current pixel value in the probability distribution.

2.4.2. Lossy Compression

Lossy compression techniques lose image data, so can not reconstruct the original image exactly. In several applications, exact reconstruction is not necessary. For illustration, it is acceptable that a reconstructed video signal is not an exact copy of the original as long as do not result in annoying artifacts.

Lossy compression is necessary to achieve high compression ratio with complex images. Images can be compressed 10 to 50 times with minimal visible information loss to maintain high quality. Newer methods, such as JPEG2000, can achieve reasonably good image quality with compression ratios as high as 100 to 200 for colour images.

Vector Quantization

Vector Quantization is a lossy compression method that maps a vector that can have lots of values to a vector that has a smaller (quantized) number of values. For image compression, the vector corresponds to a small sub image, or block.
From the theory, it is known that better compression can be achieved with vector quantization than with scalar quantization (rounding or truncating individual values). Vector quantization is achieved by use of a *codebook* that contains a fixed set of vectors, and storing the index (address) into the codebook[14].

The main advantages of VQ are the simplicity and the efficient implementation of the decoder. VQ is theoretically an efficient method for image compression and offer superior performance will be gained for large vectors. However, for use large vectors, VQ becomes complex and requires many computational resources, for example, memory and computation per pixel in order to efficiently a codebook[18].

Predictive Coding

Predictive coding has been used extensively in image compression. Predictive image coding algorithms are used primarily to exploit the correlation between adjacent pixels. They predict the value of a given pixel based on the values of the surrounding pixels. Due to the correlation property among adjacent pixels in image, the use of a predictor can reduce the amount of information bits to represent image.

This type of lossy image compression technique is not as competitive as transform coding technique used in modern lossy image compression, because predictive technique have inferior compression ratios and worse reconstructed image quality than those of transform coding[18].

Fractal Compression

The application of fractals in image compression initiated by with M.F. Barnsley and A. Jacquin[19]. Fractal image compression is a process to find a small set of mathematical equations that can describe the image. By sending the parameters of these equations to the decoder, the original image can be constructed. Fractal compression is based on the idea that various region in the image are *self-similar*, which mean that one sub image can be represented as skewed, stretched, rotated, scaled and/or translated version of another sub image.

The mathematical operations, skew, stretch, rotate and translate, are called affine transformations and can be represented by the general equations:

$$r' = k_1 r + k_2 c + k_3$$
$$c' = k_4 r + k_5 r + k_6 \qquad (2.4)$$

where *r'*and *c'* are the new coordinates and k_i are constans.

In fractal image compression, an image is divided into sub images. Some of them are selected to serve as models call *range* regions to map to the *domain* regions which represent the entire image. The range regions are the fractals, which are like basis images that can undergo affine transformations and assembled into a good representation of the image. The compressed file stores the fractals and the necessary affine transformation coefficients. Fractal image compression can achieve high compression ratio, but it is complex, costly and time consuming.

Transform Based Image Compression

The basic encoding method for transform based compression works as follows:

i. Image transform

   Divide the source image into blocks and apply the transformations to the blocks.

ii. Parameter quantization

   The data generated by the transformation are quantized to reduce the amount of information. This step represents the information within the new domain by reducing the amount of data quantization and in most cases not a reversible operation because of its lossy property.

iii. Encoding

   Encode the results of the quantization. This last step is Run Length encoding or Huffman coding. Its performance can be optimized by reducing the bit rate.

Transform based compression is one of the most useful applications. Combined with other compression techniques, this technique allows the efficient transmission, storage and display of images that otherwise would be impractical[20].

DCT-Based Transform Coding

The Discrete Cosine Transform (DCT) was first applied to image compression in the work by Ahmed, Natarajan and Rao. It is a popular transform used by the JPEG (Joint Photographic Experts Group) image compression standard for lossy compression of images. Since it is used so frequently, DCT is often referred to the literature as JPEG-DCT, DCT used in JPEG.

JPEG-DCT is a transform coding methods comprising four steps. The source image is first partitioned into sub-blocks of size 8x8 pixels in dimension. Then each block is transformed from spatial domain to frequency domain using 2-D DCT basis function. The resulting frequency coefficients are quantized and finally output to a lossless entropy coder. DCT is an efficient image compression technique since it can decorrelate pixels in the image (since the cosine basis is orthogonal) and compact most image energy to a few transformed coefficients. Additionally, DCT coefficients are generally quantized. Thus, the JPEG image file format is very efficient. This makes it very popular, especially in the World Wide Web. Nevertheless, many JPEG users preferred the wavelet-based image compression algorithms, which have better compression performance [20].

2.5. Fourier Transform

J. Fourier, the French mathematician, explained that any periodic function can be expressed as an infinite sum of periodic complex exponential functions in 19th century. The idea were generalized to non-periodic functions, and then to periodic or non-periodic discrete time signals. Fourier transform have become a very well-known tool for computer calculations.

The equation

$$F(\omega) = \int_{-\infty}^{\infty} f(t) e^{-j\omega t} dt \tag{2.5}$$

is the generally called the Fourier Transform. The equation

$$f(t) = \frac{1}{2\pi} \int_{-\infty}^{\infty} F(\omega) e^{j\omega t} d\omega \tag{2.6}$$

is called the inverse Fourier Transform.

As it can be seen in the Fourier Transform equation, the integration is from minus infinity to plus infinity over time. So, no matter when the component with frequency ω appears in time, it will affect the result of the integration equally as well. The lack of time information is one serious weakness of Fourier Transform. That is why Fourier transform is not suitable if the signal has time varying frequency, which is the signal is non-stationary.

2.6. Windowed Fourier Transform

To solve the above problem, the Windowed Fourier Transform is used. The basic idea is to divide the signal into small enough segments, where these segments can be assumed to be stationary. The width of this window must be equal to the segment of the signal where this assumption is valid.

The windowed Fourier Transform has several problems. If a window of infinite length is used, the Fourier Transform gives prefect frequency resolution, but no time information. On the other hand, in other to obtain a stationary sample, a small enough window is needed in when the signal is stationary. The narrower the window, the better the time resolution, but poorer the frequency resolution. However, the wavelet transform solves the dilemma of resolution to a certain extent, as will be seen in the next part.

2.7. Wavelet Transform

Fourier analysis expands an arbitrary signal in terms of an infinite number of sinusoidal functions of its harmonics and has been well studied by the signal processing community for decades. Fourier representation of signals is known to be very effective in analysis of time-invariant (stationary) periodic signals. In contrast to a sinusoidal function, a wavelet is a small wave whose energy is concentrated in time. An arbitrary signal can be analyzed in terms of scaling and translation of a single *mother wavelet* function (basis)[21]**.** Wavelets allow both time and frequency analysis of signals simultaneously because of the fact that the energy of wavelets is concentrated in time and still possesses the wave-like (periodic) characteristics. As a result, wavelet representation provides a versatile mathematical tool to analyze transient, time-variant (nonstationary) signals that are not statistically predictable especially at the region of discontinuities-a feature that is typical of images having discontinuities at the edges.

Wavelets are functions generated from one single function ψ, which is called mother wavelet, by dilations and translations.

$$\psi_{a,b}(t) = |a|^{-1/2} \psi(\frac{t-b}{a}) \tag{2.7}$$

where a and b are two arbitrary real numbers. The variables *a* and *b* represent the parameters for dilations and translations respectively in the time axis. From Eq. 2.7, it is noted that the mother wavelet can be essentially represented as

$$\psi(t) = \psi_{1,0}(t) . \tag{2.8}$$

For any arbitrary $a \neq 1$ and $b = 0$, a equation can be derived that

$$\psi_{a,0}(t) = \frac{1}{\sqrt{|a|}} \psi(\frac{t}{a}) . \tag{2.9}$$

Eq. 2.8 show $\psi_{a,0}(t)$ is nothing but a time-scaled (by a) and amplitude-scaled (by $\sqrt{|a|}$) version of the mother wavelet function $\psi(t)$ in the Eq. 2.8. The parameter *a* causes contraction of $\psi(t)$ in time axis whe *a* < 1and expansion or stretching when *a* > 1. That is why the parameter *a* is called *dilation* (scaling) parameter. For *a* < 0, the function $\psi_{a,b}(t)$ results in time reversal with dilation.

In Figure 2.5, there is an illustration of mother wavelet and its dilations in the time domain with the dilation parameter $a = \alpha$. For the mother wavelet $\psi(t)$ shown in Figure 2.5(a), a contraction of the signal in the time axiz when $\alpha < 1$is shown in Figure 2.5(b) and expansion of the signal in the time axis when $\alpha > 1$is shown in Figure 2.5(c).

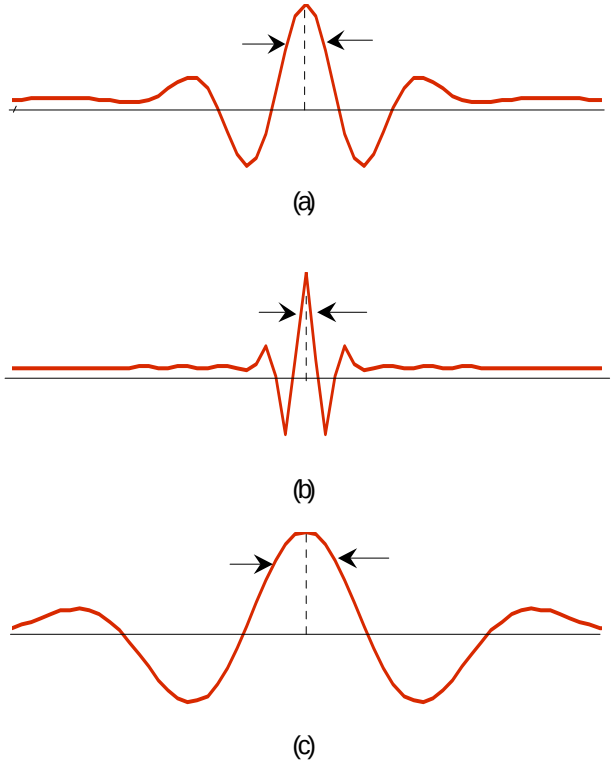

Figure 2.6 (a) A mother wavelet $\psi(t)$, (b) $\psi(t/\alpha)$: $0 < \alpha < 1$, (c) $\psi(t/\alpha)$: $\alpha > 1$

Based on this wavelet's definition, the wavelet transform (WT) of a function (signal) $f(t)$ is mathematically represented by

$$W(a,b) = \int_{-\infty}^{+\infty} \psi_{a,b}(t) f(t) dt \quad . \tag{2.10}$$

The purpose of wavelet transform is to mathematically transform the data from time-space domain to time-frequency domain which makes better compression results.

The Haar wavelet function, as the simplest form of wavelet, is defined as:

$$\psi(x) = \begin{cases} 1 & 0 \le x < 1/2 \\ -1 & 1/2 \le x < 1 \\ 0 & otherwise \end{cases} \tag{2.11}$$

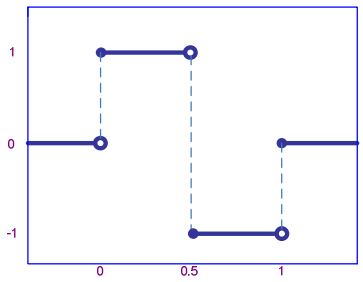

Figure 2.7 Haar wavelet[22].

The following is a simple example to show how to perform Haar wavelet transform on four sample numbers:

x(0) = 1.3; x(1) = 1.1; x(2) = -1.1; x(3) = -1.3.

For example perform Haar wavelet transform on these four numbers.

$$\begin{bmatrix} y(0) \\ y(1) \\ Y(2) \\ y(3) \end{bmatrix} = \begin{bmatrix} 1 & 1 & 0 & 0 \\ 1 & -1 & 0 & 0 \\ 0 & 0 & 1 & 1 \\ 0 & 0 & 1 & -1 \end{bmatrix} \begin{bmatrix} x(0) \\ x(1) \\ x(2) \\ x(3) \end{bmatrix} = \begin{bmatrix} 2.4 \\ 0.2 \\ -2.4 \\ 0.2 \end{bmatrix}$$

Notice an inverse transform can be carried out from x to y:

$$\begin{bmatrix} x(0) \\ x(1) \\ x(2) \\ x(3) \end{bmatrix} = \frac{1}{2} \begin{bmatrix} 1 & 1 & 0 & 0 \\ 1 & -1 & 0 & 0 \\ 0 & 0 & 1 & 1 \\ 0 & 0 & 1 & -1 \end{bmatrix} \begin{bmatrix} y(0) \\ y(1) \\ Y(2) \\ y(3) \end{bmatrix}$$

If 0.2 is below quantization threshold, it will be replaced by 0.
Then, reconstructed x will be [1.2, 1.2, -1.2, -1.2].

After first transform, keep $y(1)$ and $y(3)$ at the finest level and iterate the transform on $y(0)$ and $y(2)$ again.

$$z(0) = y(0) + y(2) = 0 \text{ and } z(2) = y(0) - y(2) = 4.8.$$

Those four numbers become [0, 0.2, 4.8, 0.2]. After quantization, they could be [0, 0, 5, 0], which are much easier to be compressed.

Reasons for Using Wavelet Based Compression

As discussed earlier, loss of some information is acceptable in image compression. Among all of the lossy compression approaches discussed, the wavelet transform based compression is chosen in this research.

For transform based compression, JPEG compression schemes based on DCT (Discrete Cosine Transform) have some advantages such as simplicity, acceptable performance and availability of special purpose hardware for implementation. However, because the input image is blocked, correlation across the block boundaries can not be eliminated. This results in noticeable and annoying “blocking artifacts” particularly at low bit rates as shown in Figure 2.7[23].

(a) (b)

Figure 2.8 (a) Original Lena image
(b) Reconstructed image to show blocking artifacts.

In the recent years, the wavelet transform has been widely used in signal processing research, particularly, in image compression. In many applications, wavelet-based schemes reach better performance than other coding schemes like the DCT based. Since there is no need to lock the input image and its basis functions have variable length, wavelet-based coding schemes can avoid blocking artifacts. Wavelet based coding also facilitates progressive transmission images[23].

2.7.1. Discrete Wavelet Transform

Since digital image is processed by a digital computer, it is practical to define the discrete version of the wavelet transform. Before the discrete wavelet transform is defined, it is essential to define the wavelets in terms of discrete value of the *dilation* and *translation* parameters *a* and *b* instead of being continuous. The most popular approach of discretizing *a* and *b* is using following equation.

$$a = a_0^m, \qquad b = nb_0a_0^m \tag{2.12}$$

where *m* and *n* are integers. Substituting *a* and *b* in Eq. 2.7 by Eq. 2.12, the discrete wavelets can be represented by Eq. 2.13.

$$\psi_{m,n}(t) = a^{-m/2}\psi(a_0^{-m}t - nb_0) \quad (2.13)$$

a_0 and b_0 can have different values. The most common choice is $a_0 = 2$ and $b_0 = 1$; thus, $a = 2^m$ and $b = n2^m$. This corresponds to sampling (discretization) of *a* and *b* in such a technique that the consecutive discrete values of *a* and *b* as well as the sampling intervals differ by a factor of two. This method of sampling is commonly known as dyadic sampling and the corresponding decomposition of the signals is called the *dyadic decomposition*. Therefore, the discrete wavelets in Eq. 2.15 can represent these values, which forms a family of orthonormal basis functions,

$$\psi_{m,n}(t) = 2^{-m/2}\psi(2^{-m}t - n) \quad (2.14)$$

Normally, the wavelet coefficients for function *f (t)* are given by

$$c_{m,n}(f) = a_0^{-m/2}\int f(t)\psi(a_0^{-m}t - nb_0)dt \quad (2.15)$$

and hence for dyadic decomposition, the wavelet coefficients can be deducted accordingly as

$$c_{m,n}(f) = 2^{-m/2}\int f(t)\psi(2^{-m}t - n)dt \quad (2.16)$$

To reconstruct the signal $f(t)$ in from the discrete wavelet coefficient use following equation

$$f(t) = \sum_{m=-\infty}^{\infty}\sum_{n=-\infty}^{\infty} c_{m,n}(f)\psi_{m,n}(t) \quad (2.17)$$

The transform shown in Eq. 2.15 is called the *wavelet series*, which is similar to the *Fourier series* since the input function *f (t)* is still a continuous function whereas the transform coefficients are discrete. This is frequently called the *discrete time wavelet*

transform (DTWT). When a digital computer execute the digital signal or image processing applications, the input signal *f (t)* desires to be discrete in nature because of the digital sampling of the original data, which is represented by a finite number of bits. After the input function *f (t)* as well as the wavelet parameters *a* and *b* are represented in discrete form, the transformation is usually referred to the *discrete wavelet transform* (DWT) of signal *f (t)[2]*.

The *discrete wavelet transform* (DWT) is a very versatile signal processing tool after Mallat [2] proposed the multiresolution representation of signals based on wavelet decomposition. The benefit of the DWT over Fourier transformation is that it executes multiresolution analysis of signals with localization both in time and frequency, generally known as time-frequency localization. As a consequence, the DWT decomposes a digital signal into different subbands so that the lower-frequency subbands have finer frequency resolution and coarser time resolution compared to the higher-frequency subbands. The DWT is being increasingly used for image compression because the DWT supports features like progressive image transmission (by quality, by resolution), simplicity of compressed image manipulation, and region of interest coding. DWT is the basis of the new JPEG2000 image compression standard[21].

2.7.2. Multiresolution Analysis Concept

The orthonormal wavelet basis functions $\psi_{m,n}(t) = 2^{-m/2}\psi(2^{-m}t - n)$ was discovered in the 1980s. The *Multiresolution analysis* theory presented a systematic approach to generate the wavelets[2][3]. The idea of multiresolution analysis is to approximate a function *f(t)* a t different levels of resolution.

In multiresolution analysis, there are two considered functions: the mother wavelet $\psi(t)$ and the *scaling function* $\phi(t)$. The dilated (scaled) and translated (shifted) version of the scaling function is given by $\phi_{m,n}(t) = 2^{-m/2}\phi(2^{-m}t - n)$. For fixed *m*, the

set of scaling functions $\phi_{m,n}(t)$ are orthonormal. By the linear combinations of the scaling function and its translations, can be generated a set of functions

$$f(t) = \sum_n \alpha_n \phi_{m,n}(t) \quad . \tag{2.18}$$

The set of all such functions generated by linear combination of the set $\{\phi_{m,n}(t)\}$ is called the span of the set $\{\phi_{m,n}(t)\}$, denoted by Span $\{\phi_{m,n}(t)\}$. Now consider V_m to be a vector space corresponding to Span $\{\phi_{m,n}(t)\}$. Assuming that the resolution increases with decreasing *m*, these vector spaces describe successive approximation vector spaces, . . . $\subset V_2 \subset V_1 \subset V_0 \subset V_{-1} \subset V_{-2}$ . . ., each with resolution 2^m (that is, each space V_{j+1} is contained in the next resolution space V_j*).* In multiresolution analysis, the set of subspaces satisfies the following properties:

i. $V_{m+1} \subset V_m$ for all *m*: This property states that each subspace is contained in the next resolution subspace.

ii. $\overline{\bigcup V_m} = L^2(\Re)$: This property indicates that the union of subspaces is dense in the space of square integrable functions $L^2(\Re)$; $\Re$ indicates a set of real numbers *(upward completeness* property).

iii. $\bigcap V_m = 0$ (an empty set): This property is called *downward complete-ness property.*

iv. $f(t) \in V_0 \leftrightarrow f(2^{-m}t) \in V_m$: Dilating a function from resolution space V_o by a factor of 2^m results in the lower resolution space V_m *(scale* or *dilation invariance* property).

v. $f(t) \in V_0 \leftrightarrow f(t-n) \in V_0$: Combining this with the scale invariance property above, this property states that translating a function in a resolution space does not change the resolution *(translation invariance* property).

vi. There exists a set $\{\phi(t-n) \in V_0$ is an integer$\}$ that forms an orthonormal

basis of V_o.

The basic principle of multiresolution analysis is that whenever the above properties are satisfied, there exists an orthonormal wavelet basis $\psi_{m,n}(t) = 2^{-m/2}\phi(2^{-m}t - n)$ such that

$$P_{m-1}(f) = P_m(f) + \sum c_{m,n}(f)\psi_{m,n}(t) \qquad (2.19)$$

where P_j is the orthogonal projection of ψ onto V_j. For each m, consider the wavelet functions $\psi_{m,n}(t)$ span a vector space W_m. It is clear from Eq. 2.19 that the wavelet that generates the space W_m, and the scaling function that generates the space V_m are not independent. W_m is exactly the orthogonal complement of V_m in V_{m-l}. Thus, any function in V_{m-l} can be expressed as the sum of a function in V_m and a function in the wavelet space W_m. Symbolically, this can be expressed as

$$V_{m-1} = V_m \oplus W_m . \qquad (2.20)$$

Since m is arbitrary,

$$V_m = V_{m+1} \oplus W_{m+1} . \qquad (2.21)$$

Thus,

$$V_{m-1} = V_{m+1} \oplus W_{m+1} \oplus W_m . \qquad (2.22)$$

Continuing in this fashion, It is can establish that

$$V_{m-1} = V_k \oplus W_k \oplus W_{k-1} \oplus W_{k-2} \oplus ...W_m . \qquad (2.23)$$

for any $k \geq m$.

Thus, if there is a function that belongs to the space V_{m-l} (that is., the function can be exactly represented by the scaling function at resolution *m* - l), it can be decomposed into a sum of functions starting with lower-resolution approximation followed by a sequence of functions generated by dilations of the wavelet that represent the loss of information in terms of details. The image representation with fewer and fewer pixels at successive levels of approximation should be considered. The wavelet coefficients can then be considered as the additional detail information needed to go from a coarser to a finer approximation. Therefore, in each decomposition level, the signal can be decomposed into two parts, one is the coarse approximation of the signal in the lower resolution and the other is the detail information that was lost because of the approximation. The wavelet coefficients derived by Eq. 2.15 or 2.16, therefore, describe the information (detail) lost when going from an approximation of the signal at resolution 2^{m-1} to the coarser approximation at resolution 2^m.

2.7.3. Extension to Two-Dimensional Signals

The 2D extension of DWT is essential for transformation images. A two-dimensional signal (image) can be represented by a 2D array *X* [*M* ,*N*] with *M* rows and *N* columns, where *M* and *N* are nonnegative integers. The simple approach for 2D implementation of the DWT is to perform the one-dimensional DWT row-wise to create an intermediate result and then perform the same one-dimensional DWT column-wise on this intermediate result to produce the final result. This is shown in Figure 2.7(a). This is possible because the two-dimensional scaling functions can be expressed as separable functions which are the products of two one-dimensional scaling functions such as $\phi_2(x,y) = \phi_1(x)\phi_1(y)$. The similar is true for the wavelet function $\psi(x,y)$ as well. Applying the one-dimensional transform in each row, two subbands in each row are produced. When the low-frequency subbands of all the rows (L) are put together, it looks like a thin version (of size *M* x $\frac{N}{2}$) of the input signal as shown in Figure 2.7(a). Similarly that put together the high-frequency subbands of all

the rows to produce the H subband of size M x $\frac{N}{2}$, which contains mainly the high-frequency information around discontinuities (edges in an image) in the input signal.

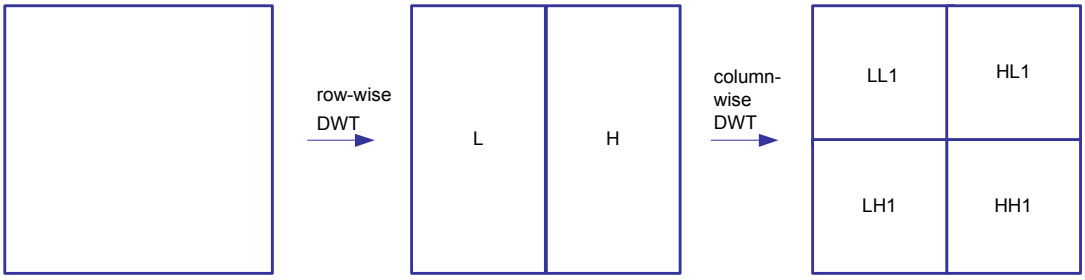

(a) First level of decomposition

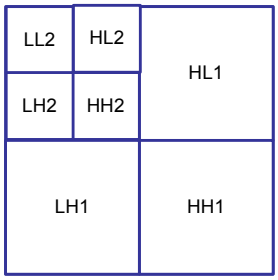

(b) Second level of decomposition

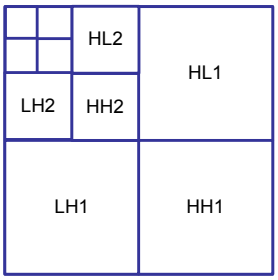

(c) Third level of decomposition

Figure 2.9 Row-Column computation of two-dimensional DWT.

Then applying a one-dimensional DWT column-wise on these L and H subbands (intermediate result), we produce four subbands LL, LH, HL, and HH of size $\frac{M}{2}$ x $\frac{N}{2}$ respectively, as shown in Figure 2.8(a). LL is a coarser version of the original input signal. LH, HL, and HH are the high-frequency subband containing the detail information. It should be noted the one-dimensional DWT column-wise first and then row-wise to achieve the same result could be applied.

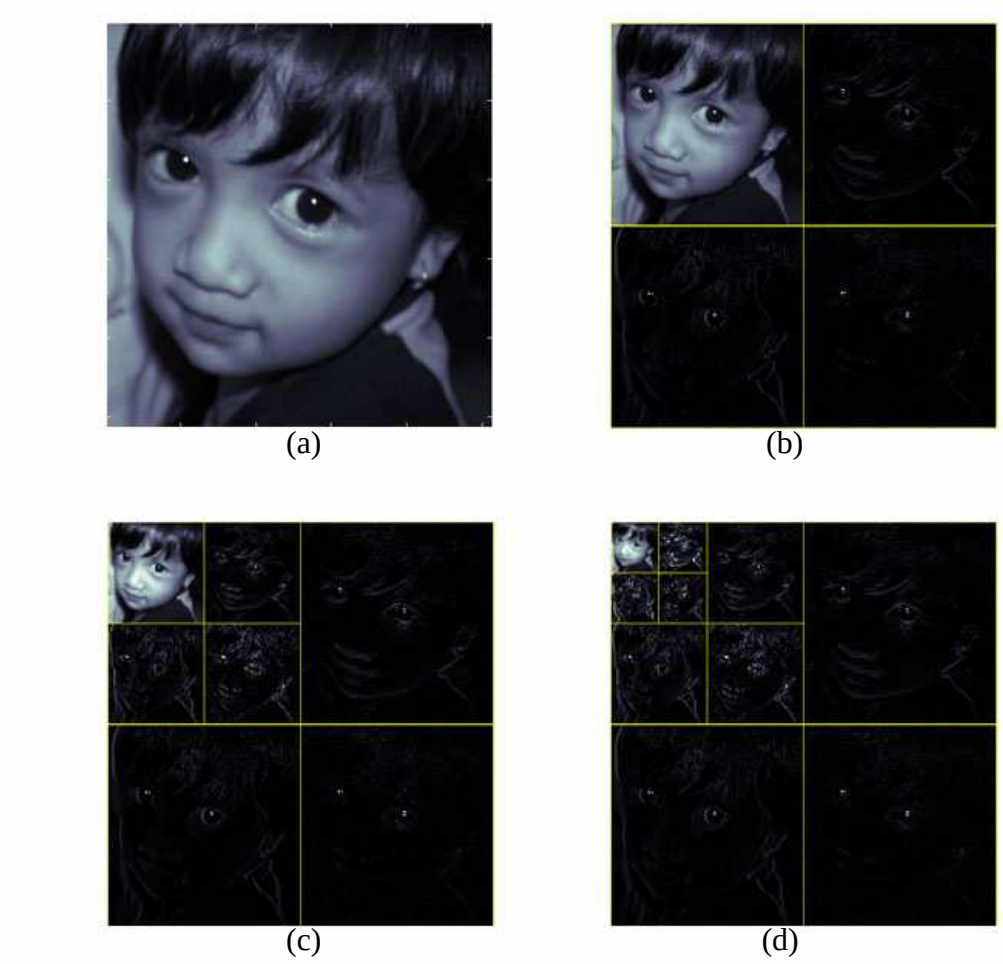

Figure 2.10 (a) Original `chicha.bmp` (b) after level 1, (c) after level 2, (d) after level 3 decomposition.

As shown in Figure 2.8(b), the LL1 subband can be further decomposed into four subbands LL2, HL2, LH2, and HH2 based on the principle of multiresolution analysis. The same computation can continue to further decompose LL2 into higher levels. In Figure 2.9 shows the result of the wavelet transform at different levels with a real-life image provided by the JPEG2000 standard committee. The subbands have been normalized to 8 bits for the purpose of display.

2.8. Wavelet-Based Colour Image Compression

There are some image compressions that based on the wavelet. Set Partitioning in Hierarchical Trees (SPIHT) dan Embedded Zerotrees of Wavelet Transforms (EZW) are described in the following section.

2.8.1. Set Partitioning in Hierarchical Trees (SPIHT)

Set Partitioning in Hierarchical Trees (SPIHT) is an image compression algorithm that exploits the inherent similarities across subbands in a wavelet decomposition of an image. It implies uniform quantization and bit allocation applied after wavelet decomposition and was proposed by Amir Said and William Pearlman[24].

Wavelet transform can be applied several times to an image, creating regions or subbands. Different wavelet filters produce different results depending on the image type, but it is currently not clear what filter is the best for any given image type. In spite of the particular filter used, the image is decomposed into subbands, such that lower subbands correspond to higher image frequencies (they are the highpass levels) and higher subbands correspond to lower image frequencies (lowpass levels), where most of the image energy is concentrated (Figure 2.10). This is the reason why the detail coefficients can be expected to get smaller as the moving from high to low levels. An image part, such as an edge, occupies the same spatial position in each subband. These features of the wavelet decomposition are exploited by the SPIHT method [24].

Optimal progressive transmission, as well as for compression problem was considered can be solved by SPIHT. SPIHT has one of the important, perhaps a unique feature, that is at any point during the decoding of an image, the quality of the displayed image is the best that can be achieved for the number of bits input by the decoder up to that moment.

SPIHT also has another essential feature that it uses of embedded coding. This feature is defined as follows: If an embedded coding encoder produces two files, a large one

of size M and a small one of size m, then the smaller file is identical to the first m bits of the larger file.

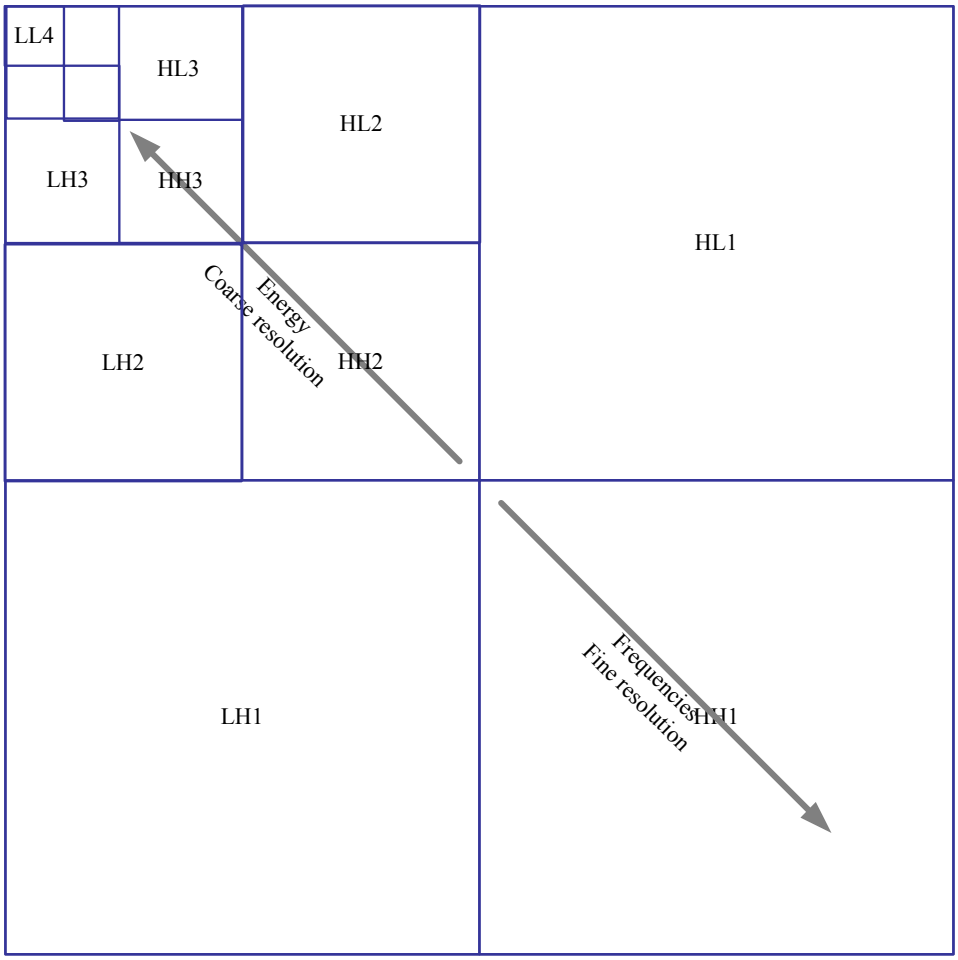

Figure 2.11 Subbands and levels in wavelet Decomposition.

The following example appropriately illustrates the meaning of this definition. If there are three users wait for the sending of a certain compressed image, but they need different image qualities. The first one needs the quality contained in a 10 Kb file. The second and third users require the image qualities at 20 Kb and 50 Kb file sizes, respectively. Most lossy image compression methods would have to compress the same image three times, at different qualities, to generate three files with the right sizes. SPIHT, on the other hand, produces one file and then three chunks—of lengths

10 Kb, 20 Kb, and 50 Kb, all starting at the beginning of that file—can be sent to the three users, thereby satisfying their needs.

The major steps of the SPIHT encoder are expressed as follows:

i. Step 1: Given an image to be compressed, perform its wavelet transform using any suitable wavelet filter, decompose it into transform coefficients $c_{i,j}$, and represent the resulting coefficients with a fixed number of bits. The first assumption is that the coefficients are represented as 16-bit signed-magnitude numbers. The leftmost bit is the sign, and the remaining 15 bits are the magnitude. (Notice that the sign-magnitude representation is different from the 2's complement method, which is used by computer hardware to represent signed numbers.) Such numbers can have values from $-(2^{15}-1)$ to $2^{15}-1$. Set n to $\lfloor \log_2 \max_{i,j}(c_{i,j}) \rfloor$. In our case n will be set to $\lfloor \log_2 (2^{15}-1) \rfloor = 14$.
ii. Step 2: Sorting pass: Transmit the number l of coefficients $c_{i,j}$ that satisfy $2^n \leq |c_{i,j}| < 2^{n+1}$. Follow with the l pairs of coordinates and the l sign bits of those coefficients.
iii. Step 3: Refinement pass: Transmit the nth most significant bit of all the coefficients satisfying $|c_{i,j}| \geq 2^{n+1}$. These are the coefficients that were selected in previous sorting passes (not including the immediately preceding sorting pass).
iv. Step 4: Iterate: Decrement n by 1. If more iterations are needed (or desired), go back to Step 2.

The last iteration is typically performed for $n = 0$, but the encoder can stop earlier, in which case the least important image information (some of the least significant bits of all the wavelet coefficients) will not be transmitted. This is the natural lossy option of SPIHT. Because the coefficients are transmitted in sorted order, it is equivalent to scalar quantization, but it produces better results than what is usually reached with scalar quantization. An alternative is for the encoder to transmit the entire image (that is, all the bits of all the wavelet coefficients) and the decoder can stop decoding when the reconstructed image reaches a certain quality. This quality can either be predetermined by the user or automatically determined by the decoder at run time.

Spatial Orientation Trees [25]

The sets T_k are created and partitioned using a special data structure called a spatial orientation tree. This structure is defined in a way that exploits the spatial relationships between the wavelet coefficients in the different levels of the subband pyramid[25].

The spatial orientation trees are illustrated in Figure 2.10a and 2.10b for a 16×16 image. The figure shows two levels, level 1 (the highpass) and level 2 (the lowpass). Each level is divided into four subbands. Subband LL2 (the lowpass subband) is divided into four groups of 2×2 coefficients each. Figure 4.2a shows the top-left group, and Figure 4.2b shows the bottom-right group. In each group, each of the four coefficients (except the top-left one, marked in gray) becomes the root of a spatial orientation tree. The arrows show examples of how the various levels of these trees are related. The thick arrows indicate how each group of 4×4 coefficients in level 2 is the parent of four such groups in level 1. In general, a coefficient at location *(i, j)* in the image is the parent of the four coefficients at locations (2*i*, 2*j*), (2*i* + 1, 2*j*), (2*i*, 2*j* + 1), and (2i + 1, 2*j* + 1).

The roots of the spatial orientation trees of our example are located in subband LL2. In general, they are located in the top-left LL subband, which can be of any size, but any wavelet coefficient, except the gray ones on level 1 (also except the leaves), can be considered the root of some spatial orientation subtree. The leaves of all those trees are located on level 1 of the subband pyramid. In our example, subband LL2 is of size 4×4, so it is divided into four 2×2 groups, and three of the four coefficients of a group become roots of trees. Thus, the number of trees in the example is 12. In general, the number of trees is 3/4 the size of the highest LL subband.

Each of the 12 roots in subband LL2 in our example is the parent of four children located on the same level. However, the children of these children are located on level 1. This is true in general. The roots of the trees are located on the highest level, and

their children are on the same level, but from then on, the four children of a coefficient on level k are themselves located on level $k - 1$.

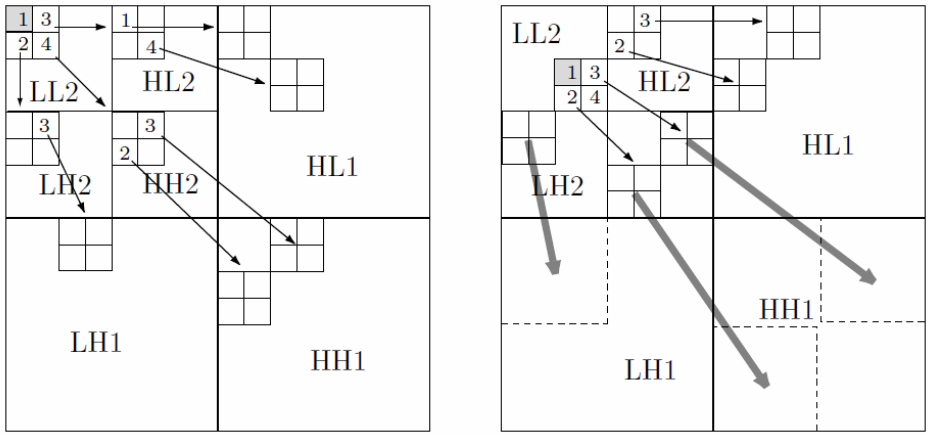

(a) (b)

Figure 2.12 Spatial orientation trees in SPIHT[25].

The coding algorithm therefore uses three lists called list of significant pixels (LSP), list of insignificant pixels (LIP), and list of insignificant sets (LIS). The LIP contains coordinates of coefficients that were insignificant in the previous sorting pass. In the current pass they are tested, and those that test significant are moved to the LSP. In a similar way, sets in the LIS are tested in sequential order, and when a set is found to be significant, it is removed from the LIS and is partitioned. The new subsets with more than one coefficient are placed back in the LIS, to be tested later, and the subsets with one element are tested and appended to the LIP or the LSP, depending on the results of the test. The refinement pass transmits the nth most significant bit of the entries in the LSP.

The SPIHT algorithm is illustrated as follow in detail.

i. Set the threshold. Set LIP to all root nodes coefficients. Set LIS to all trees (assign type D to them). Set LSP to an empty set.
ii. Sorting pass: Check the significance of all coefficients in LIP:
    ii.a. If significant, output 1, output a sign bit, and move the coefficient to the LSP.

ii.b. If not significant, output 0.

iii. Check the significance of all trees in the LIS according to the type of tree:

a) For a tree of type D:

- If it is significant, output 1, and code its children:
  - If a child is significant, output 1, then a sign bit, add it to the LSP
  - If a child is insignificant, output 0 and add the child to the end of LIP.
  - If the children have descendants, move the tree to the end of LIS as type L, otherwise remove it from LIS.
- If it is insignificant, output 0.

b) For a tree of type L:

- If it is significant, output 1, add each of the children to the end of LIS as an entry of type D and remove the parent tree from the LIS.
- If it is insignificant, output 0.

iv. Loop: Decrement the threshold and go to step 2 if needed.

2.8.2. Embedded Zerotrees of Wavelet Transforms

Embedded Zerotrees of Wavelet Transforms (EZW) is a lossy image compression algorithm. At low bit rates, that is high compression ratios most of the coefficients produced by a subband transform (such as the wavelet transform) will be zero, or very close to zero. This occurs because "real world" images tend to contain mostly low frequency information (highly correlated). However where high frequency information does occur (such as edges in the image) this is particularly important in terms of human perception of the image quality, and thus must be represented accurately in any high quality coding scheme.

In zerotree based image compression scheme such as EZW and SPIHT, the intent is to use the statistical properties of the trees in order to efficiently code the locations of the significant coefficients. Since most of the coefficients will be zero or close to zero, the spatial locations of the significant coefficients make up a large portion of the total size of a typical compressed image. A coefficient (likewise a tree) is considered significant if its magnitude (or magnitudes of a node and all its descendants in the case of a tree)

is above a particular threshold. By starting with a threshold which is close to the maximum coefficient magnitudes and iteratively decreasing the threshold, it is possible to create a compressed representation of an image which progressively adds finer detail. Due to the structure of the trees, it is very likely that if a coefficient in a particular frequency band is insignificant, then all its descendants (the spatially related higher frequency band coefficients) will also be insignificant.

The EZW method, as implemented in practice, starts by performing the 9-tap symmetric quadrature mirror filter (QMF) wavelet transform. The main loop is then repeated for values of the threshold that are halved at the end of each iteration. The threshold is used to calculate a significance map of significant and insignificant wavelet coefficients. Zerotrees are used to represent the significance map in an efficient way. The main steps are as follows:

i. Initialization: Set the threshold T to the smallest power of 2 that is greater than $\max_{(i,j)} | c_{i,j} |/2$, where $c_{i,j}$ are the wavelet coefficients.
ii. Significance map coding: Scan all the coefficients in a predefined way and output a symbol when $| c_{i,j} | > T$. When the decoder inputs this symbol, it sets $ci,j = \pm 1.5T$.
iii. Refinement: Refine each significant coefficient by sending one more bit of its binary representation. When the decoder receives this, it increments the current coefficient value by $\pm 0.25T$.
iv. Set $T = T/2$, and go to step 2 if more iterations are needed.

A wavelet coefficient ci,j is considered insignificant with respect to the current threshold T if $| c_{i,j} | \leq T$. The zerotree data structure is based on the following experimental result[25]: If a wavelet coefficient at a coarse scale (that is, high in the image pyramid) is insignificant with respect to a given threshold T, then all of the coefficients of the same orientation in the same spatial location at finer scales (that is., located lower in the pyramid) are very likely to be insignificant with respect to T.

In each iteration, all the coefficients are scanned in the order shown in Figure 2.11. This guarantees that when a node is visited, all its parents will already have been

scanned. The scan starts at the lowest frequency subband LL_n, continues with subbands HL_n, LH_n, and HH_n, and drops to level $n - 1$, where it scans HL_{n-1}, LH_{n-1}, and HH_{n-1}. Each subband is fully scanned before the algorithm proceeds to the next subband.

Each coefficient visited in the scan is classified as a zerotree root (ZTR), an isolated zero (IZ), positive significant (POS), or negative significant (NEG). A zerotree root is a coefficient that is insignificant and all its descendants (in the same spatial orientation tree) are also insignificant. Such a coefficient becomes the root of a zerotree. It is encoded with a special symbol and is denoted by ZTR. The important point is that its descendants do not have to be encoded in the current iteration. When the decoder inputs a ZTR symbol, it assigns a zero value to the coefficients and to all its descendants in the spatial orientation tree. These values are refined in subsequent iterations. An isolated zero is a coefficient that is insignificant but has some significant descendants. Such a coefficient is encoded with the special IZ symbol. The other two classes are coefficients that are significant and are positive or negative.

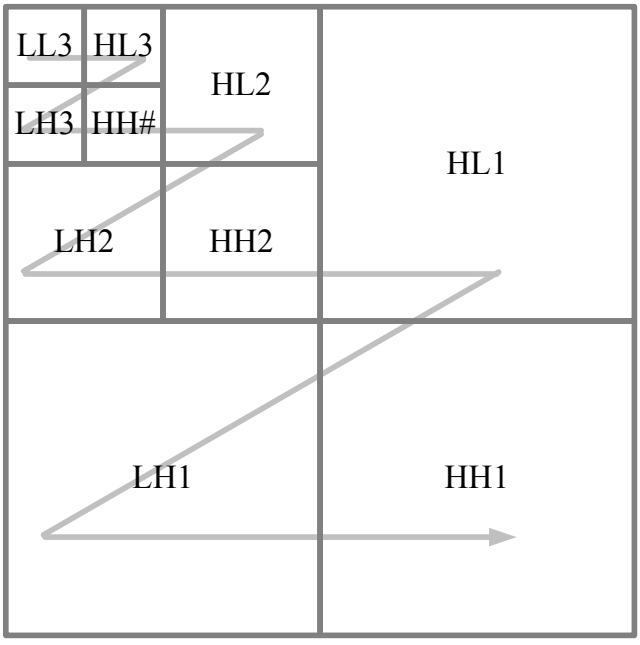

Figure 2.13 Scanning a zerotree.

2.9. Image Features Influence on The Wavelet-based Image Codec

Study on relationship of several image features and wavelet-based image codec have been evaluated by Saha and Vemuri[8-11]. Saha and Vemuri investigated the statistical image features of images that influence to coding performance in gray scale images. The research results show the strong correlation of the features against the wavelet-based codec performance. Nevertheless, this result is only a statistical association and cannot conclusively prove causality

There are other researchers, that is Eskicioglu and Fisher that evaluated image quality measures like spatial frequency and their performance for gray scale images [12]. In this study the spatial frequency (SF) is used to evaluate the image features. N. Sprljan, S. Grgic and M Grgic, investigated spectral flatness measure (SFM) in images [13].

However, gray scale images are not realistic today, because the digital colour image technology has growth rapidly. However, the idea of their researches conducted in gray scale, can be explored in colour image. Therefore, this research will discuss how the characteristics of colour images affect the performance of a wavelet-based codec.

S. Gladston Raj, K. Revathy, and G. Raju examined the influence of image properties on the selection of suitable wavelet filters. They considered a set of spatial, spectral as well as statistical features of image. The images are compressed by applying different families of wavelets. For a given image, a wavelet filter giving the best performance is decided based on the compression ratio and quality of the reconstructed image. The choice of filter for each image was found, and this information was given to different classifiers like neural, nearest neighbor, discriminant and classification tree to predict the best filter for image compression based on image features. The study reveals that the parameters used in this investigation are not sufficient for the selection of appropriate wavelet filters [26].

The results from this study showed that image gradient and spatial frequency have a strong correlation with PSNR, CR and bpp. The magnitude of the relation between the

variables, that is, image gradient and the coding performance and spatial frequency and coding performance is strong. In other words, one variable could be predicted based on the other.

Because this result is only a statistical relationship and cannot conclusively prove causality. This research has also investigated the cause-effect relationship as the logical direction. The cause-effect study using hypothesis statistical test could help better understand which image characteristics influence the coding performance of a wavelet-based image compression system. Therefore, this thesis hypothesizes that an adaptive wavelet-based compression system would be feasible based on the image characteristics. The adaptive wavelet-based compression system could use a neural-network, which would select the most appropriate wavelet based on image characteristics.

2.10. Wavelet Selection in Image Compression

In recent years, wavelet transforms have established their popularity in image compression applications. Various different kinds of wavelets exist currently. In wavelet based image compression techniques, the selection of filters influences the compression performance. The choice of a suitable wavelet functions for image coding is still an open question. Many interesting image coding schemes based on wavelets have recently been offered in many applications. The illustration of two compressed images of an image using two different wavelets (appropriate and inappropriate chosen) is shown in Figure 2.13.

O. Rioul conducted investigation to choose of wavelet filters for still image compression[4]. T. Buschgens and F. Hartenstein also tried to find the most appropriate wavelet for image compression [5]. S. Masud and J.**V.** Mc Canny have evaluated several kinds of wavelet to compress gray scale image in their research. These researchers explained that the results obtained indicate that of the wavelets studied the biorthogonal 9&7 taps wavelet is the most suitable from a compression

perspective and that the Daubechies 8 taps gives best performance when assessed solely in terms of statistical measures [1].

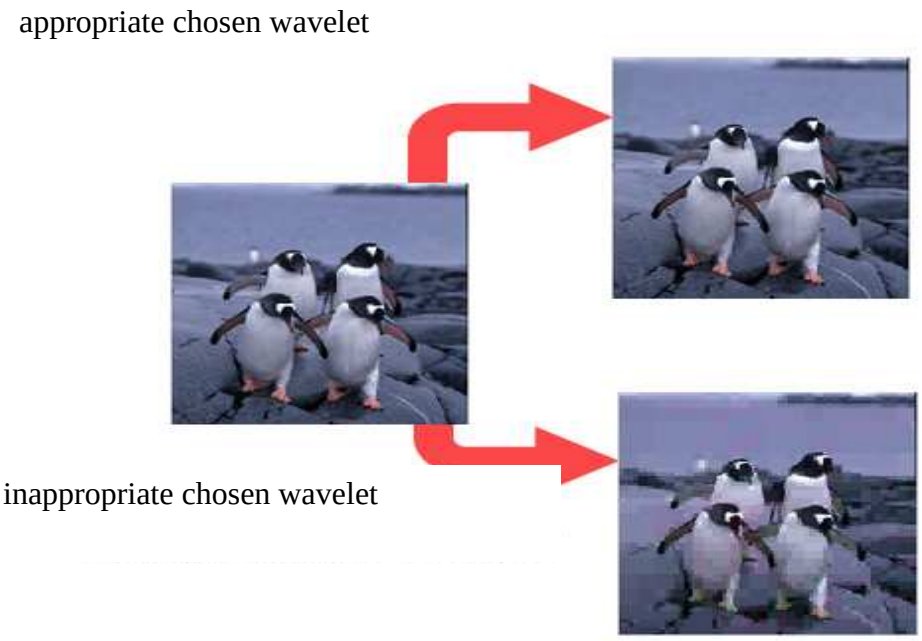

Figure 2.14 Image compressions using appropriate and inappropriate chosen wavelet.

J.D. Villasenor, B. Belzer, and J. Lio analyze of all reasonable length minimum order biorthogonal perfect reconstruction filters using these metrics identified filter banks that are well suited to image compression. They evaluated several wavelet filters taken from 4300 candidate filter banks, and then represented several chosen wavelets[6]. They suggested using some wavelet types for all images, without considering the image classification.

In the past, researches have recommended one wavelet filter for all type of images, without considering the image characteristics. The filter suitable for one image needs not be the best for another.

This research proposes a method that can select the most appropriate wavelet for general image types adaptively. The artificial neural network will be used in the selection stage by considering the image features [7].

2.11. Artificial Neural Network in Image Processing

Artificial Neural Networks are recent development tools that are modeled from biological neural networks. The powerful side of this new tool is its ability to solve problems that are very hard to be solved by traditional computing methods that is by algorithms to solve problems. It has been used over a wide range of area including, virus detection, robot control, intrusion detection systems, pattern (image, fingerprint, noise) recognition and so on.

In image processing field, artificial Neural Networks have been extensively used, especially in image segmentation and object classification problems[27][28]. Several approaches have also used to solve image compression problems. Some researches use neural network approach instead of the "classical" method such as lossy or lossless compression for coding and decoding evaluation [29][30]. S. Saha and R. Vemuri described the possibility of adaptive wavelet filters in image coders [31][32]. But they have not developed the adaptive wavelet based image compression.

As discussed earlier, the most important issue in wavelet-based codec is the wavelet type chosen. An appropriate choice of wavelet significantly improves coding performance, fidelity and image perceptual quality. If a inappropriate wavelet is chosen, the resultant compressed image would be visually poor. This research proposed to put MLP neural network on the wavelet-based colour image compression scheme. The neural network will be used as an adaptive tool for the wavelet selection. The study of relationship of image features; image gradient and spatial frequency (IAM and SF) against the wavelet-based image codec performance (PSNR, CR and bpp) will provide useful information to implement an neural network based image compression system [7]. Therefore, the image codec scheme can be shown as Figure 2.14.

The Basic of Artificial Neural Networks

The ability to adapt, learn, generalize, cluster or organize data is characteristic of ANNs. There are many structures of ANNs including, Percepton, Adaline, Madaline, Kohonen, BackPropagation and various others. The most common neural network model is the multilayer perceptron (MLP) using backpropagation algorithm. This type of neural network is known as a supervised network because it requires a desired output in order to learn. The goal of this type of network is to create a model that correctly maps the input to the output using historical data so that the model can then be used to produce the output when the desired output is unknown. This research will deal with BackPropagation ANNs.

Multi layer perceptron (MLP) contain one or more layers each of which are linked to the next layer. The first layer is called the "input layer" which assembles the initial input and so does the last one "output layer" which usually holds the input's identifier. The layers connecting input and output layers are called "hidden layer(s)" which only propagate the previous layer's outputs to the next layer and (back) propagates the following layer's error to the previous layer. Actually, these are the main procedures of training a BackPropagation that used in MLP which follows a few steps.

A graphical representation of an MLP is depicted as Figure 2.15.

The extreme left nodes are the initial inputs. The network training involves two stages. In the first stage, the inputs are propagated forward to compute the outputs for each output node. Then, each of these outputs is subtracted from its desired output, causing an error (for each output node). In the second stage, each of these output errors is passed backward and the weights are fixed. These two stages are repeated until the sum of (square of output errors) achieves an acceptable value.

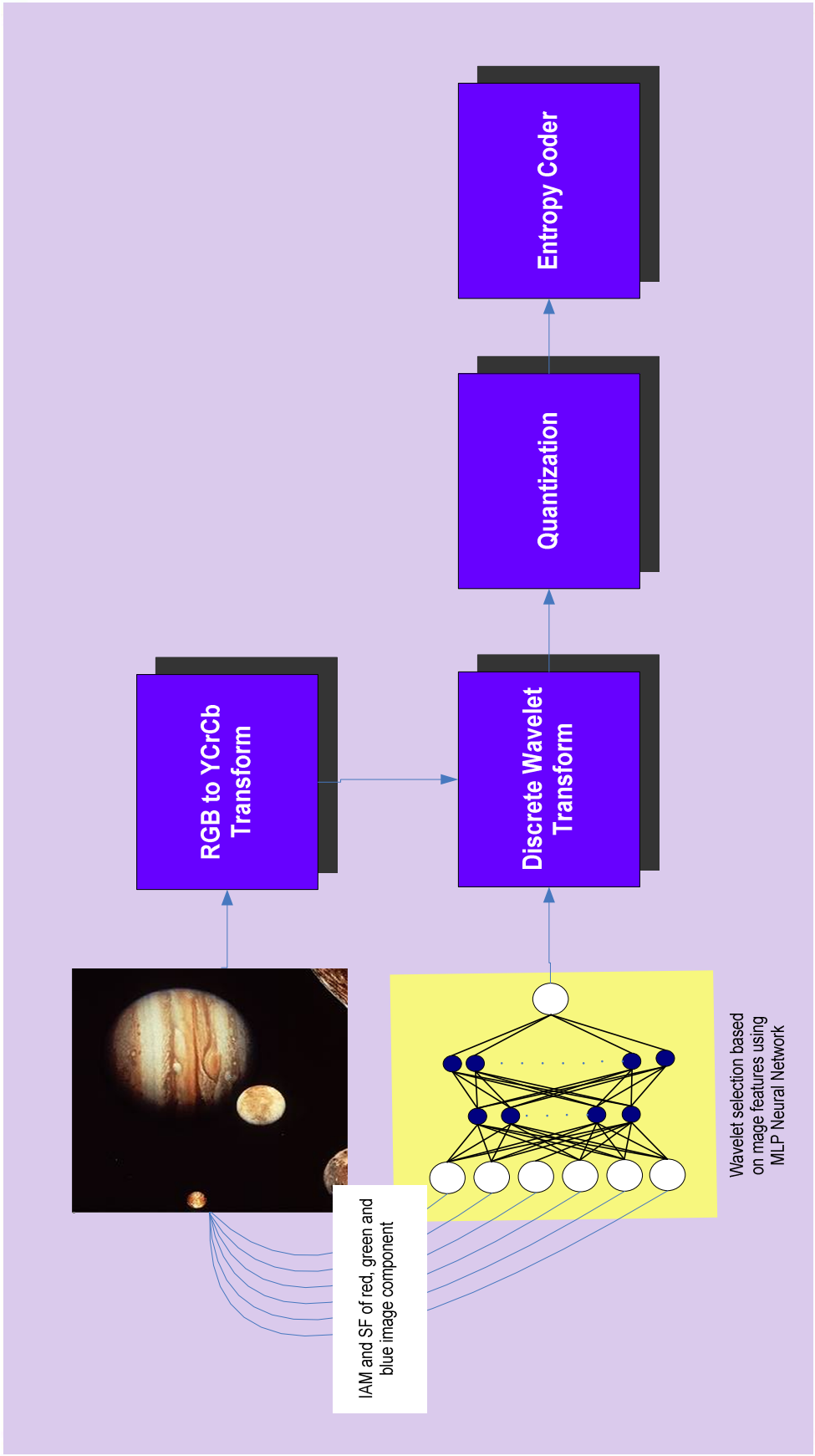

Figure 2.14 Block diagram of an adaptive wavelet selection in colour image

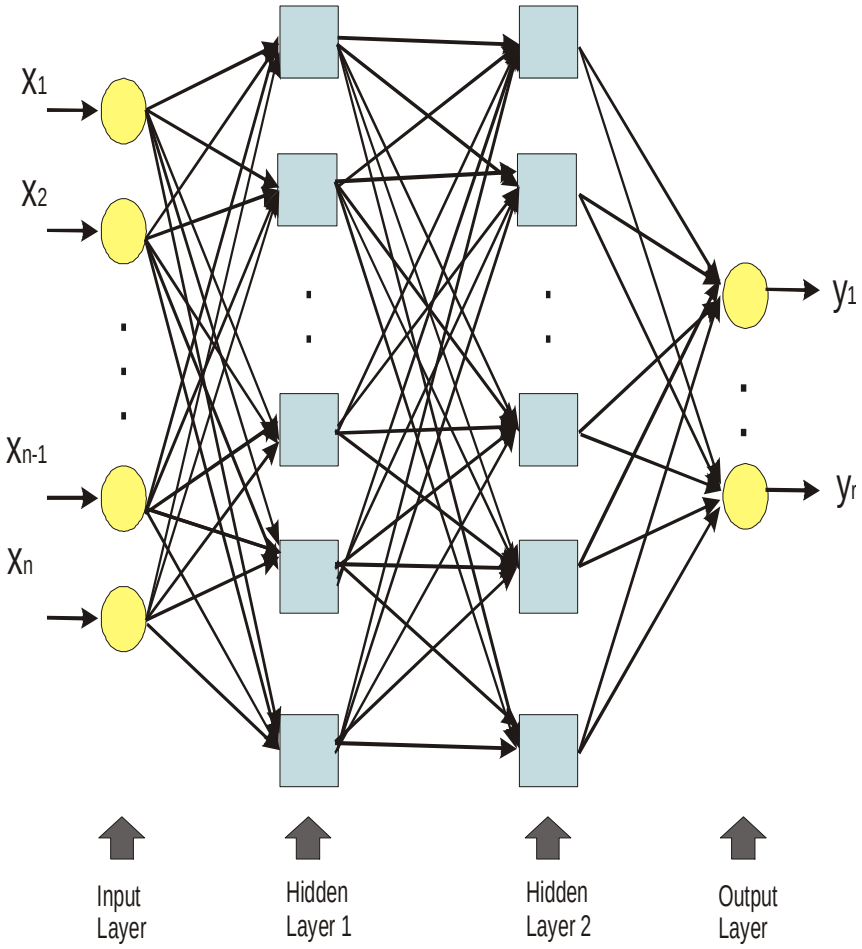

Figure 2.15 Block diagram of a two hidden layer multiplayer perceptron (MLP).

2.12. Summary

In this chapter, the basic knowledge about colour image, its representation and the colour space and human perception are discussed. The image feature analysis is also briefly introduced. Some ordinary used algorithms image compression including both lossless and lossy methods are mentioned in this chapter. The basic of wavelet transform is described. The relationship of wavelet based codec and the image features are also cited here.

In this chapter, the wavelet theory and its implementation in image compression are discussed. This chapter also discussed the theoretical foundation of the discrete wavelet transform (DWT). The multiresolution analysis features of the wavelet transform that make it appropriate for image compression application are also explained here.

This chapter has discussed the wavelet-based colour image compression. This chapter discussed the Set partitioning in hierarchical trees (SPIHT) and Embedded Zerotrees of Wavelet Transforms (EZW) as the popular advanced schemes.

Some researches have been evaluated the most suitable wavelet filter for image compression application. This research proposes the MLP neural network as a adaptive tool for wavelet selection by considering the image characteristics.

CHAPTER 3

METHODOLOGY

This chapter will discuss the methodology part of this research, as well as description on the data samples of images and features evaluation of images used. The wavelet based image compression, analyses of the relation of image features and codec performance and development of adaptive wavelet compression system using neural network are also discussed. The details of the experiments are also elaborated in this chapter. The methodology is divided in two main parts: identify the image features and codec performance correlation/relationship and develop the adaptive wavelet codec. The diagram in Figure 3.1 describes the methodology.

3.1 Data Samples of Images

A set of 450 BMP (bitmap) colour images having a size of 256 x 256 pixels is used in this research. The large number of images used is to ensure the system designed is objective because the various types of images used. In order to achieve acceptable statistical results, a large number of images are required.

The images used are from different types of images and they are grouped into natural and synthetic image classifications. In this research, a natural image is defined as an image taken from real object in the world using photograph. Synthetic image is defined as image generated by a computer, or cartoon image.

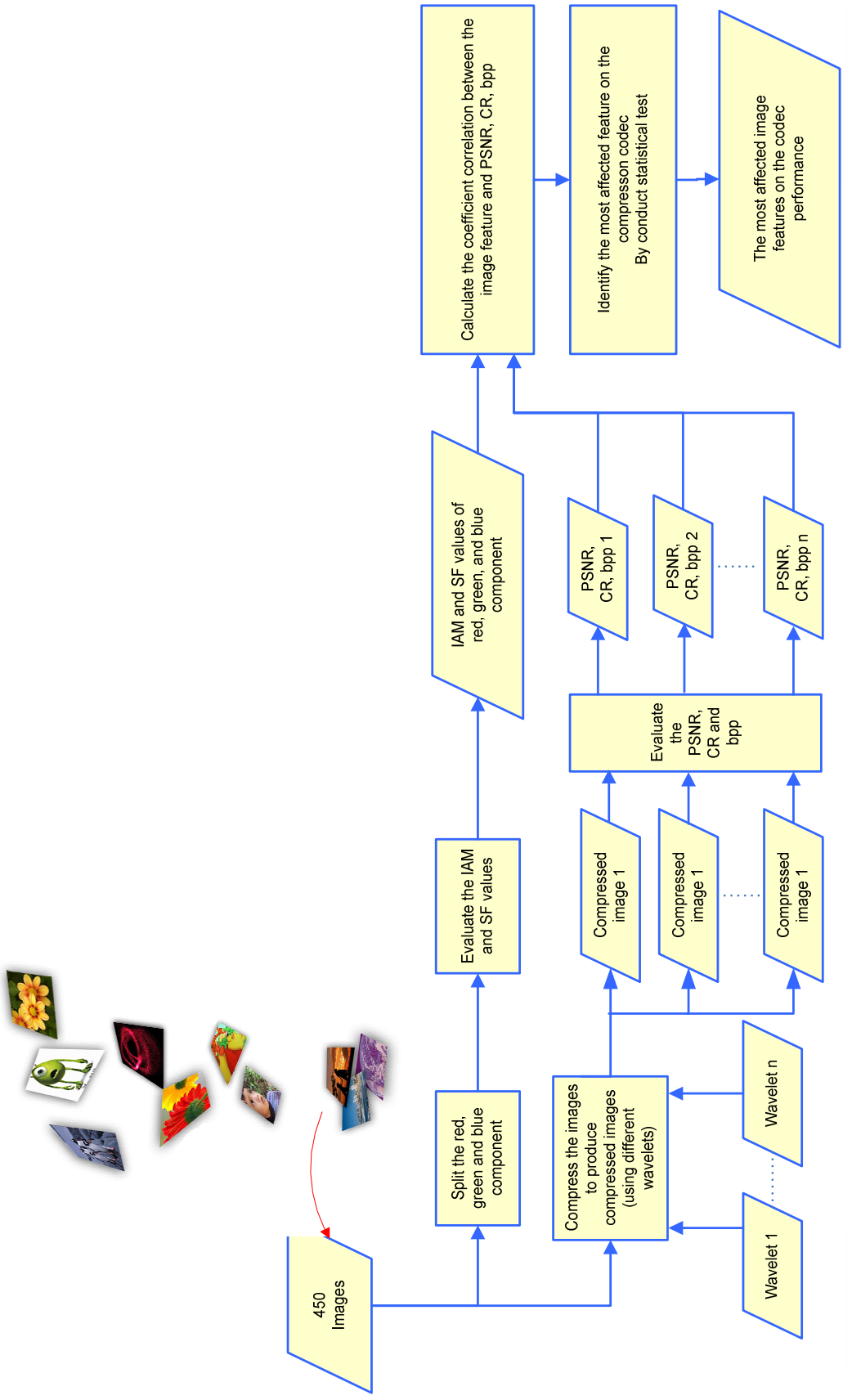

Figure 3.1 Diagram of the most affected image feature on wavelet codec identification.

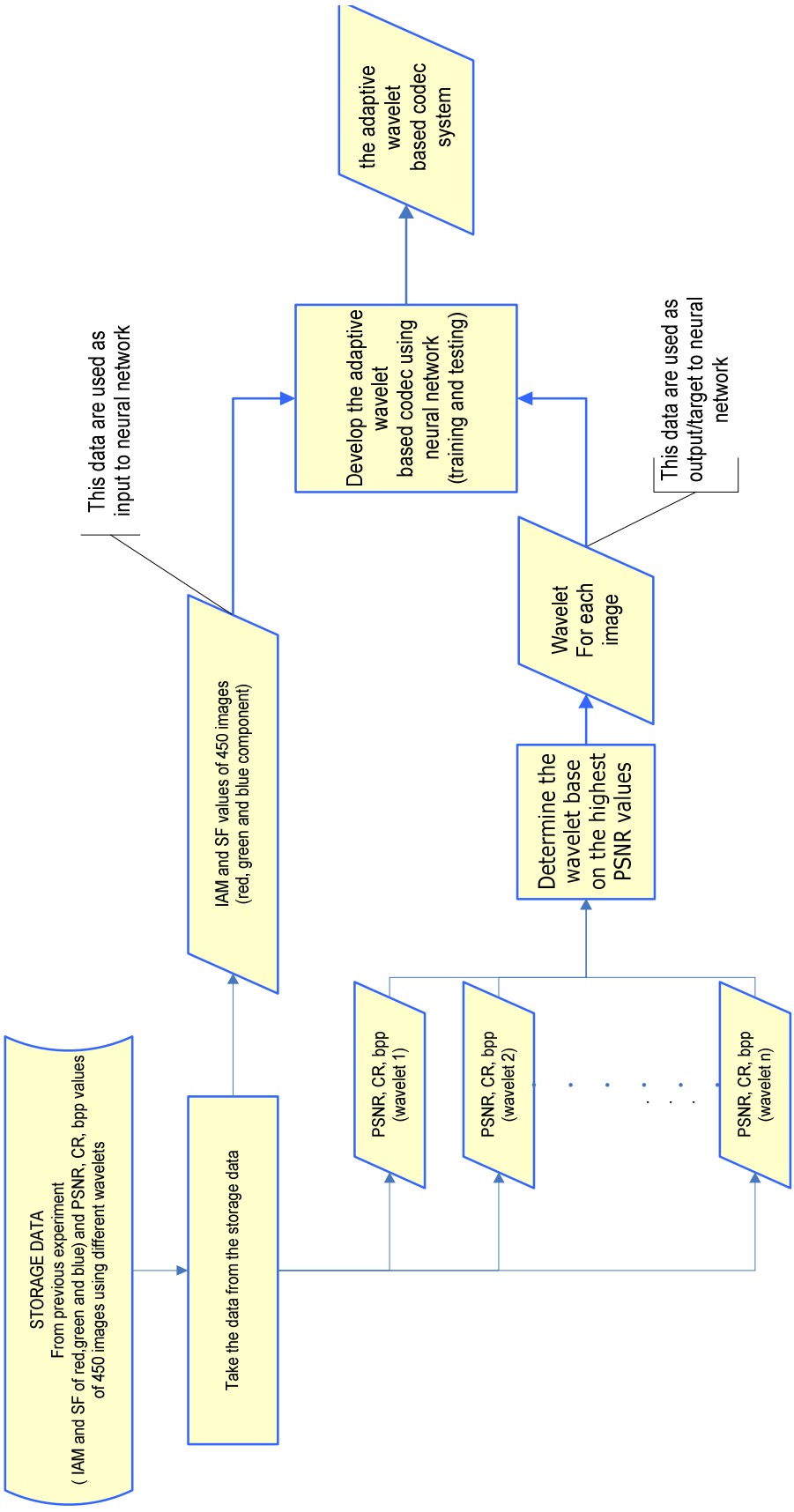

Figure 3.3 Diagram of adaptive wavelet codec system development.

Synthetic images differ from natural images in that synthetic images have sharp artificial colour transitions. Conversely, natural images have gradual colour transition, for example photographs. Furthermore, sharp transition can occur between two different regions of constant colour in a synthetic image. In contrast, natural images do not have sharp edges like synthetic images instead the edges are often blurred. Also some synthetic images have fewer colours than natural images. Cartoons and clip-arts are basically human drawings and therefore will have very well defined edges as compared to natural images.

The images are arbitrarily classified into animal, flower and plant, satellite, people, space/telescope and scene images are classified as natural images. The classification of images samples in this research is shown in Figure 3.3.

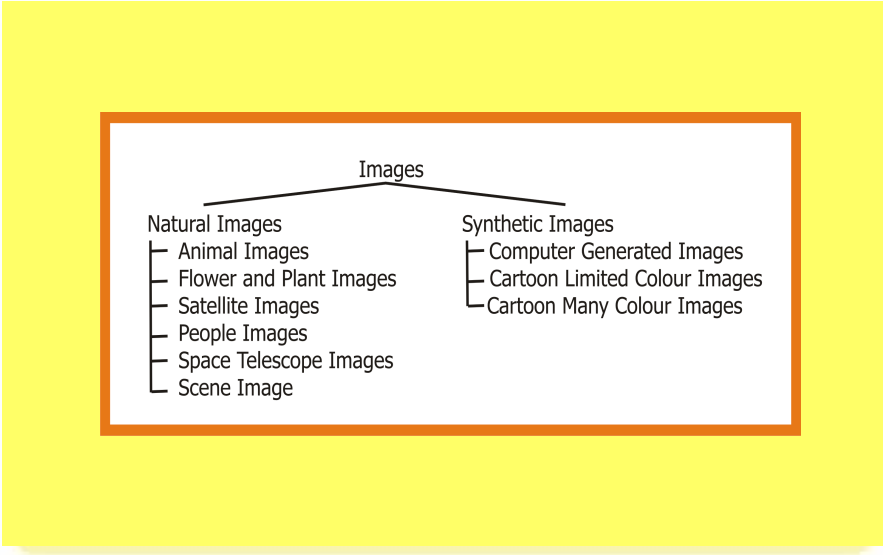

Figure 3.5 Image classification.

There are nine classes in this thesis, six for natural image classes and three classes for synthetic image classes. There are 50 images in each class. Figure 3.4 shows sample images from every class, two images representative other images.

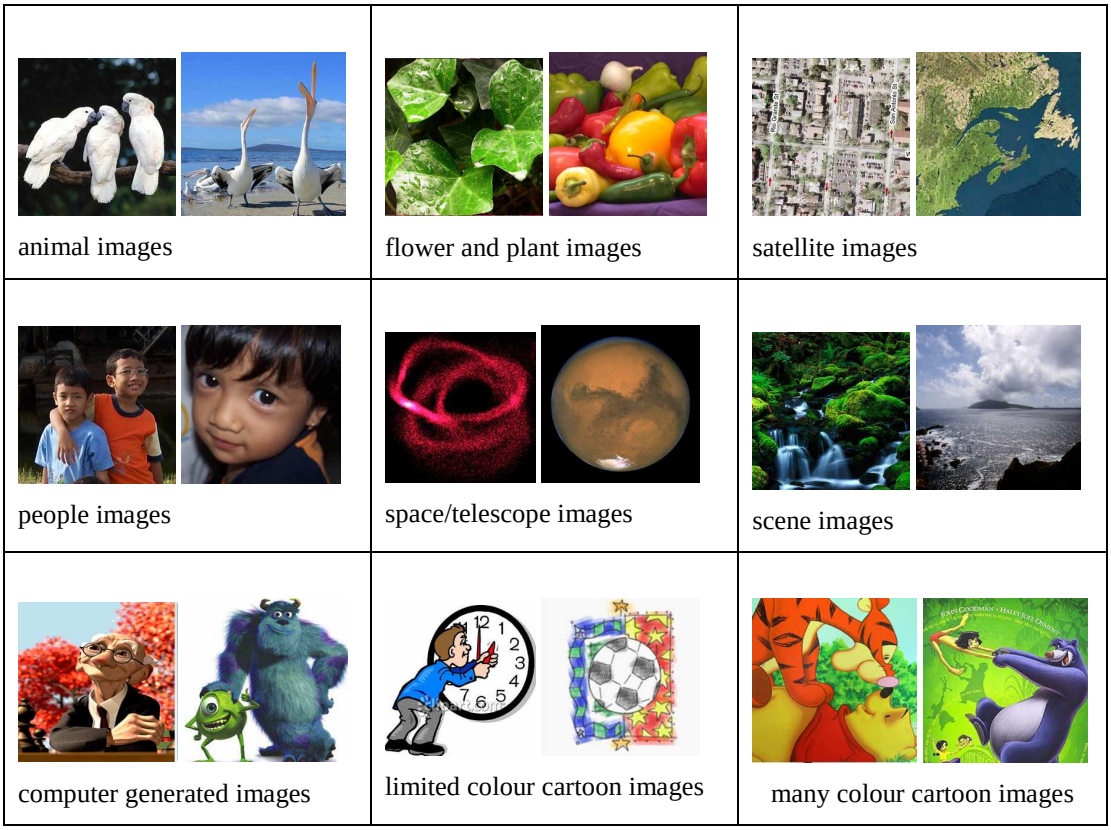

Figure 3.6 Sample images for each class.

3.2 Image Features Evaluation

A colour image consists of three colour component, namely red, green and blue. The first step to evaluate a colour image is to divide the image into three colour component. An example is shown in Figure 3.5.

Figure 3.7 RGB dividing image.

The histogram features and spatial characteristics of each colour component (red, green and blue) are evaluated for all images. The histogram features are statistically based features and they provide information about the characteristics of the colour distribution of a colour image. This features include first order statistics that is, range, mean, median, different (mean-median), standard deviation, variance, coefficient variance, skewness, kurtosis, brightness energy[10], gray/color energy, zero-order entropy, first-order entropy, second-order entropy. The spatial characteristics explored include image gradient[9], spatial frequency (SF) [12]and spectral flatness measure (SFM)[13].

3.2.1 Image Statistic Features

Characteristics of a grey-level image can be evaluated using statistical analysis of histogram statistics. Mean, standard deviation, variance, skewness, kurtosis, and entropy as the common statistical feature [9][17] are used in the evaluation. The following sections will give a brief explanation of the image statistics used in this research.

Mean

Mean also can be called average, which shows the general brightness of the m by n image and is given by:

$$mean = \sum_{m}\sum_{n}\frac{I_{(m,n)}}{(M * N)} \tag{3.1}$$

where $I_{(m,n)}$is the values of the image at m row and n column. Mean can be evaluated by summing of all pixel values, then divided by *(M*N)*, where *(M*N)* is the size of the image [33]. An image with a high mean indicates that the image is a bright image and other wise a dark image will have a low mean.

Median

The median is the middle of a distribution: half the scores are above the median and half are below the median. The median value can be found by arranging the values in order and then selecting the one in the middle. In an image, total number of values in the image is even, and then the median is the mean of the two middle numbers. The median is useful in cases where the distribution has very large extreme values which would otherwise skew the data.

Standard Deviation

The standard deviation of an image is a measure of spreading of pixel values of that image. The standard deviation is usually denoted with the letter σ (lowercase sigma). It is defined as the root-mean-square (RMS) deviation of the values from their mean, or as the square root of the variance. If many data points are close to the mean, then the standard deviation is small; if many data points are far from the mean, then the standard deviation is large. The standard deviation (Std. Dev.) can be calculated by:

$$StDev = \sigma = \sqrt{\frac{\sum_m \sum_n (I_{(m,n)} - mean)^2}{M * N - 1}} \qquad (3.2)$$

where $\sum_m \sum_n (I_{(m,n)} - mean)^2$ is the sum of the squares of all pixel values that have subtracted by mean of all pixel values of the image[33].

Variance

The variance of an image is one measure of statistical dispersion, averaging the squared distance of its possible values from the expected value (mean). The variance is the square of the standard deviation and is calculated using[34]:

$$Variance(\sigma) = StDev^2 = \frac{1}{M * N - 1} \sum_m \sum_n (I_{(m,n)} - mean)^2 \tag{3.3}$$

An image with a high variance means that the image has a high contrast, and an image with a low variance indicates that the image has a low contrast.

Coefficient of Variation

Coefficient of variation of an image is evaluated by calculating the standard deviation divided by the mean of the image[9].

$$\eta = \frac{StDev}{mean} \tag{3.4}$$

Skewness

Skewness of an image is a measure of the asymmetry of the pixels' values in the image around the mean. A distribution or data set is symmetric, if it looks the same to the left and right of the centre point. When the skewness is negative, the data are spread out more to the left of the mean than to the right. If skewness is positive, the data are spread out more to the right. The skewness of the normal distribution (or any perfectly symmetric distribution) is zero.
Skewness is calculated by using:

$$s = \frac{1}{M * N} \sum_m \sum_n \left[\frac{I_{(m,n)} - mean}{StDev} \right]^3 \tag{3.5}$$

where $M*N$ is the number of pixels[34].

Kurtosis

Kurtosis is a measure of whether the data is peaked or flat relative to a normal distribution. Data sets with high kurtosis tend to have a distinct peak near the mean, decline rather rapidly, and have heavy tails. Kurtosis is calculated by using

$$k = \frac{1}{M * N} \sum_m \sum_n \left[\frac{I_{(m,n)} - mean}{StDev} \right]^4 - 3 \tag{3.6}$$

where *N* is the number of pixels[34].

Brightness energy

A bright image will have more energy than a dark image. The formula of brightness energy is[9]:

$$BrightnessEnergy = \frac{1}{M * N} \sum_m \sum_n I_{(m,n)}^{\ 2} \tag{3.7}$$

where *M* is the number of row and *N* is column's number of an image, therefore I is the image intensity in *m* row and *n* column.

Colour energy

How color levels are distributed is measured by gray/colour energy[17].

$$ColourEnergy = \sum_{g=0}^{L-1} \left[I_{(m,n)} \right]^2 \tag{3.8}$$

If the gray/colour energy is high, it means that the number of gray levels in the image is few, that is, the distribution is concentrated in only a small number of different gray levels.

Entropy

Assuming an information source with *n* possible symbols *x* and that symbol *i* will occur with probability $p(x_i)$ then the entropy associated with the source of the symbols *X* is defined, in general, as:

$$H(x) = -\sum_{i=1}^{n} p(x_i)\log(p(x_i)) \tag{3.9}$$

where entropy is measured in bits/symbol[34].

If an image is thought of as a source of symbols, or grey levels, then entropy is the measure of information content of an image[34]. The entropy of an image in this research is measured by:

a. **zero-order entropy**,

$$H(0) = \log_2 N_i \tag{3.10}$$

where N_i is the different number of pixels. The zero order entropy is $\log_2$ of different values of pixels or average number of bits required to represent one pixel[13].

b. **first-order entropy**,

$$H(1) = -\sum_{i=1}^{n} P_i \log_2 P_i \quad \text{. bits/pixel [34]} \tag{3.11}$$

c. **second-order entropy**,

$$H(2) = -p(i,j) * \log_2 p(i,j) \tag{3.12}$$

where *p(i,j)* denotes the probability that a pixel has value *i* while its neighbouring pixel has value *j*[13].

3.2.2 Image Gradient

Image gradient is a measure of image edge strength and orientation. An edge is defined by a change in colour level. This change of colour level in an image is big near an edge and small in areas where the grey level is regular. Image gradient can be used to provide an indication of how busy the image is in terms of edges. Saha and Vemuri [10]defined image gradient as:

$$IAM=\frac{1}{M*N}\left[\sum_{i=1}^{M-1}\sum_{j=1}^{N}\left|I(i,j)-I(i+1,j)\right|-\sum_{i=1}^{M}\sum_{j=1}^{N-1}\left|I(i,j)-I(i,j+1)\right|\right] \quad (3.13)$$

where *I(i,j)* is the values of the image at *i* row and *j* column. *M* is the number of row and *N* is the number of column of an image.

3.2.3 Spatial Frequency

An additional characteristic used to analyse the sample images is the spatial frequency (SF) in the spatial domain [12]. SF is the mean difference between neighbouring pixels and it indicates the overall activity in an image. It is defined as:

$$SF=\sqrt{\left[\frac{1}{M*N}\sum_{i=1}^{M}\sum_{j=1}^{N}(I_{i,j}-I_{i,j-1})^2\right]+\left[\frac{1}{M*N}\sum_{i=1}^{M}\sum_{j=1}^{N}(I_{i,j}-I_{i-1,j})^2\right]} \quad (3.14)$$

where *I(i,j)* is the values of the image at *i* row and *j* column. *M* is the number of row and *N* is the number of column of an image.

3.2.4 Spectral Flattness Measure

The spectral flatness measure (SFM) of a digital image is defined as:

$$SFM(\Theta) = \frac{\left[\prod_{i=0}^{M-1}\prod_{j=0}^{N-1}\left|I(i,j)\right|^2\right]^{\frac{1}{M*N}}}{\frac{1}{M*N}\sum_{i=0}^{M-1}\sum_{j=0}^{N-1}\left|I(i,j)\right|^2} \qquad (3.15)$$

where *ΠΙ(k,l)* refers to the Fourier coefficients[13].

The SFM provides an indication of the overall activity of a digital image. A digital image with a SFM of 1 indicates that all the pixels have the same value, except one. A lower SFM indicates that the energy of image is concentrated in fewer coefficients. Sprljan [35] cited that if an image has a flat or near-flat spectrum then the quality of any prediction will be poor.

Original Image	R Image	G Image	B Image
	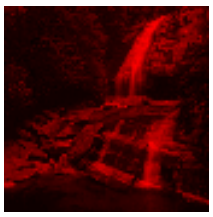		
range	254	255	255
mean	62.4896	65.1429	48.8272
median	45	53	29
diff	17.4896	12.1429	19.8272
st dev	47.5969	48.7158	54.4079
variance	2265.4658	2373.2261	2960.2145
coeff. variance	0.76168	0.74783	1.1143
skewness	1.4337	1.2024	1.7882
kurtosis	1.6993	1.5069	2.8838
brightness energy	6170.3767	6616.7851	5344.2687
color/gray energy	0.010135	0.0079752	0.013107
Zero-order entropy	7.9944	8	8
1st-order entropy	7.0812	7.2774	6.9448
2nd-order entropy	6.3701	6.4999	6.2415
Image Gradient	20.718	22.0276	20.9735
Spatial Frequency	23.1655	24.2089	24.0974
Spectral Flatness Measure	0.011051	0.010993	0.013272

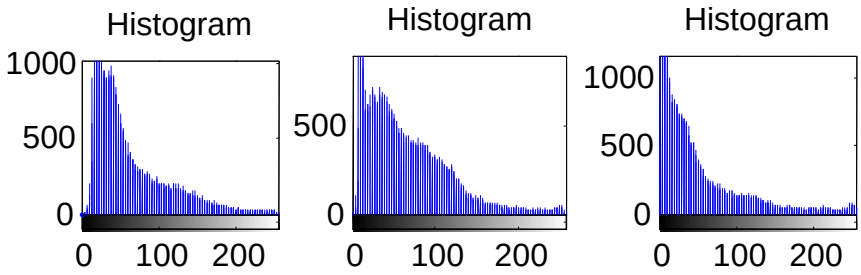

Figure 3.8 An example of the image features evaluated.

3.3 Colour Image Compression using Wavelet Codec

The block diagram of wavelet-based colour image lossy compression is represented in Figure 3.7. The first step of the system is transforming the RGB image to the YCrCb image. Discrete wavelet transform using various wavelets is applied in the next step. After the image was transformed, quantization and coding are carried out. After that the decompression process is executed. The original image is then compared with the compressed image to obtain the compression ratio.

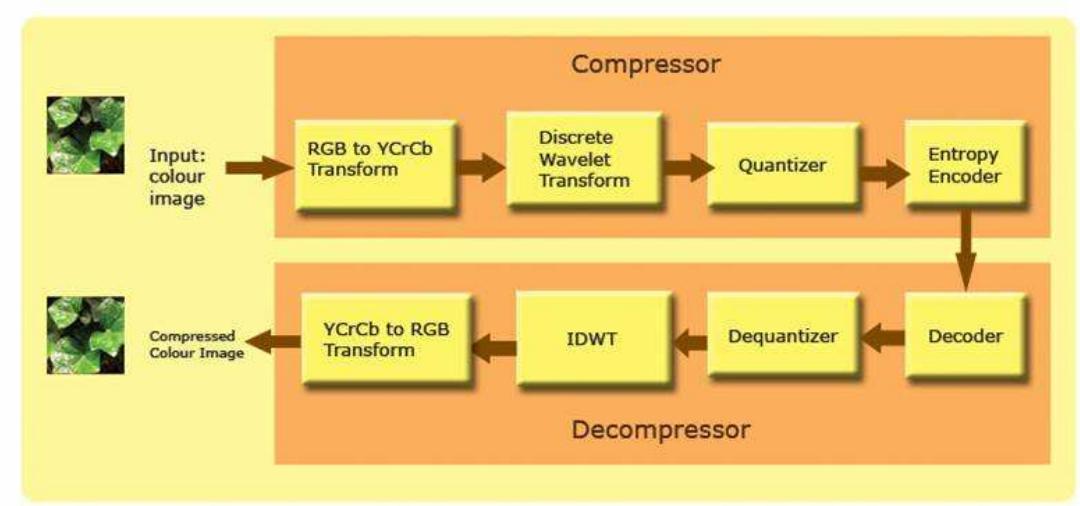

Figure 3.9 Diagram of wavelet-based colour image codec.

Quantization

Quantization refers to the process of approximating the continuous set of values in the image data with a finite set of values. The input to a quantizer is the original data, and the output is one among a finite number of levels. The quantizer is a function whose set of output values are discrete, and usually finite. This is a process of approximation, and a good quantizer is one which represents the original signal with minimum loss or distortion.

There are two types of quantization - Scalar Quantization and Vector Quantization. In scalar quantization, each input symbol is treated separately in producing the output,

while in vector quantization the input symbols are clubbed together in groups called vectors, and processed to give the output. This research uses the scalar quantization compare to the vector quantization that has increased computational complexity. Scalar quantization evaluates data by rounding or truncating individual values, so this is simpler in calculation. However, vector quantization is achieved by using of a *codebook* that contains a fixed set of vectors, and storing the index (address) into the codebook. Vector quantization become complex and requires many computational resources, such as memory and computational per pixel in order to efficiently construct and search a codebook. Vector quantization has simple decompression, but complex compression [14][18].

Entropy Coder using Huffman Coder

After the data has been quantized into a finite set of values, it can be encoded using an Entropy Coder to give additional compression. By entropy, we mean the amount of information present in the data, and an entropy coder encodes the given set of symbols with the minimum number of bits required to represent them.

Two of the most popular entropy coding schemes are Huffman coding and Arithmetic coding, and this study uses the Huffman coding. Huffman coding developed by D. A. Huffman is a classical data compression technique. It has been used in various applications including image compression.

Various wavelets are used to compress images to investigate the coding performance. Peak signal-to-noise ratio (PSNR) compression ratio (CR) and bits-per-pixel (bpp) are the parameter for comparing the coding performance.

For image compression, the most commonly measure that is used is the standard peak signal-to-noise ratio PSNR, defined [36] as

$$PSNR = 10 * \log_{10}(2^B - 1)^2 / MSE \tag{3.16}$$

for this research, the images have 256 * 256 size, so the PSNR become

$$PSNR = 10 * \log_{10}(255^2 / MSE) \tag{3.17}$$

$$MSE = \frac{1}{M*N} \sum_{m}^{M} \sum_{n}^{N} [I_{(m,n)} - \hat{I}_{(m,n)}]^2 \tag{3.18}$$

where M and N are the row and column of the image respectively. I is the original image and $\hat{I}$ is the compressed image.

However, the PSNR of a colour image with red, green and blue components is mentioned by [36]

$$PSNR = 10 * \log_{10} \left\{ \frac{255^2}{\left[\frac{MSE(red) + MSE(green) + MSE(blue)}{3} \right]} \right\} \tag{3.19}$$

A high value of PSNR is good because it means that the signal-to-noise ratio is high which means less error in the image. In image compression, the 'signal' is the original image, and the 'noise' is the error in reconstruction. The PSNR is expressed in decibel (dB). Good reconstructed images typically have PSNR values of 30 dB or more[36].

Image compression involves reducing the size of image data, while retaining necessary information. The reduced file is known as the compressed file. Compression ratio is defined by[17]:

$$CR = \frac{Uncompressed \quad file \quad size}{Compressed \quad file \quad size} \tag{3.20}$$

.

An alternative way to state the compression is to use the terminology bits-per-pixel, which is defined by[17]:

$$bpp = \frac{No.\ of\ bits}{No.\ of\ pixels} \tag{3.21}$$

Wavelet Filters Used

Wavelet filters used in this thesis are Haar, daubechies two, daubechies four, biorthogonal 4.4, biorthogonal 6.8, coiflets 4 and symlet 4 that are taken from the Matlab toolbox. The wavelets used in the research are `haar`, `db2`, `db4`, `bior4.4`, `bior6.8`, `coif4`, and `sym4` respectively. The first, second, third, fourth and fifth level decompositions can be used in image compression. However, all wavelet used here are applied in fifth level decomposition. It is chosen because the higher level of decomposition gives higher the image quality (PSNR). From the third level of decomposition, the image quality is better [37].

The wavelet names 'db*N*', 'bior*N*r.*N*d', 'coif'*N*', and 'sym*N*' are short names for daubechies, biorthogonal, coiflets and symlets. The *N*, *N*r, and *N*d are the order and they are integers. *N* is known as the length of support.

Haar wavelet is the simplest wavelet filter bank, so any explanation of wavelets begins with Haar wavelet, the first and simplest. Haar wavelet is discontinuous, and looks like a step function. It represents the same wavelet as Daubechies db1. Figure 3.8 shows the wavelet function of Haar wavelet [38].

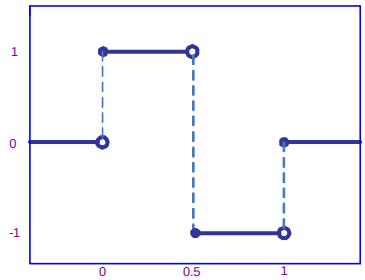

Figure 3.10 Wavelet function of `haar` wavelet[22].

The orthogonal wavelets that contructed by Daubechies are used here. In the Matlab, the names of the Daubechies family wavelets are written dbN, where N is the order, and db the "family name" of the wavelet. The db1 wavelet, as mentioned above, is the same as Haar wavelet. Figure 3.9 represents the wavelet functions of the db2 and db4:

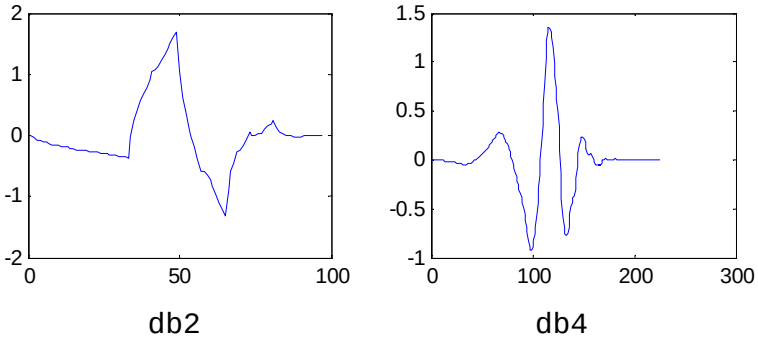

Figure 3.11 The wavelet functions of the `db2` and `db4` [39].

Biorthogonal family of wavelets exhibits the property of linear phase, which is needed for signal and image reconstruction. By using two wavelets, one for decomposition (on the left side) and the other for reconstruction (on the right side) instead of the same single one, interesting properties are derived. The wavelet function of biorthogonal 4.4 and 6.8 are shown in Figure 3.10.

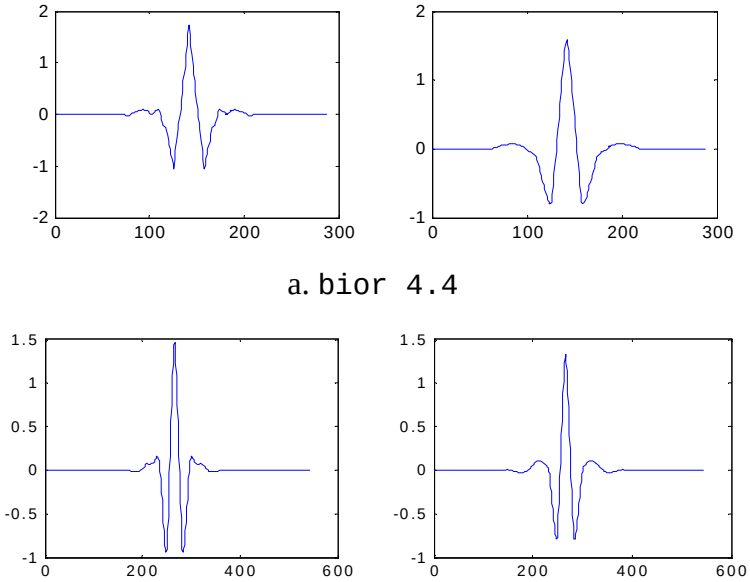

Figure 3.12 The wavelet function of biorthogonal 4.4 and 6.8[39].

The Coiflet wavelet function has 2N moments equal to 0 and the scaling function has 2N-1 moments equal to 0. The two functions have a support of length 6N-1. The symlets are nearly symmetrical wavelets proposed by Daubechies as modifications to the db family. The properties of the two wavelet families are similar. Figure 3.11 shows the wavelet function of coiflet 4 and symlet 4 that are used in this study.

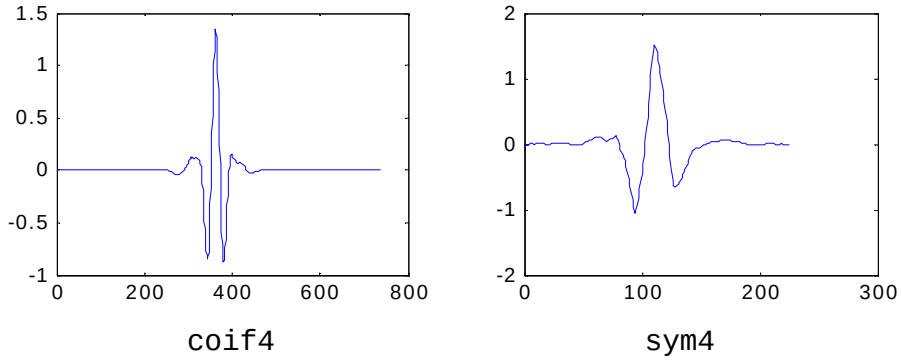

Figure 3.13 The wavelet function of `coiflet 4` and `symlet 4` [40].

These wavelet filters applied as the transform in the compression, therefore the performance of each wavelet can be evaluated based on the PSNR, CR and bpp values. Because various classes of images have different characteristic, the wavelets give different compressed image for each image.

3.4 Correlation Coefficients between Image Features and Wavelet Codec Performance

Correlation coefficients between image features and PSNR-CR-bpp are evaluated to find the relationships between them. The coefficient of correlation (r) between the image statistic of each colour component and coding performance measure is computed using the following definition:

$$r_{xy} = \frac{\sum x_i y_i - n\bar{x}\bar{y}}{(n-1)s_x s_y} = \frac{n\sum x_i y_i - \sum x_i \sum y_i}{\sqrt{n\sum x_i^2 - (\sum x_i)^2}\sqrt{n\sum y_i^2 - (\sum y_i)^2}} \qquad (3.22)$$

where $\bar{x}$ and $\bar{y}$ are the sample means of X and Y, s_x and s_y are the sample standard deviations of X and Y and the sum is from $i = 1$ to n.

The relation between two or more variables can be viewed by coefficient correlation measure. The r between the image features and coding performance indicates the strength of the relationship between the variables. A strong relationship or connection in which one variable affects or depends on the other will be indicated by a big r value. A weak correlation will indicate the contrary.

As there is no defined method for determining whether a connection is weak or strong, for this research a good negative correlation coefficients (R-square) is define as the absolute value greater than 0.5.

3.5 Non Parametric Statistical Test

It was determined that certain features (IAM and SF) have strong correlation with PSNR, CR and bpp [8-11][31][41] . However, this only a statistical association and cannot conclusively prove causality. For that reason, this research carried out a detailed investigation on the cause-effect relationship. The cause-effect study could help better understand which image characteristics affect the coding performance of a wavelet-based image compression system. It is envisaged that an adaptive wavelet-based compression system would be possible based on the image characteristics [9].

To investigate the effect of IAM and SF and wavelet based colour image codec, the hypothesis test is conducted. One of statistical purpose of a hypothesis test is to investigate the real effects of the population (images) from the effects computed from a sample (image used in this research) indicate.

Choosing the right test to compare measurements is a bit difficult, because there are two families of tests: parametric and nonparametric. Many statistical tests are based upon the assumption that the data are sampled from a Gaussian distribution. These tests are referred to as parametric tests. Tests that do not make assumptions about the population distribution are referred to as nonparametric tests.

Nonparametric tests are sometimes called *distribution free* statistics because they do not require that the data fit a normal distribution. Nonparametric statistics are methods of hypothesis testing and estimation that require less restrictive assumptions about the normality of data [42].

There are two types of statistical tests, which are parametric and nonparametric statistic. Parametric statistics are used for normally distributed *variables*. In this research, v*ariables* are images that we measure, control, or manipulate.

Figure 3.12 and 3.13 show the data set distribution of IAM and SF. From these figures can be seen that both IAM and SF distribution are not Gaussian or normal distribution. This study refers to use nonparametric method because the IAM and SF of images data in this study is not a normal distribution data, so non parametric test is suitable for testing.

All commonly used nonparametric tests rank the outcome variable from low to high and then analyze the ranks. These tests include the Wilcoxon, Mann-Whitney test, and Kruskal-Wallis tests, Friedman test, Spearman correlation, and nonparametric regression. These tests are also called distribution-free tests.

Kruskal-Wallis test and Friedman test are suitable for comparing three or more groups[43]. Kruskal-Wallis test and Friedman test are two type of nonparametric statistical test that are investigated in this research.

Statistical analysis of PSNR-IAM, PSNR-SF, CR-IAM, CR-SF, bpp-IAM and bpp-SF were computed. The Kruskal-Wallis and Friedman's statistical tests are applied to test the results obtained.

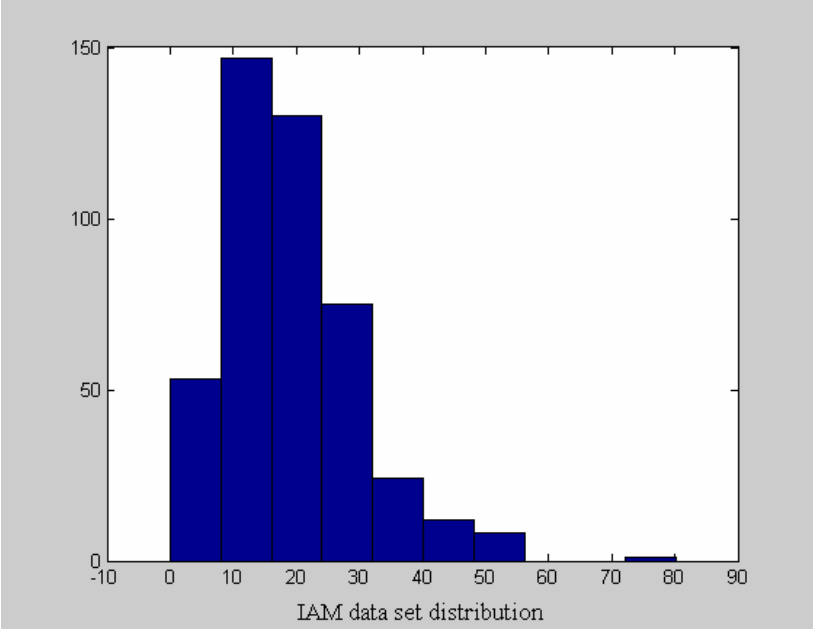

Figure 3.14 The IAM data set distribution.

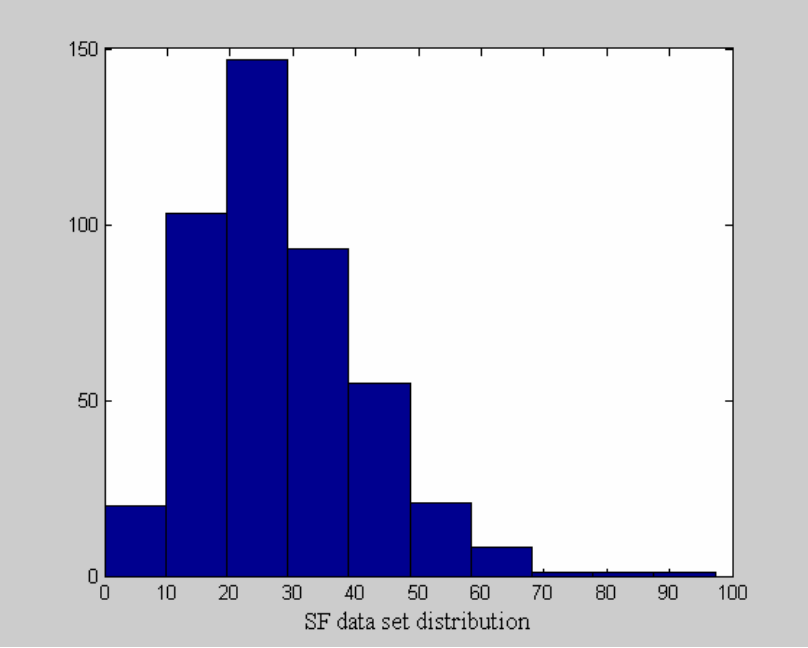

Figure 3.15 The SF data set distribution.

Kruskal-Wallis Test

Kruskal-Wallis is a nonparametric method for testing equality of population medians among groups. In this study, the term “factor“ in the test is the type of wavelet, so by Kruskall-Waliss test, the PSNR, CR and bpp value are tested separately for each kind wavelet.

The method of the test is as follow[44].

1 Rank all data from all groups together; that is, rank the data from 1 to n ignoring group membership. Assign any tied values the average of the ranks they would have received had they not been tied.

2 The test statistic is given by:

$$KW = \frac{12}{n(n+1)} \sum_{i=1}^{k} n_i (\overline{R_i} - \overline{R})^2 \qquad (3.23)$$

where

1 k = number of samples (groups)

2 n_i = number of observations for the i-th sample or group

3 n = total number of observations (sum of all the n_i)

4 $\overline{R_i}$ = sum of ranks for group i

$\overline{R}$

6) = average of R_i.

An example can illustrate the calculation in the Kruskal-Wallis test. Table 3.1 shows these measures for each subject in each of the three groups (A, B and C). Thus, the measures that appear in the following table on the left are replaced by their respective ranks, as shown in the table on the right.

Table 3.1 An example for for Kruskal-Wallis test.

Raw Measures			Ranked Measures			
A	B	C	A	B	C	
6.4	2.5	1.3	11	2	1	A, B, C Combined
6.8	3.7	4.1	12	3	4	
7.2	4.9	4.9	13	5.5	5.5	
8.3	5.4	5.2	17	8	7	
8.4	5.9	5.5	18	10	9	
9.1	8.1	8.2	19	14	15.5	
sum of ranks			90	43.5	42	175.5
average of ranks			15	7.25	7	9.75

The squared deviate for any particular group mean is equal to the squared difference between that group mean and the mean of the overall array of data, multiplied by the number of observations on which the group mean is based. Thus, for each of our current three groups.

Table 3.2 The squared deviate for the example.

A: $6(15—9.75)^2 = 165.375$

B: $6(7.25—9.75)^2 = 037.5$

C: $6(7—9.75)^2 = 045.375$

$\sum_{i=1}^{k} n_i(\overline{R_i} - \overline{R})^2 = 248.25$

Then, the Kruskal-Wallis value can be calculated by:

$$KW = \frac{12}{n(n+1)} \times 248.25 = 8.710526$$

And then, treating this result as though it were a value of chi-square, we can refer it to the sampling distribution of chi-square with df=3—1=2. The following graph, shows the outlines of this particular chi-square distribution. In brief: by the Kruskal-Wallis test, the observed aggregate difference among the three samples is significant a bit beyond the .01 level.

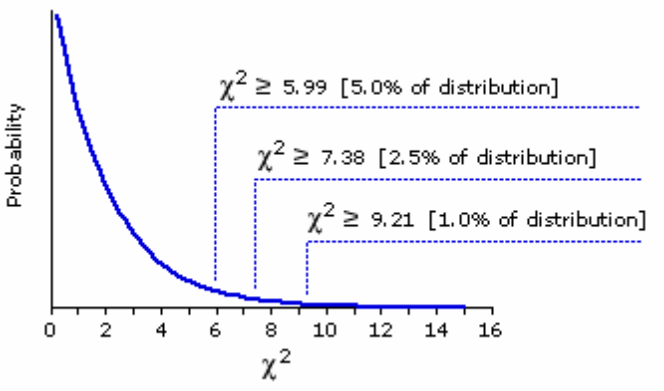

Figure 3.16 Theoretical Sampling Distribution of Chi-Square for df=2

Friedman Test

Friedman's test is also a nonparametric test used to identify differences in treatments across multiple test attempts. The procedure involves ranking each row (or *block*) together, followed by considering the values of ranks by columns. The Friedman test is used for two-factor repeated measures analysis of variance by ranks. In its use of its ranking is similar to the Kruskal-Wallis one-factor analysis of variance by ranks. This test used to compare column effects in a two-way layout. The tests only for column effects after adjusting for possible row effects. The test is based on an analysis of variance using the ranks of the data across categories of the row factor.

Methods of Friedman's test are[44]:

a. The test evaluates $\{x_{ij}\}_{n\times k}$ whether *k*-paired samples, each with *n treatments* (*n* rows and *k* columns), are from the same population or from populations with

continuous distributions and the same median. The variable being tested must be at least of ordinal type.

b. The test procedure starts by assigning natural ordered ranks from 1 to *k* to the matched case values in each row, from the smallest to the largest. Tied ranks are substituted by their average.

The test statistic is:

$$F_r = \frac{12\sum_{i=1}^{k} R_i^2 - 3n^2k(k+1)^2}{nk(k+1)}, \quad (3.24)$$

where *Ri* = the sum of ranks for sample *i.*

The purpose of this study is to establish that gradient and spatial frequency is the cause effect of PSNR, CR and bpp. To implement Kruskal-Wallis test, the data *x* of PSNR, CR and bpp are arranged in table or matrix with the columns are the various intervals of image gradient and SF.

IAM or SF interval

$$\begin{bmatrix} x_{11} & x_{21} & x_{31} & x_{41} & x_{51} \\ x_{12} & x_{22} & x_{32} & x_{42} & x_{52} \\ . & . & . & . & . \\ . & . & . & . & . \\ x_{145} & x_{245} & x_{345} & x_{445} & x_{545} \end{bmatrix}$$

Figure 3.17 Matrix modeling for Kruskal-Wallis test analysis.

In using Friedman's test, the columns are the various intervals of image gradient and SF. The matrix shown in Figure 3.16 illustrates the format for a set-up where column factor IAM or SF interval has five levels, row factor wavelet kind has two levels, and there are forty-five replicates (reps=45). The subscripts indicate row, column, and replicate, respectively. The values of *x* are PSNR, CR or bpp that tested.

IAM or SF interval

45 repicates for each wavelet

$$\begin{Bmatrix} \begin{bmatrix} x_{111} & x_{121} & x_{131} & x_{141} & x_{151} \\ x_{112} & x_{122} & x_{132} & x_{142} & x_{152} \\ . & . & . & . & . \\ x_{1145} & x_{1245} & x_{1345} & x_{1445} & x_{1145} \end{bmatrix} \\ \begin{bmatrix} x_{211} & x_{221} & x_{231} & x_{241} & x_{251} \\ x_{211} & x_{221} & x_{231} & x_{242} & x_{252} \\ . & . & . & . & . \\ x_{2145} & x_{2245} & x_{2345} & x_{2445} & x_{2545} \end{bmatrix} \end{Bmatrix}$$

Figure 3.18 Matrix modeling for Friedman test analysis.

Kruskal-Wallis and Friedman test return the p-value for the null hypothesis that the column (the IAM or SF intervals) effect to the PSNR, CR and bpp equals to 0. The null hypothesis is the PSNR, CR and bpp are identical for different IAM and SF groups. If the p-value is next to zero, this casts reject on the null hypothesis. A satisfactorily small p-value suggests that at least one column-sample median is significantly different from the others; that is, there is a main effect due to factor of image gradient or spatial frequency.

The selection of a critical p-value to establish whether a result is "statistically significant" is researcher arbitrary. It is common to state a result significant if the p-value is less than 0.05 or 0.01. But those classifications represent is only arbitrary conventions that are only informally based on general research experience[45].

The 450 random selected images have different IAM and SF values. For IAM to PSNR, the tests are conducted for each colour component IAM. The IAM values are divided in 5 interval values for each colour component. The test for IAM to CR and bpp are also conducted using interval. Therefore the test for SF to PSNR, CR and bpp are carried out in that way as well. In this research, 45 images are used as a sample that represents image population in IAM and SF interval. For this reason this work can not use all of 450 images but 45 images for each red, green, blue IAM and SF interval. If every test using 5 intervals, there are 225 images involve statistical test, perhaps different images randomly taken from the 450 images.

Figure 3.17 shows the diagram of the cause-effect test of certain image characteristics which affect the coding performance of a wavelet-based image compression system.

3.6 Neural Network

An Artificial Neural Network (ANN) is an information processing paradigm that is encouraged by the way biological nervous systems, such as the brain, process information. ANNs, like people, learn by example. An ANN is configured for a specific application, such as pattern recognition or data classification, through a learning process. Learning in biological systems involves adjustments to the synaptic connections that exist between the neurones. A highly important property in neural network is nonlinearity, it is appropriate for the problem in this study, because there is no linear relationship between the input and output.

Input-output mapping describes the popular paradigm in neural network, namely learning involves modification of the synaptic weights. In learning there is training samples process that can reaches a steady state where there are further significant changes in the synaptic weights[27].

A neuron is a processing unit in a neural-network. It is a node that processes all fan-in from other nodes and generates an output according to a transfer function called the activation function. The activation function used here are sigmoid functions (logarithmic and tanh) and denoted by *f(.).* A neuron is linked to other neurons by variable synapses (weights)[46].

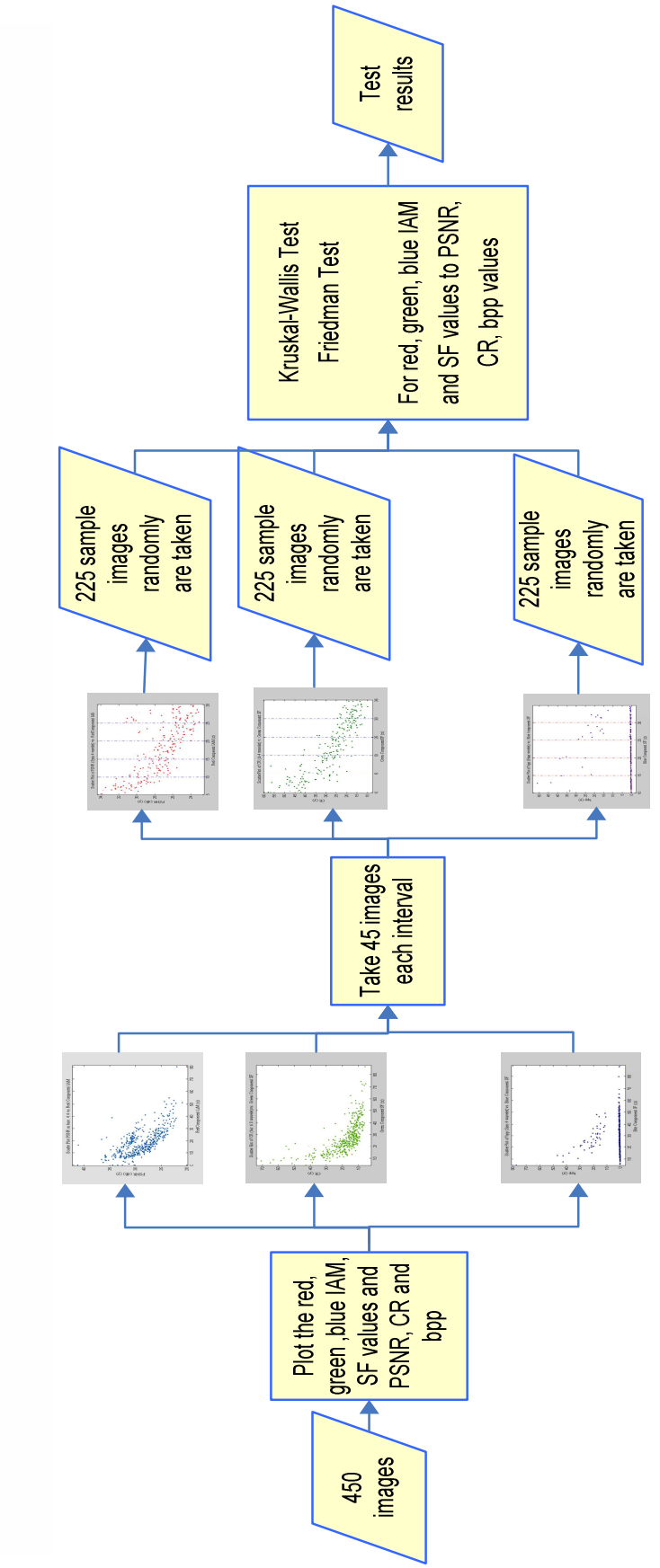

Figure 3.17 Diagram of non parametric statistical test implementation.

Figure 3.18 illustrates the simple neuron model. The output of the neuron is given by:

$$net = \sum_{i=1}^{m} w_i x_i - \theta \tag{3.26}$$

$$y = f(net) \tag{3.27}$$

where x_i is the ith input, w_i is the link weight from the ith input, θ is a threshold or bias, and m is the number of inputs. The activation function $f(.)$ is usually some continuous or discontinuous function.

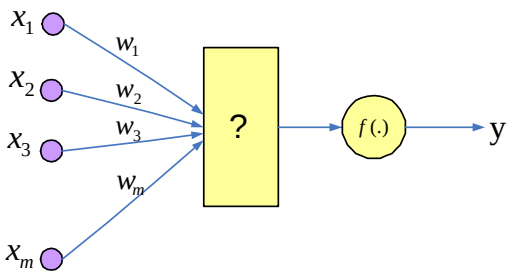

Figure 3.20 Mathematical model of neuron.

The sigmoid function is usually used in MLP. Two sigmoid functions are logistic and hyperbolic tangent function defined in Equation (3.28) and (3.29). Both approaches are used in this research; the curves of both sigmoid functions are graphed in Figure 3.19.

$$f(v) = \frac{1}{(1+\exp(-av))} \quad a>0 \text{ and } -\infty < v < \infty \tag{3.28}$$

$$f(v) = a\tanh(bv) \quad (a,b) > 0 \tag{3.29}$$

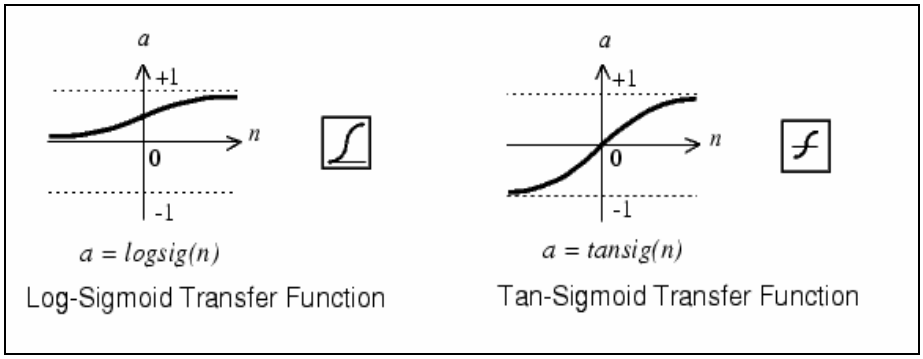

Figure 3.21 Graphic of two sigmoid functions [46]

Learning Method

It is not an easy task to decide which training algorithm will be the fastest for a given problem and it will depend on many factors, which includes the complexity of the problem, the number of data points in the training set, the number of weights and biases in the network, the error goal, and whether the network is being used for pattern recognition (discriminant analysis) or function approximation (regression).

The Levenberg-Marquardt algorithm is very efficient for training small to medium-size networks and very successful for nonlinear least-squares optimization problems[46]. The Levenberg-Marquardt (LM) algorithm is the most widely used optimization algorithm, and this is used in this research.

Neural Network Implementation

Back propagation is a specific technique a multilayer feedforward network. In back propagation learning, the training process usually is started to compute the synaptic weight of MLP. One of the mayor advantages of neural network is their ability to generalize. This means that a trained network could classify data from the same class as the learning data that it has never seen before [27]. In real world applications developers normally have only a small part of all possible patterns for the generation of a neural network. To reach the best generalization, the dataset should be split into two parts:

a. The training set is used to train a neural net. The error of this dataset is minimized during training.
b. A testing set for finally checking the over all performance of a neural net.

For the purpose of the neural network implementation the images used are separated into two sets of images. The first set, consisting of 80% of the total images are used as training data and the remaining 20% are used as the testing data. The training data consists of 360 images and the testing data consists of 90 images. The training data set is used in network design; however the testing data set is used to see generalization ability of the network designed. The generalization is computed by evaluate the network's accuracy on testing data set.

Figure 3.20 shows the neural network implementation for adaptive wavelet based codec development.

accuracy of each topology can be evaluated. The results from the simulation are compared to target values. When the result equal to the target, the accuracy of test = 1, otherwise = 0. The accuracy of N number of test run is defined as:

$$A_{total} = \frac{1}{N}\sum_{i=1}^{N} A_{test(i)} \quad . \tag{3.30}$$

The accuracy value is used to measure the performance of the network. A better neural network topology has higher testing accuracy.

The number neuron of input layer is static (6 neurons), these comes from the IAM and SF of red, green and blue image component. The one hidden layer and two hidden layers are applied in this research. The numbers of neuron for hidden layer are 4, 5, 6, 10, 12, 13, 15, 16, 17, 18, 23, 25, 27, 35 and 45. For output neuron is both 1 and 8. The wavelet names are coded in number 1, 2, 3 .. to 8 for one neuron output layer. The codes are also changed in 8 digit number (using 1 and 0) to make sure the output is desired result. Therefore it can be executed for 8-output at the network. The code of the wavelet can be changed in digital form as shown in Table 3.3.

Table 3.3 1 to 8 digit wavelet code.

1 digit wavelet code	8 digit wavelet code
1	10000000
2	01000000
3	00100000
4	00010000
5	00001000
6	00000100
7	00000010
8	00000001

Many multi layer perceptron (MLP) topologies are investigated to get the weights of the network. The systems are simulated on the training and testing data set. The

There are no standard to decide how many number of hidden layer and neuron to be used. A useful guide to the maximum number of layers comes from a theorem put forward in 1957 by the Soviet mathematician A. N. Kolmogorov. This theorem states effectively that a three layer perceptrons with $n(2n+1)$ nodes using continuously increasing non-linearities can compute any continous function of n variables. Previous researches have also shown that three layers are sufficient[47]. Even though Picton cited that only three layers are needed, in this research, three layers and four layers are applied.

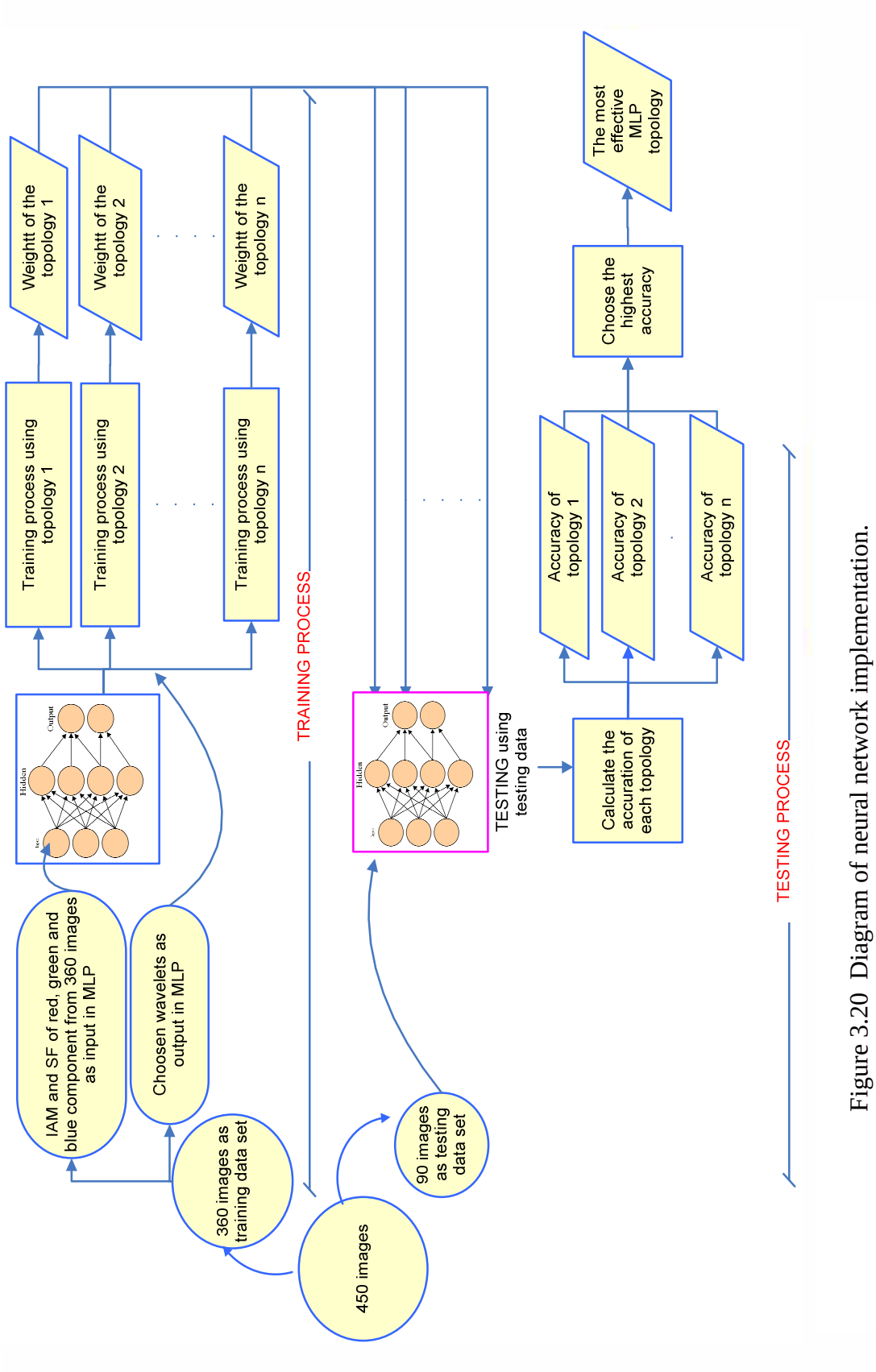

Figure 3.20 Diagram of neural network implementation.

The MLP topologies that used in this research are listed in the Table 3.4.

Table 3.4 MLP topologies used in the research.

One hidden layer – eight output neurons topologies	Two hidden layers – eight output neurons topologies
6-4-8	6-13-15-8
6-5-8	6-13-18-8
6-6-8	6-13-21-8
6-10-8	
6-12-8	
6-13-8	
6-15-8	
6-16-8	
6-18-8	
6-20-8	
6-23-8	
6-35-8	

After the all of various MLP topologies accuracies are evaluated, choosing the most effective MLP topology for adaptive wavelet based codec for colour image compression. The topology that has the highest accuracy and lest number of neuron, is considered as the most effective design for the system.

3.7 Summary

This chapter has shown the methodology of this research to develop adaptive wavelet based colour image compression using neural network. The neural network is developed based on the colour image characteristics. The data samples used in this research consist of 256x256 size 450 colour images. The images are classified in two categories, namely natural and synthetic image.

The histogram image features that are evaluated in this research are range, mean, median, different (mean-median), standard deviation, variance, coefficient variance, skewness, kurtosis, brightness energy [23], gray/color energy, zero-order entropy, first-order entropy, second-order entropy. The spatial characteristics explored include image gradient[8], spatial frequency (SF) [12]and spectral flatness measure (SFM)[35]. Those features of three colour components (red, green and blue) are evaluated.

All images are compressed by wavelet codec using several wavelet types. The PSNR, CR and bpp values are calculated. Coefficient correlations between all features and the PSNR, CR and bpp are also evaluated. The initial results show there are strong correlation between certain features (image gradient and spatial frequency) and the wavelet codec performance (PSNR, CR and bpp).

Statistical test is needed to understand the cause effect of image gradient (IAM) and spatial frequency (SF) to the PSNR, CR and bpp values. Kruskal-Wallis test and Friedman test are used to establish the causal effect relation of IAM and SF to PSNR, CR and bpp. That means those features can be used as the input into a neural network system.

MLP Neural Network is used in this research. The input is the IAM and SF of three colour components and the output is the chosen wavelet type. Several topologies are implemented to select the optimum network design.

CHAPTER 4

RESULT AND DISCUSSION

In this chapter, the results from the experiments are analyzed and explained. The main aim of the study is to identify the relationship between characteristics of the colour image and the coding performance. It is envisage that the study can help identify the features that influence the wavelet based colour image compression.

Another concern of this research is to establish, which wavelet filter is best suited to compress different types of images. The result from the previous study can be used as the input for deciding the wavelet type. Certain image features will be used to determine the most effective wavelet that used in different types colour images compression. This study utilizes neural network as the learning process to identify the image characteristics and the coding performance relationship.

4.1 Image Features Evaluation

The image features that are evaluated in this study consist of statistical image features such as range, mean, media, standard deviation, variance, coefficient variance, skewness, kurtosis, brightness energy, gray/color energy, zero-order entropy. 1st-order entropy, 2nd-order entropy and others features like image gradient, spatial frequency and spectral flatness measure.

Table 4.2 Image features in red part of images.

	bear	cactus	Two	sulawesi	tulip	mars	bugs	smile	walt
				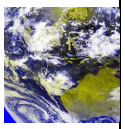			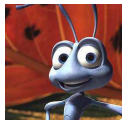		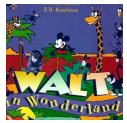
range	255	252	255	255	250	255	199	247	255
mean	117.94	138.4	73.45	130.07	142.02	76.12	144.9	216.87	98.53
median	108	140	47	129	154	91	140	254	73
stand deviation	64.77	55.89	65.02	65.92	53.99	70.71	36.92	62.11	76.83
variance	4195.1	3123.2	4227.8	4344.9	2914.8	5000.5	1363.4	3858.2	5902.5
coef. Variance	0.55	0.4	0.89	0.51	0.38	0.93	0.25	0.29	0.78
Skewness	0.29	-0.06	0.8	0.06	-0.35	0.17	0.11	-1.52	0.75
Kurtosis	-0.85	-1.04	-0.61	-1.02	-0.83	-1.4	-0.83	0.95	-0.55
brightness energy	18105	22277	9623	21263	23084	10794	22358	50892	15611
color energy	0.0045	0.0049	0.0076	0.0043	0.0057	0.1667	0.0088	0.2328	0.0095
zero-order entropy	8	7.98	8	8	7.97	8	7.61	7.86	8
1st-order entropy	7.9	7.74	7.46	7.9	7.64	5.34	7.09	4.47	7.34
2nd-order entropy	6.78	7.18	6.2	7.2	6.61	4.13	5.89	3.55	6.53
Image gradient	18.4	38.74	13.81	35.81	19.32	6.18	10.28	15.31	31.4
Spatial frequency	19.02	40.77	21.15	38.03	23.56	9.41	13.11	27.38	43.47
Spectral Flatness Measure	0.002	0.0104	0.0042	0.0069	0.0021	0.0009	0.0008	0.0007	0.0118

Table 4.2 Image features in green part of images.

	bear	cactus	Two	sulawesi	tulip	mars	bugs	smile	walt
				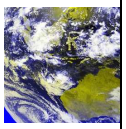					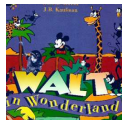
range	254	252	255	255	255	255	208	247	255
mean	83.25	129.56	53.45	130.12	117.63	57.36	146.74	210.47	95.41
median	66	128	35	129	105	78	151	254	80
stand deviation	64.59	48.78	51.88	66.39	66.21	50.97	45.3	63.09	64.91
variance	4171.5	2379.1	2691.1	4407.6	4383.8	2598.2	2052.4	3980.1	4213.7
coef. Variance	0.78	0.38	0.97	0.51	0.56	0.89	0.31	0.3	0.68
Skewness	0.68	0.13	1.6	0.06	0.12	0.05	-0.12	-1.22	0.94
Kurtosis	-0.63	-0.72	2.25	-1.02	-1.45	-1.23	-1.48	0.22	0.18
brightness energy	11103	19166	5548	21339	18220	5889	23586	48277	13316
color energy	0.0057	0.0057	0.0098	0.0043	0.0054	0.1637	0.0116	0.2282	0.0088
zero-order entropy	7.98	7.98	8	8	7.98	7.99	7.67	7.88	8
1st-order entropy	7.68	7.6	7.13	7.91	7.69	4.84	6.88	4.65	7.41
2nd-order entropy	6.62	7.08	5.94	7.22	6.53	3.63	5.64	3.72	6.59
Image gradient	18.31	36.64	12.91	36.5	18.03	3.98	9.99	14.63	28.05
Spatial frequency	19.51	38.05	20.82	38.81	22.65	8.1	13.04	25.54	38.68
Spectral Flatness Measure	0.0033	0.0112	0.0071	0.0071	0.0027	0.0013	0.0007	0.0006	0.0123

Table 4.3 Image features in blue part of images.

	bear	cactus	Two	sulawesi	tulip	mars	bugs	smile	walt
				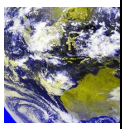					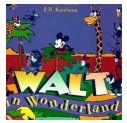
range	245	255	255	255	255	255	239	250	255
mean	73.09	100.94	50.55	130.31	102.32	37.63	142.82	213.46	99.33
median	55	99	25	130	49	55	127	254	112
stand deviation	62.86	56.38	59	70.92	89.28	34.43	63.3	71.15	60.97
variance	3951.2	3178.1	3480.9	5029.9	7970.5	1185.5	4006.8	5063	3717.5
coef. Variance	0.86	0.56	1.17	0.54	0.87	0.91	0.44	0.33	0.61
Skewness	0.78	0.4	1.74	-0.04	0.43	0.68	-0.07	-1.57	0.01
Kurtosis	-0.53	-0.25	2.18	-1.08	-1.65	2.33	-1.74	0.94	-0.96
brightness energy	9292.8	13366	6036.1	22010	18441	2601.6	24403	50629	13585
color energy	0.0078	0.0052	0.0129	0.0041	0.0089	0.1725	0.0146	0.2349	0.0079
zero-order entropy	7.94	8	8	8	7.99	7.97	7.86	7.97	8
1st-order entropy	7.48	7.73	6.92	7.97	7.15	4.1	6.71	4.33	7.42
2nd-order entropy	6.48	7.22	5.86	7.2	6.09	3.12	5.55	3.37	6.72
Image gradient	18.33	41.62	12.97	34.07	15.46	3.82	10.16	13.84	28.97
Spatial frequency	19.8	42.5	20	35.08	18.9	9.97	13.35	26.37	35.57
Spectral Flatness Measure	0.004	0.0201	0.0063	0.0067	0.0021	0.005	0.0007	0.0006	0.0119

The features of 450 images are evaluated in this research. Table 4.1, 4.2, and 4.3 show samples of the results of image statistics in the red, green, blue colour space respectively. Each table shows nine images that taken from nine categories.

Table 4.1 shows the image features in red part of nine images. For example, "bear.bmp" image is taken form animal (natural) images, "cactus.bmp" is taken from flower and plant (natural) images, "Two sons.bmp" is taken from people (natural) images, "sulawesi.bmp" is taken from satellite (natural) images, "tulip.bmp" is taken from scene (natural) images, "mars.bmp" is taken from space/telescope (natural) images, "bugs.bmp" is taken from computer generated (synthetic) images, "smile.bmp" is taken from cartoon limited colour (synthetic) images and "walt.bmp" is taken from cartoon many colour (synthetic) images. Table 4.2 and Table 4.3 show the image features in green and blue part of same images respectively.

4.2 Colour Image Compression using Wavelet Codec

The images are compressed using wavelet based codec. In this research, the fifth level decomposition wavelet is used. After the images are compressed using many wavelet types, the original and compressed image are compared. The performance indicators used are the peak-signal-to-noise ratio (PSNR), compression ratio (CR) and bit-per-pixel (bpp). PSNR is the most commonly used to evaluate the objective image compression quality[20].

To compare the compression result of different wavelets, other parameters are made fix. The following tables show the PSNR, CR and bpp of 10 samples from 450 images using various wavelets. Table 4.4 shows the PSNR values of 10 images, that is, "Big boy.bmp", "bird.bmp", "peppers.bmp", "ali.bmp", "cool.bmp", "map.bmp", "Alaska.bmp", "briere.bmp", "Saturn.bmp" and "surface.bmp" evaluated using haar, db2, db4, bior4.4, bior 4.8,

`coif4` and `sym4` wavelet. Table 4.5 and Table 4.6 illustrate the CR and bpp values of same images and same wavelet.

Table 4.5 PSNR values of 10 images by using different wavelets.

	Big boy	bird	peppers	ali	cool	map	alaska	briere	Saturn	surface
haar	28.07	34.28	26.52	27.50	25.72	22.26	27.78	22.29	33.31	26.05
db2	28.75	35.14	26.93	28.63	26.48	22.36	27.47	22.20	34.67	27.59
db4	28.86	35.04	26.90	27.94	26.53	21.87	27.55	21.98	35.21	26.47
bior 4.4	29.51	35.82	27.76	29.52	27.32	22.50	28.02	22.45	36.18	27.47
bior 6.8	29.52	35.69	27.52	29.58	27.27	22.52	28.24	22.11	36.29	26.85
coif4	28.79	35.01	27.32	28.74	26.76	22.34	28.16	22.15	35.42	26.49
sym4	28.89	35.58	27.23	28.82	26.74	22.15	27.47	21.89	35.41	26.72

Table 4.6 CR values of 10 images by using different wavelets.

	Big boy	bird	Peppers	ali	cool	map	alaska	briere	Saturn	surface
Haar	40.25	74.19	19.08	40.15	30.31	13.60	26.64	19.15	68.60	32.09
Db2	42.45	72.12	20.27	42.46	32.26	13.22	28.25	18.78	81.48	32.06
Db4	40.21	69.92	17.68	38.10	28.79	12.07	25.36	17.14	77.93	29.61
bior 4.4	40.61	65.65	17.01	37.61	29.11	11.93	26.97	16.99	77.65	29.28
bior 6.8	31.92	48.73	11.66	25.83	20.91	9.29	20.57	13.46	64.99	21.40
coif4	23.51	36.23	8.30	19.70	15.68	7.40	16.44	11.23	55.18	16.63
sym4	38.50	64.13	17.45	38.12	28.83	12.17	26.70	17.37	78.42	29.90

Table 4.7 bpp values of 10 images by using different wavelets.

	Big boy	bird	Peppers	ali	cool	map	alaska	briere	Saturn	surface
haar	0.199	0.108	0.419	0.199	0.264	0.588	0.300	0.418	0.117	0.249
Db2	0.188	0.111	0.395	0.188	0.248	0.605	0.283	0.426	0.098	0.250
Db4	0.199	0.114	0.452	0.210	0.278	0.663	0.315	0.467	0.103	0.270
bior 4.4	0.197	0.122	0.470	0.213	0.275	0.671	0.297	0.471	0.103	0.273
bior 6.8	0.251	0.164	0.686	0.310	0.383	0.861	0.389	0.594	0.123	0.374
coif4	0.340	0.221	0.964	0.406	0.510	1.081	0.487	0.712	0.145	0.481
sym4	0.208	0.125	0.458	0.210	0.277	0.658	0.300	0.461	0.102	0.268

Table 4.4 shows that the highest PSNR are attained when the `bior 4.4` or `bior 6.8` wavelet selected, however this is not enough to conclude that both wavelets are the most suitable for all colour image classes, natural and synthetic images. These initial results are also used as data for the next evaluation process.

Table 4.5 and 4.6 show that CR and bbp is a different parameter that used to measure image quality. The results indicate that a wavelet gives high PSNR value, but the CR and bpp values are not high. The results also show that it is not possible to get the highest PSNR, CR and bpp all simultaneously.

To determine which wavelet is the most appropriate wavelet for each image, this study will use PSNR, CR and bpp as the parameters. This study uses PSNR as the essential parameter in the wavelet selection. The reason is PSNR relate to image quality that human eye perceive. A wavelet that produces a high PSNR will be considered as the appropriate wavelet, even though the CR and bpp that are produced by a wavelet are not the highest values, as long as the CR and bpp values can be accepted.

4.3 Correlation Coefficients between image features and Wavelet Codec Performance

To understand how the image features influence the wavelet based colour image compression performance, the correlation coefficients between the colour image features and the PSNR, CR and bpp values are evaluated. Table 4.7. shows the correlation coefficient values between red component colour image characteristics and PSNR, CR and bpp of 50 images using different wavelets (`Haar, daubechies 2, daubichies 4, biorthogonal 4.4, biorthogonal 6.8, coiflet 4` and `symlet 4`). Therefore the correlation coefficient values between green component colour image characteristics and PSNR, CR and bpp of these images using different wavelets are shown in Table 4.8. Table 4.9 shows the evaluation result of the correlation coefficient values between blue component of 50 images. The 50 images used in these three tables are taken from people images category.

Table 4.7 Correlation coefficient values between red component colour image characteristics and PSNR, CR and bpp of 50 images using different wavelets.

	Haar			db2			db4			bior 4.4			bior 6.8			coif4			Sym4		
	PSNR	CR	bpp	PSNR	CR	bpp	PSNR	CR	bpp	PSNR	CR	bpp	PSNR	CR	bpp	PSNR	CR	bpp	PSNR	CR	bpp
range	-0.24	-0.34	0.24	-0.29	-0.28	0.21	-0.26	-0.28	0.22	-0.24	-0.27	0.22	-0.24	-0.21	0.19	-0.24	-0.17	0.17	-0.25	-0.29	0.22
mean	-0.17	0.11	-0.07	-0.15	0.09	-0.07	-0.20	0.13	-0.10	-0.16	0.19	-0.13	-0.17	0.30	-0.17	-0.21	0.36	-0.20	-0.19	0.16	-0.11
median	-0.16	0.08	-0.06	-0.15	0.07	-0.06	-0.21	0.11	-0.09	-0.17	0.16	-0.11	-0.18	0.25	-0.15	-0.21	0.31	-0.18	-0.19	0.14	-0.10
stand dev	-0.37	-0.36	0.30	-0.32	-0.36	0.30	-0.28	-0.33	0.28	-0.29	-0.38	0.31	-0.29	-0.40	0.31	-0.32	-0.38	0.28	-0.29	-0.38	0.31
variance	-0.35	-0.31	0.26	-0.30	-0.31	0.26	-0.27	-0.28	0.24	-0.26	-0.33	0.26	-0.27	-0.34	0.26	-0.31	-0.31	0.23	-0.27	-0.33	0.27
coef. variance	0.02	-0.16	0.12	0.03	-0.15	0.12	0.09	-0.16	0.12	0.06	-0.21	0.16	0.06	-0.27	0.17	0.07	-0.31	0.17	0.07	-0.20	0.15
Skewness	-0.05	-0.23	0.18	-0.03	-0.23	0.19	0.02	-0.26	0.21	-0.02	-0.32	0.24	-0.01	-0.42	0.29	0.02	-0.47	0.32	0.01	-0.29	0.23
Kurtosis	0.16	0.35	-0.29	0.13	0.33	-0.29	0.08	0.34	-0.29	0.12	0.39	-0.32	0.11	0.48	-0.36	0.09	0.52	-0.37	0.10	0.37	-0.31
brightness energy	-0.17	0.12	-0.09	-0.14	0.11	-0.09	-0.19	0.15	-0.12	-0.15	0.21	-0.14	-0.16	0.33	-0.19	-0.21	0.40	-0.23	-0.18	0.18	-0.13
color energy	0.05	0.24	-0.21	0.02	0.24	-0.21	-0.01	0.28	-0.23	0.02	0.33	-0.25	0.01	0.47	-0.29	-0.02	0.56	-0.33	0.00	0.29	-0.23
zero-order entropy	-0.34	-0.44	0.31	-0.42	-0.40	0.29	-0.40	-0.39	0.29	-0.37	-0.38	0.30	-0.37	-0.31	0.27	-0.37	-0.26	0.24	-0.38	-0.40	0.30
1st-order entropy	-0.17	-0.37	0.33	-0.13	-0.36	0.33	-0.07	-0.40	0.36	-0.13	-0.45	0.38	-0.11	-0.58	0.43	-0.07	-0.65	0.46	-0.10	-0.42	0.36
2nd-order entropy	-0.30	-0.50	0.47	-0.28	-0.49	0.47	-0.21	-0.54	0.50	-0.27	-0.58	0.52	-0.26	-0.68	0.56	-0.21	-0.74	0.59	-0.25	-0.55	0.50
Image gradient	-0.81	-0.83	0.89	-0.81	-0.84	0.89	-0.75	-0.86	0.90	-0.81	-0.86	0.91	-0.80	-0.82	0.90	-0.77	-0.77	0.87	-0.79	-0.86	0.91
Spatial frequency	-0.84	-0.85	0.88	-0.88	-0.87	0.89	-0.86	-0.86	0.88	-0.89	-0.85	0.89	-0.89	-0.76	0.85	-0.87	-0.68	0.81	-0.88	-0.86	0.89
S F M	-0.48	-0.65	0.62	-0.55	-0.67	0.63	-0.49	-0.68	0.64	-0.55	-0.70	0.66	-0.56	-0.66	0.62	-0.52	-0.61	0.58	-0.53	-0.69	0.65

Table 4.8 Correlation coefficient values between green component colour image characteristics and PSNR, CR and bpp of 50 images using different wavelets.

	Haar			db2			db4			bior 4.4			bior 6.8			coif4			Sym4		
	PSNR	CR	bpp	PSNR	CR	bpp	PSNR	CR	bpp	PSNR	CR	bpp	PSNR	CR	bpp	PSNR	CR	bpp	PSNR	CR	bpp
range	-0.48	-0.54	0.42	-0.50	-0.50	0.40	-0.49	-0.51	0.41	-0.47	-0.46	0.39	-0.47	-0.39	0.38	-0.46	-0.34	0.36	-0.49	-0.49	0.40
mean	-0.16	0.16	-0.11	-0.16	0.15	-0.11	-0.21	0.17	-0.12	-0.15	0.23	-0.15	-0.16	0.34	-0.19	-0.21	0.42	-0.22	-0.18	0.20	-0.14
median	-0.09	0.16	-0.12	-0.12	0.15	-0.12	-0.18	0.18	-0.14	-0.12	0.23	-0.17	-0.12	0.34	-0.21	-0.17	0.41	-0.23	-0.14	0.21	-0.16
stand dev	-0.57	-0.37	0.30	-0.57	-0.37	0.30	-0.59	-0.34	0.27	-0.55	-0.33	0.27	-0.57	-0.27	0.23	-0.62	-0.23	0.19	-0.56	-0.35	0.28
variance	-0.55	-0.35	0.28	-0.55	-0.35	0.28	-0.58	-0.32	0.25	-0.53	-0.31	0.24	-0.55	-0.26	0.21	-0.60	-0.21	0.17	-0.54	-0.33	0.26
coef. variance	-0.06	-0.26	0.19	-0.05	-0.24	0.18	0.00	-0.25	0.18	-0.05	-0.28	0.20	-0.05	-0.32	0.20	-0.03	-0.35	0.19	-0.03	-0.27	0.20
Skewness	-0.05	-0.20	0.16	-0.02	-0.21	0.16	0.04	-0.23	0.18	-0.01	-0.29	0.21	-0.01	-0.38	0.25	0.02	-0.44	0.27	0.02	-0.26	0.20
Kurtosis	0.19	0.19	-0.21	0.13	0.19	-0.21	0.11	0.20	-0.20	0.12	0.23	-0.22	0.12	0.29	-0.23	0.13	0.35	-0.25	0.11	0.21	-0.21
brightness energy	-0.15	0.16	-0.12	-0.16	0.15	-0.11	-0.21	0.18	-0.13	-0.15	0.24	-0.16	-0.16	0.37	-0.21	-0.22	0.45	-0.24	-0.18	0.21	-0.14
color energy	0.02	0.16	-0.16	-0.03	0.17	-0.17	-0.06	0.22	-0.19	-0.03	0.27	-0.21	-0.04	0.41	-0.26	-0.07	0.51	-0.30	-0.05	0.22	-0.19
zero-order entropy	-0.59	-0.60	0.47	-0.65	-0.59	0.46	-0.65	-0.58	0.45	-0.62	-0.54	0.44	-0.62	-0.45	0.41	-0.61	-0.36	0.38	-0.64	-0.57	0.45
1st-order entropy	-0.19	-0.30	0.30	-0.12	-0.31	0.30	-0.07	-0.35	0.33	-0.11	-0.40	0.35	-0.10	-0.53	0.41	-0.08	-0.62	0.45	-0.09	-0.36	0.33
2nd-order entropy	-0.35	-0.49	0.48	-0.30	-0.49	0.48	-0.23	-0.54	0.51	-0.29	-0.58	0.53	-0.28	-0.68	0.58	-0.24	-0.74	0.61	-0.26	-0.54	0.51
Image gradient	-0.84	-0.86	0.91	-0.83	-0.87	0.91	-0.78	-0.88	0.91	-0.84	-0.88	0.92	-0.83	-0.83	0.91	-0.80	-0.78	0.88	-0.82	-0.88	0.92
Spatial frequency	-0.86	-0.88	0.89	-0.89	-0.89	0.90	-0.88	-0.88	0.88	-0.91	-0.86	0.88	-0.92	-0.75	0.84	-0.90	-0.67	0.80	-0.91	-0.87	0.89
S F M	-0.40	-0.62	0.58	-0.44	-0.64	0.59	-0.40	-0.64	0.59	-0.48	-0.65	0.60	-0.48	-0.61	0.56	-0.44	-0.56	0.52	-0.45	-0.65	0.60

Table 4.9 Correlation coefficient values between blue component colour image characteristics and PSNR, CR and bpp of 50 images using different wavelets.

	Haar			db2			db4			bior 4.4			bior 6.8			coif4			Sym4		
	PSNR	CR	bpp	PSNR	CR	bpp	PSNR	CR	bpp	PSNR	CR	bpp	PSNR	CR	bpp	PSNR	CR	bpp	PSNR	CR	bpp
range	-0.14	-0.09	0.11	-0.19	-0.08	0.11	-0.16	-0.10	0.13	-0.11	-0.08	0.13	-0.11	-0.05	0.11	-0.14	-0.02	0.09	-0.13	-0.08	0.12
mean	-0.14	0.15	-0.13	-0.16	0.14	-0.12	-0.21	0.17	-0.15	-0.15	0.24	-0.18	-0.16	0.35	-0.22	-0.22	0.41	-0.24	-0.18	0.20	-0.16
median	-0.07	0.17	-0.14	-0.10	0.16	-0.14	-0.15	0.19	-0.17	-0.10	0.25	-0.20	-0.11	0.36	-0.24	-0.16	0.42	-0.26	-0.12	0.22	-0.18
stand dev	-0.47	-0.22	0.21	-0.48	-0.23	0.22	-0.50	-0.23	0.22	-0.44	-0.20	0.20	-0.46	-0.14	0.17	-0.53	-0.10	0.14	-0.46	-0.22	0.22
variance	-0.48	-0.24	0.23	-0.49	-0.26	0.24	-0.51	-0.25	0.23	-0.46	-0.23	0.22	-0.48	-0.17	0.19	-0.55	-0.13	0.15	-0.48	-0.25	0.23
coef. variance	0.00	-0.18	0.15	-0.01	-0.17	0.14	0.04	-0.19	0.16	0.00	-0.22	0.17	0.00	-0.25	0.17	0.02	-0.27	0.17	0.01	-0.20	0.16
Skewness	-0.02	-0.20	0.16	-0.01	-0.21	0.16	0.03	-0.23	0.18	-0.01	-0.29	0.21	-0.01	-0.38	0.25	0.04	-0.44	0.28	0.01	-0.26	0.20
Kurtosis	0.25	0.12	-0.15	0.20	0.13	-0.16	0.18	0.14	-0.15	0.17	0.15	-0.16	0.17	0.19	-0.16	0.21	0.21	-0.16	0.16	0.14	-0.16
brightness energy	-0.13	0.16	-0.13	-0.15	0.15	-0.13	-0.20	0.19	-0.16	-0.14	0.25	-0.19	-0.16	0.37	-0.24	-0.21	0.45	-0.27	-0.17	0.21	-0.17
color energy	0.01	0.14	-0.15	-0.04	0.16	-0.16	-0.07	0.20	-0.18	-0.04	0.26	-0.20	-0.05	0.39	-0.25	-0.08	0.49	-0.29	-0.06	0.20	-0.18
zero-order entropy	-0.25	-0.17	0.17	-0.30	-0.17	0.17	-0.28	-0.17	0.18	-0.23	-0.15	0.17	-0.23	-0.08	0.14	-0.27	-0.04	0.12	-0.25	-0.16	0.17
1st-order entropy	-0.16	-0.22	0.26	-0.09	-0.24	0.27	-0.05	-0.28	0.29	-0.07	-0.33	0.31	-0.06	-0.45	0.36	-0.05	-0.54	0.40	-0.05	-0.28	0.29
2nd-order entropy	-0.33	-0.44	0.47	-0.27	-0.45	0.47	-0.21	-0.49	0.50	-0.25	-0.53	0.52	-0.24	-0.64	0.56	-0.22	-0.70	0.60	-0.23	-0.50	0.50
Image gradient	-0.80	-0.82	0.92	-0.78	-0.83	0.93	-0.74	-0.84	0.93	-0.79	-0.84	0.94	-0.78	-0.79	0.93	-0.77	-0.74	0.90	-0.77	-0.84	0.93
Spatial frequency	-0.82	-0.82	0.89	-0.85	-0.84	0.90	-0.83	-0.83	0.88	-0.86	-0.81	0.89	-0.87	-0.71	0.85	-0.86	-0.64	0.81	-0.85	-0.83	0.89
S F M	-0.34	-0.56	0.56	-0.37	-0.57	0.57	-0.33	-0.58	0.57	-0.42	-0.59	0.59	-0.41	-0.55	0.55	-0.36	-0.50	0.52	-0.38	-0.58	0.58

Many image features such as range, mean, median, standard deviation, variance, coefficient variance, skewness, kurtosis, brightness energy, gray/color energy, zero-order entropy, 1st-order entropy, 2nd-order entropy and spectral flatness measure (SFM) have no strong correlation. However, the results show that the image gradient (IAM) and spatial frequency (SF) have strong correlations with the colour image compression performance.

Table 4.7 gives results of coefficient correlation between red component colour image characteristics and PSNR, CR and bpp of 50 images using different wavelets. The absolute of coefficient correlation range values are 0 to 0.91. Almost all of the statistical features have coefficient correlation values (from 0 to 0.74), except the IAM, that is between 0.75 and 0.91 and SF, from 0.68 to 0.89.

The coefficient correlations between green component colour image characteristics and coding performance measures using different wavelets are computed to verify any relationship. The results are showed in Table 4.8. The results show the features have no correlation except the IAM, that is 0.78 to 0.92 and SF, from 0.67 to 0.92.

Similar to the red and green component, the blue component of images are also evaluated to find the coefficient correlation values between colour image characteristics and PSNR, CR and bpp using different wavelets. Table 4.9 shows the results. Many features have small coefficient correlation values, but the IAM, that is, between 0.74 and 0.94 and SF, from 0.64 to 0.9.

These results indicate that there is a strong negative correlation between the image gradient and spatial frequency against PSNR and CR. The results also indicate that there is a strong positive correlation between IAM and SF against bpp.

There is no defined method for determining whether a connection is weak or strong. The closer the coefficient is to either −1 or 1, in other words the absolute coefficient correlation value closer to 1, shows the stronger the correlation between the image features and codec performance. The IAM and SF have high absolute coefficient

correlation value close to 1. This indicates that both features have the stronger correlation to the wavelet based colour image compression performance.

Scatter plot of each image feature against the PSNR values is plotted to verify relationship between any of the image features and the PSNR values obtained. The plots are shown in Figure 4.1(a) through 4.1(n). These figures shown that the gray-level based features used in this research namely range, mean, median, standard deviation, variance, coefficient variance, skewness, kurtosis, brightness energy, gray/color energy, zero-order entropy, 1st-order entropy, 2nd-order entropy and spectral flatness measure (SFM) have a weak relation with the coding performance. Figure 4.1(a) through Figure 4.1(n) show the scatter plot of PSNR using biorthogonal 4.4 wavelet in several green component features. Figure 4.1(a) shows the scatter plot of PSNR vs. range, Figure 4.1(b) shows the scatter plot of PSNR vs. mean, Figure 4.1(c) shows the scatter plot of PSNR vs. median, Figure 4.1(d) shows the scatter plot of PSNR vs. standard deviation, Figure 4.1(e) shows the scatter plot of PSNR vs. variance, Figure 4.1(f) shows the scatter plot of PSNR vs. coefficient variance, Figure 4.1(g) shows the scatter plot of PSNR vs. skewness, Figure 4.1(h) shows the scatter plot of PSNR vs. kurtosis, Figure 4.1(i) shows the scatter plot of PSNR vs. brightness energy, Figure 4.1(j) shows the scatter plot of PSNR vs. gray/color energy, Figure 4.1(k) shows the scatter plot of PSNR vs. zero-order entropy, Figure 4.1(l) shows the scatter plot of PSNR vs. 1st-order entropy, Figure 4.1(m) shows the scatter plot of PSNR vs. 2nd-order entropy, Figure 4.1(n) shows the scatter plot of PSNR vs. Spectral Flatness Measure. It can be seen from these results that there are no correlation between PSNR and those features. The scatter plots of other colour components, both red and blue, are not shown here. The plots also show that there are no correlations between any features and PSNR.

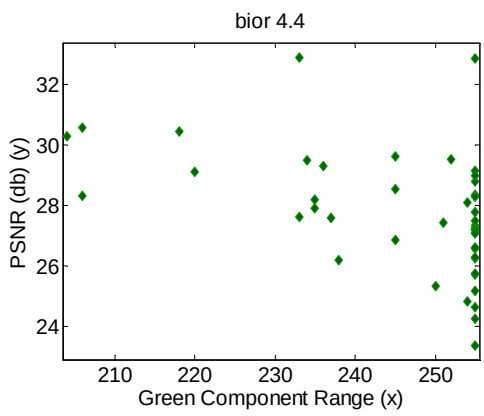
bior 4.4
PSNR (db) (y)
Green Component Range (x)

(a)

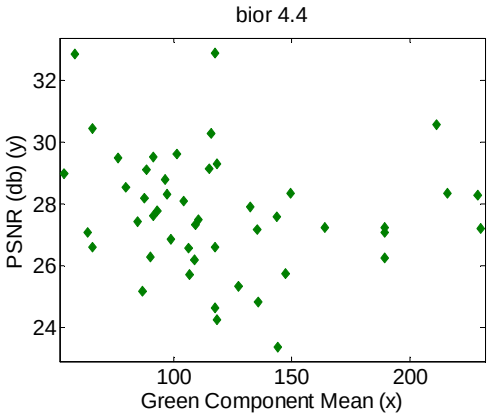
bior 4.4
PSNR (db) (y)
Green Component Mean (x)

(b)

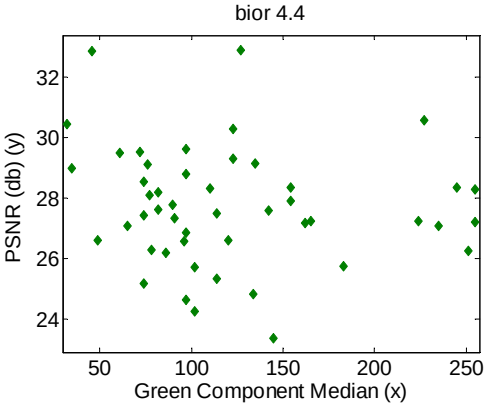
bior 4.4
PSNR (db) (y)
Green Component Median (x)

(c)

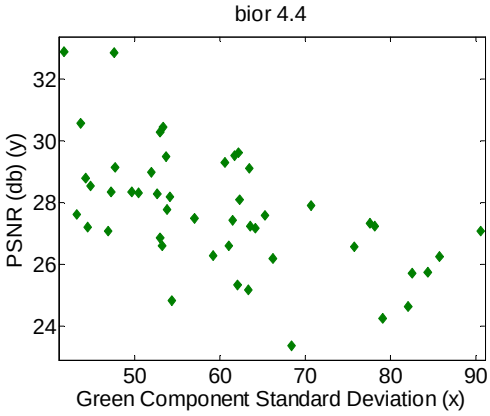
bior 4.4
PSNR (db) (y)
Green Component Standard Deviation (x)

(d)

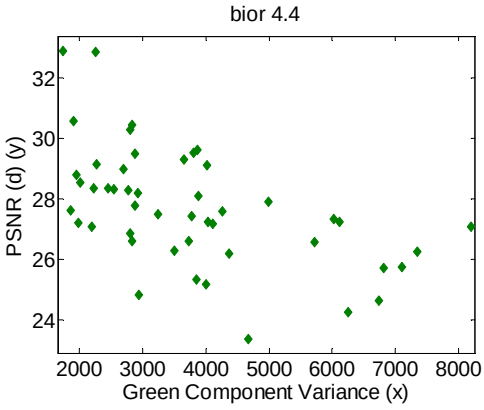
bior 4.4
PSNR (d) (y)
Green Component Variance (x)

(e)

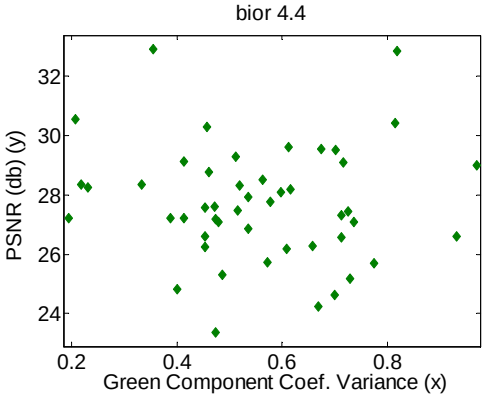
bior 4.4
PSNR (db) (y)
Green Component Coef. Variance (x)

(f)

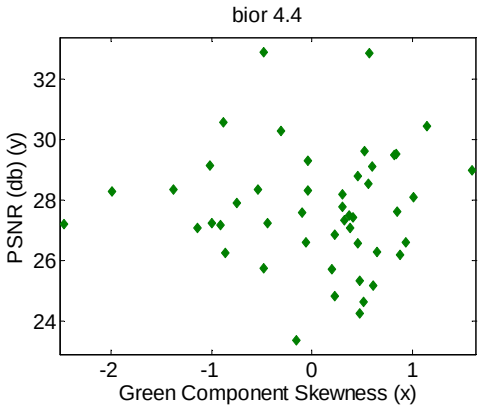
bior 4.4
PSNR (db) (y)
Green Component Skewness (x)

(f)

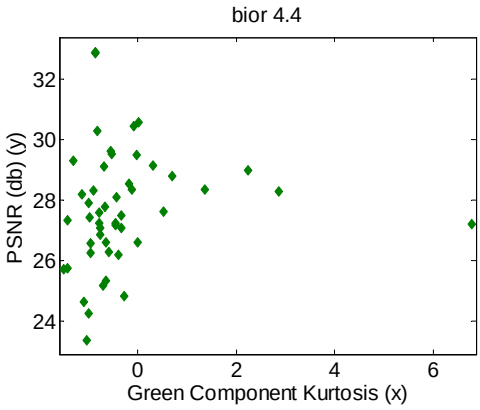
bior 4.4
PSNR (db) (y)
Green Component Kurtosis (x)

(h)

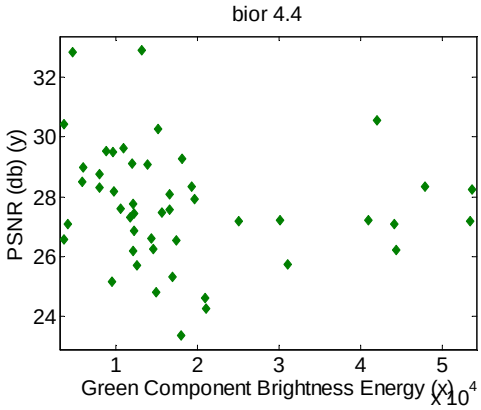
bior 4.4
PSNR (db) (y)
Green Component Brightness Energy (x)
X 10^4

(i)

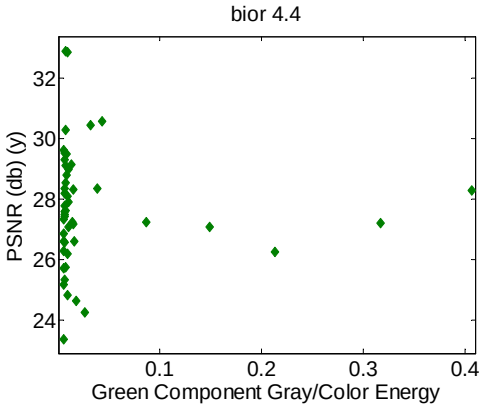
bior 4.4
PSNR (db) (y)
Green Component Gray/Color Energy

(j)

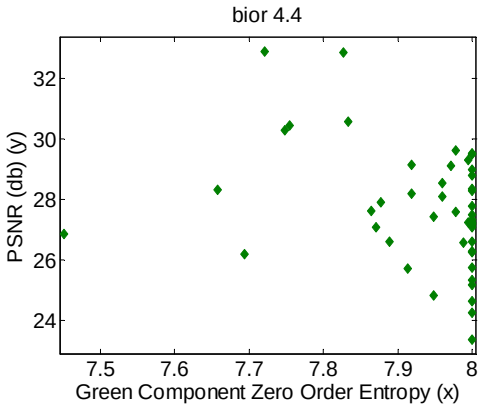
bior 4.4
PSNR (db) (y)
Green Component Zero Order Entropy (x)

(k)

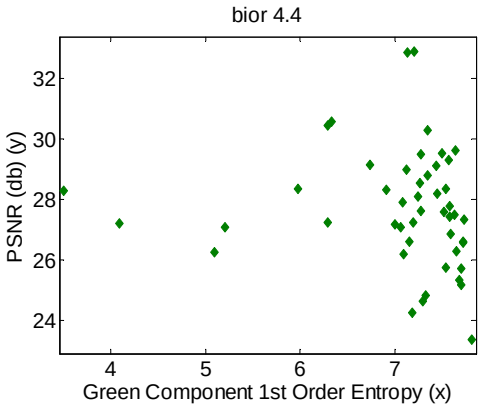
bior 4.4
PSNR (db) (y)
Green Component 1st Order Entropy (x)

(l)

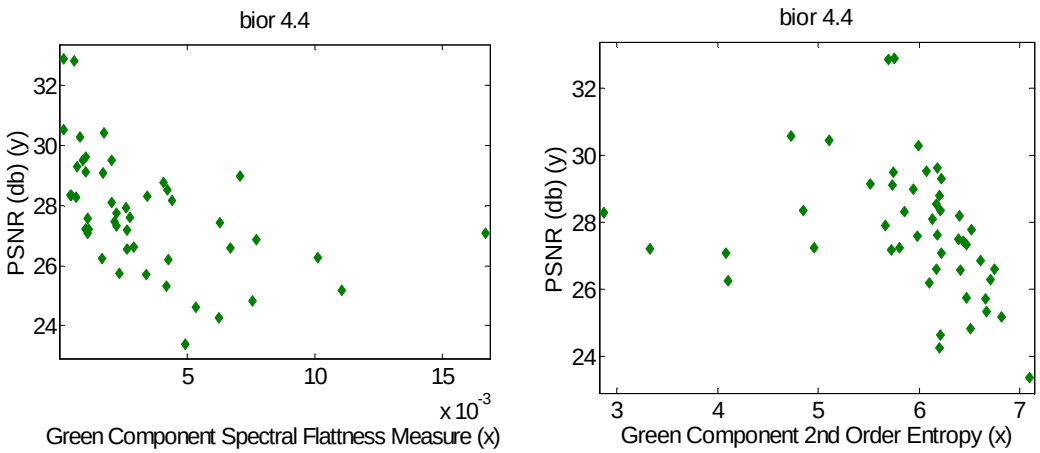

(m) (n)

Figure 4.1 Scatter plots of the green component's features and PSNR values.

Scatter plots of other any feature images colour in red, green and blue vs. the CR and bpp values are not shown here, because the results show a weak correlation.

Furthermore, the PSNR values (using `bior 4.4` wavelet) are plotted against the image gradient values of red, green and blue components are exposed in Figure 4.2(a), 4.2(b) and 4.2(c). These figures show there is a clear inverse relationship between the image gradient (IAM) and the PSNR values. Images with low image gradient value gives a much higher PSNR value than image with high image gradient value.

The scatter plots show that the correlation varies between 0.6758 for the red component and 0.7679 for the green component. As mentioned earlier, for this research a good correlation coefficients (R-square) is defined as the absolute value greater than 0.5.

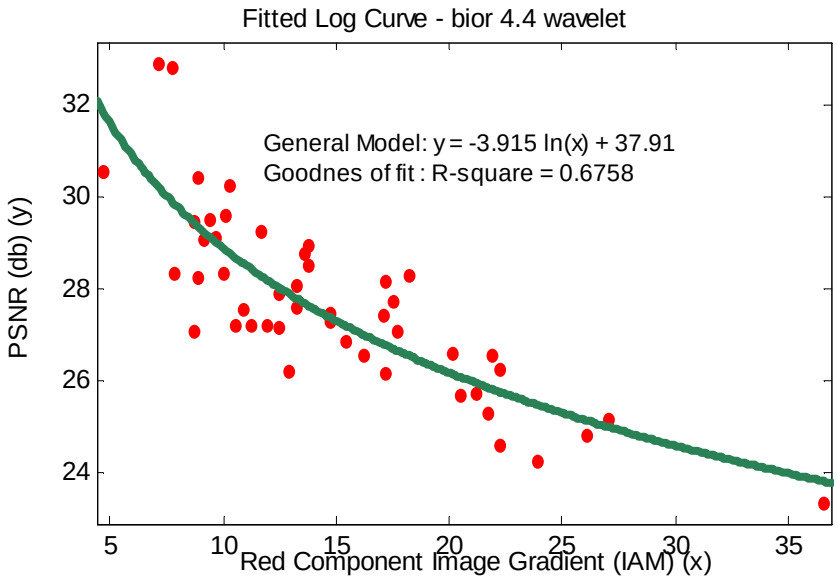
Fitted Log Curve - bior 4.4 wavelet
General Model: y = -3.915 ln(x) + 37.91
Goodnes of fit : R-square = 0.6758
PSNR (db) (y)
Red Component Image Gradient (IAM) (x)
32
30
28
26
24
5
10
15
20
25
30
35

(a)

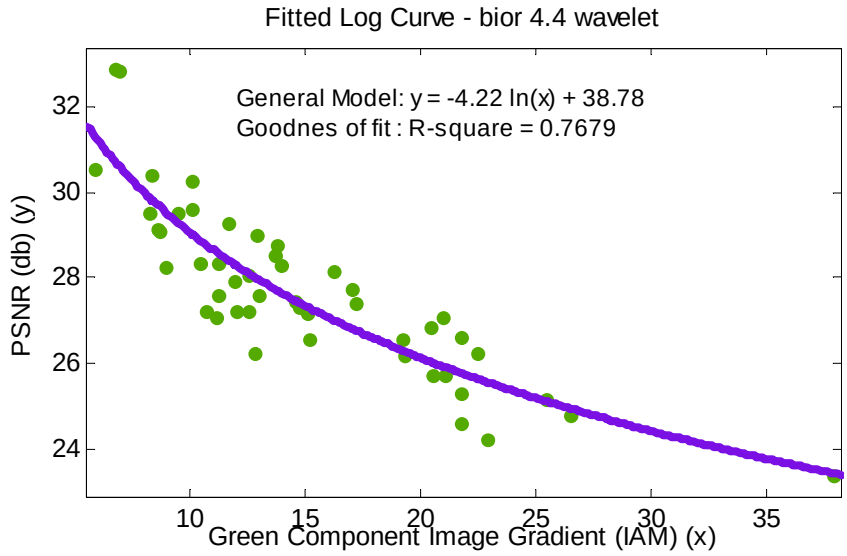
Fitted Log Curve - bior 4.4 wavelet
General Model: y = -4.22 ln(x) + 38.78
Goodnes of fit : R-square = 0.7679
PSNR (db) (y)
Green Component Image Gradient (IAM) (x)
32
30
28
26
24
10
15
20
25
30
35

(b)

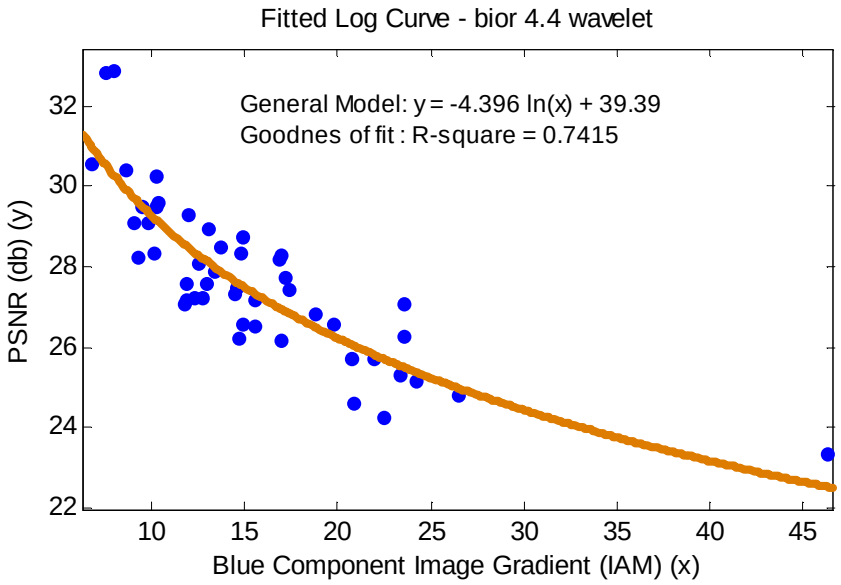

(c)

Figure 4.2

(a) Scatter plots PSNR vs. red components IAM of 50 images.

(b) Scatter plots PSNR vs. green components IAM of 50 images.

(c) Scatter plots PSNR vs. blue components IAM of 50 images.

Scatter plots of the SF vs. PSNR (using `bior 6.8` wavelet) from red, green and blue components are shown in Figure 4.3(a), 4.3(b), and 4.3(c) correspondingly. These figures also show that there is a clear inverse relationship between the spatial frequency (SF) and the PSNR values. Images with low spatial frequency value gives a much higher PSNR value than image with high spatial frequency value. It can be observed that the correlation varies between 0.8398 for the red component and 0.8951 for the green component.

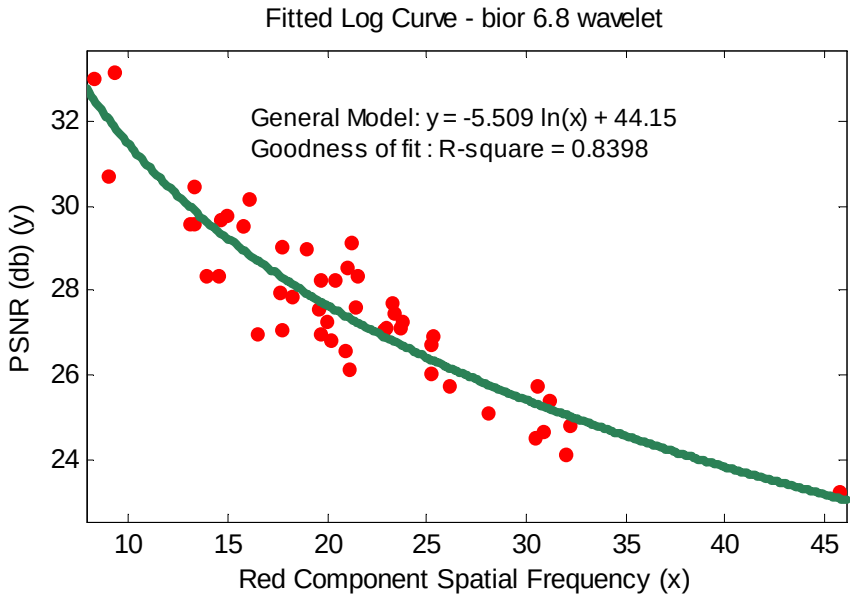
Fitted Log Curve - bior 6.8 wavelet
General Model: y = -5.509 ln(x) + 44.15
Goodness of fit : R-square = 0.8398
PSNR (db) (y)
Red Component Spatial Frequency (x)
32
30
28
26
24
10
15
20
25
30
35
40
45

(a)

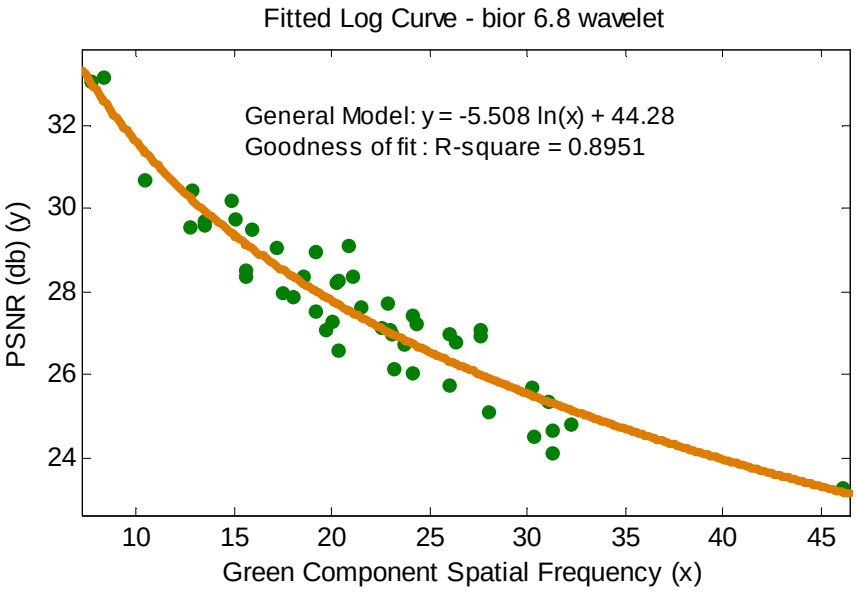
Fitted Log Curve - bior 6.8 wavelet
General Model: y = -5.508 ln(x) + 44.28
Goodness of fit : R-square = 0.8951
PSNR (db) (y)
Green Component Spatial Frequency (x)
32
30
28
26
24
10
15
20
25
30
35
40
45

(b)

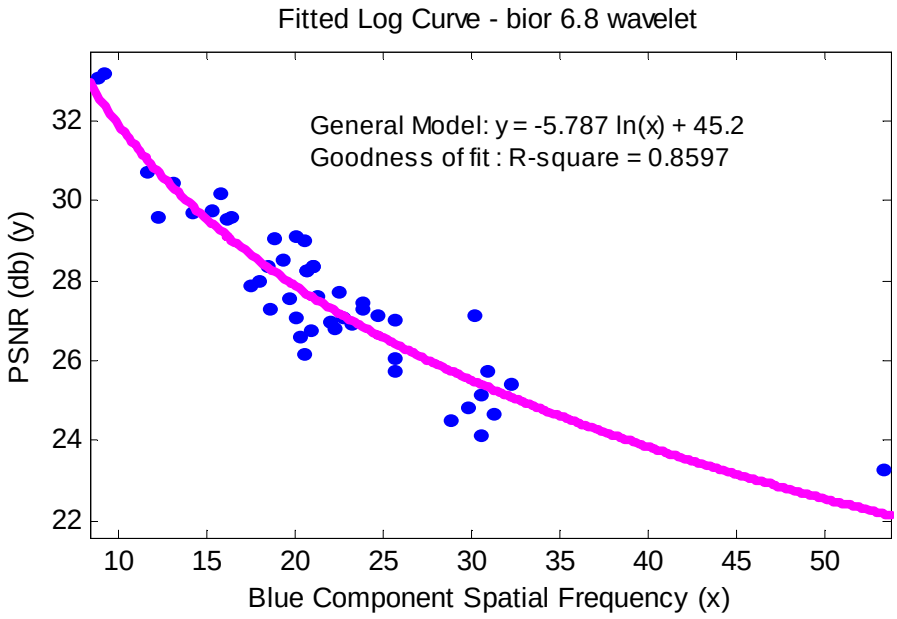

(c)

Figure 4.3

(a) Scatter plots PSNR vs. red components SF of 50 images.

(b) Scatter plots PSNR vs. green components SF of 50 images.

(c) Scatter plots PSNR vs. blue components SF of 50 images.

In addition, the CR values (using `bior 4.4` wavelet) are plotted against the image gradient (IAM) values of red, green and blue components are exposed in Figure 4.4(a), 4.4(b) and 4.4(c). These figures illustrate there is a clear inverse relationship between the image gradient (IAM) and the CR values, as well. Images with low image gradient value gives a much higher CR value than image with high image gradient value. R-square varies between 0.8023 and 0.8453 indicating a strong correlation between IAM and CR.

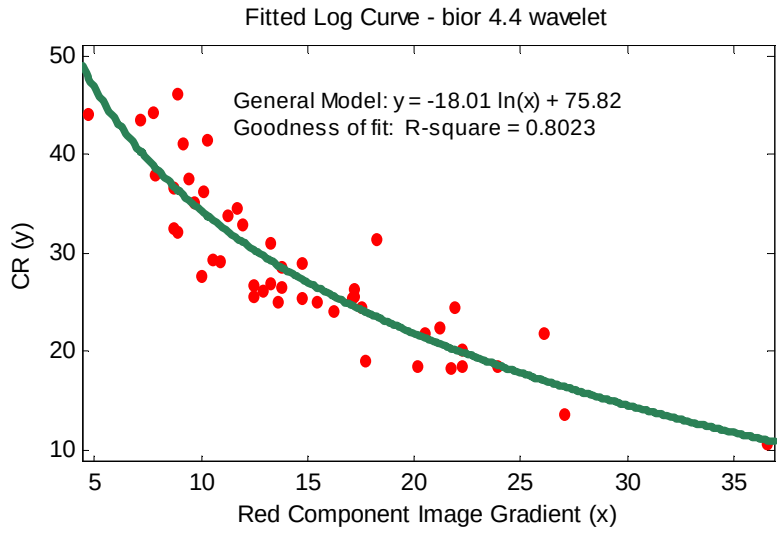
Fitted Log Curve - bior 4.4 wavelet
General Model: y = -18.01 ln(x) + 75.82
Goodness of fit: R-square = 0.8023
CR (y)
Red Component Image Gradient (x)
50
40
30
20
10
5
10
15
20
25
30
35

(a)

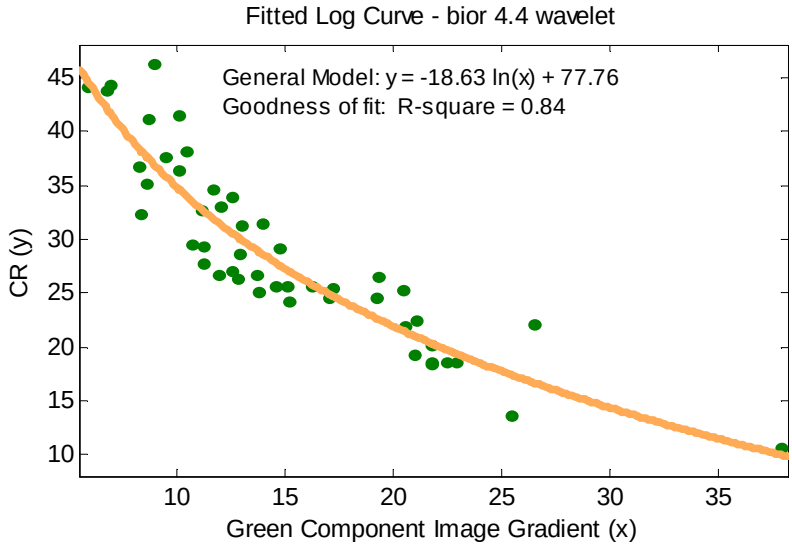
Fitted Log Curve - bior 4.4 wavelet
General Model: y = -18.63 ln(x) + 77.76
Goodness of fit: R-square = 0.84
CR (y)
Green Component Image Gradient (x)
45
40
35
30
25
20
15
10
10
15
20
25
30
35

(b)

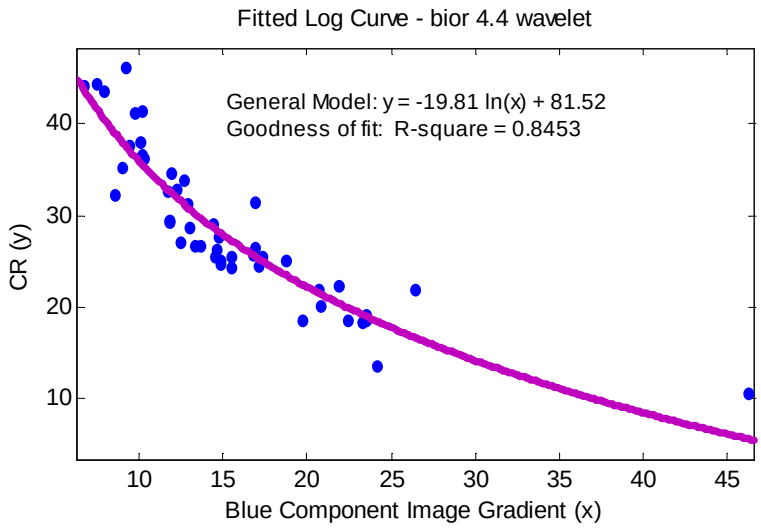

(c)

Figure 4.4

(a) Scatter plots CR vs. red components IAM of 50 images.

(b) Scatter plots CR vs. green components IAM of 50 images.

(c) Scatter plots CR vs. blue components IAM of 50 images.

Scatter plots of SF vs. CR (using daubechies 4 wavelet) from red, green and blue components are shown in Figure 4.5(a), 4.5(b) and 4.5(c). R-square varies between 0.748 and 0.7712.

The results show that the colour histogram statistics of the images e.g. range, mean, median, different (mean-median), standard deviation, variance, coefficient variance, skewness, kurtosis, brightness energy, gray/color energy, zero order entropy, first-order entropy, second-order entropy, and spectral flatness measure do not influence the coding performance. However, image gradient and spatial frequency of colour images have good correlation with the PSNR, CR and bpp.

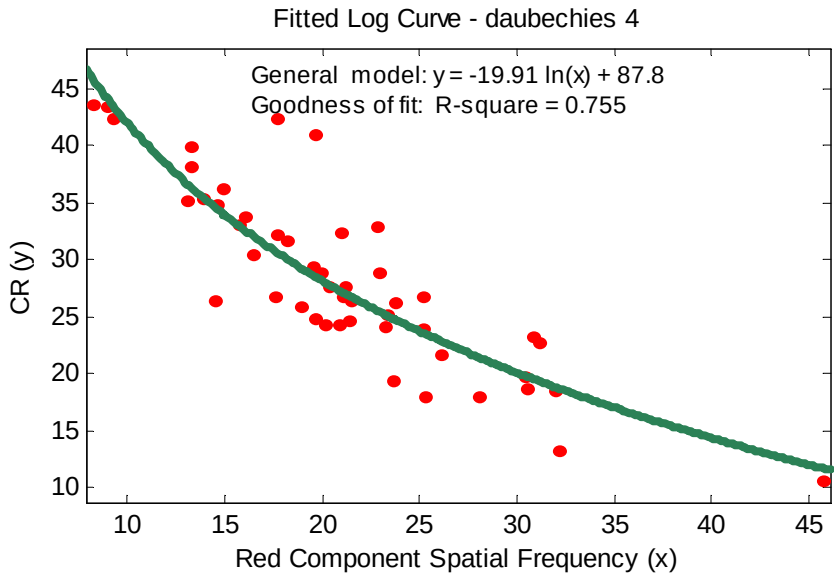
Fitted Log Curve - daubechies 4
General model: y = -19.91 ln(x) + 87.8
Goodness of fit: R-square = 0.755
CR (y)
Red Component Spatial Frequency (x)
10
15
20
25
30
35
40
45

(a)

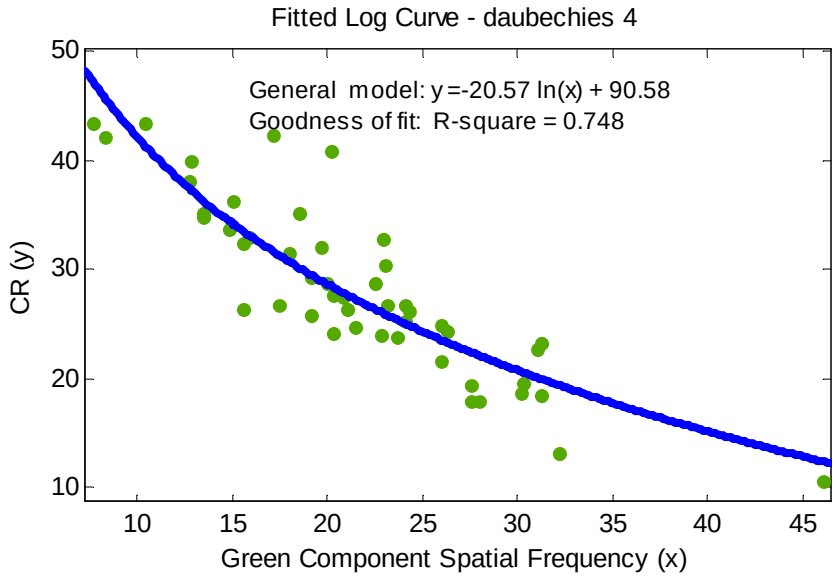
Fitted Log Curve - daubechies 4
General model: y =-20.57 ln(x) + 90.58
Goodness of fit: R-square = 0.748
CR (y)
Green Component Spatial Frequency (x)
10
20
30
40
50
15
25
35
45

(b)

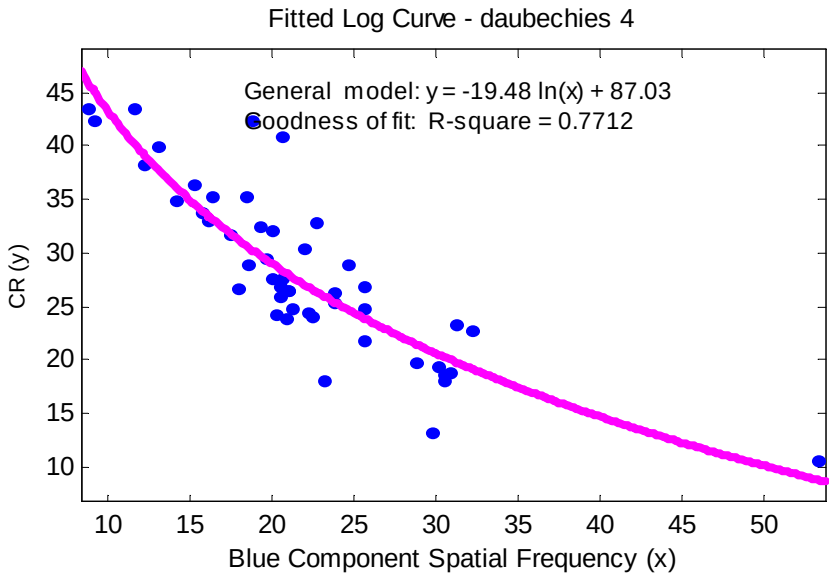

(c)

Figure 4.5

(a) Scatter plots CR vs. red components SF of 50 images.

(b) Scatter plots CR vs. green components SF of 50 images.

(c) Scatter plots CR vs. blue components SF of 50 images.

4.4 Logarithmic Equation

An equation is established to describe the relationship between IAM and PSNR and SF and PSNR. This equation is a logarithmic equation in a form of

$$Y = a\ ln(x) + b$$

where a and b are values to be determined . This equation can be used to predict the PSNR and CR from the IAM or SF for a given image. Table 4.10 is the summary of the fitted logarithmic equation and R-square of 12 scatter plots. R-square values vary from 0.67 to 0.89, and it is shown that both IAM and SF have good correlation with PSNR and CR. Similarly with CR, bpp has strong correlation.

Table 4.11 Summary of the logarithmic fitted equation and the R-square.

Scatter plot	Logarithmic fitted equation	R – square
IAM vs. PSNR (red)	Y = -3.91 ln(x) + 37.91	0.6758
IAM vs. PSNR (green)	Y = -4.22 ln(x) + 38.78	0.7679
IAM vs. PSNR (blue)	Y = -4.39 ln(x) + 39.39	0.7415
SF vs. PSNR (red)	**Y = -5.51 ln(x) + 44.15**	**0.8398**
SF vs. PSNR (green)	**Y = -5.51 ln(x) + 44.28**	**0.8951**
SF vs. PSNR (blue)	**Y = -5.78 ln(x) + 45.2**	**0.8597**
IAM vs. CR (red)	**Y = -18.01 ln(x) +75.82**	**0.8023**
IAM vs. CR (green)	**Y = -19.29 ln(x) +80.55**	**0.8264**
IAM vs. CR (blue)	**Y = -19.81 ln(x) + 81.52**	**0.8453**
SF vs. CR (red)	Y = -20.81 ln(x) + 90.99	0.755
SF vs. CR (green)	Y = -19.93 ln(x) + 88.84	0.748
SF vs. CR (blue)	Y = -21.13 ln(x) + 92.75	0.7712

Table 4.10 gives information of the fitted logarithmic equation. The equation of IAM vs. PSNR for red component is Y = -3.91 ln(x) + 37.91 and the R-square value is 0.6758. The equation of IAM vs. PSNR for green component is Y = -4.22 ln(x) + 38.78, with the R-square 0.7679 and for blue component, the equation is Y = -4.39 ln(x) + 39.39 with R-square value is 0.7415. Therefore, the fitted logarithmic equation of SF vs. PSNR followed by R-square values for red, green and blue component are Y = -5.51 ln(x) + 44.15; 0.8398, Y = -5.51 ln(x) + 44.28; 0.8951, and Y = -5.78 ln(x) + 45.2; 0.8597, respectively.

The fitted logarithmic curves of IAM vs. CR for red, green and blue component and their R-square values are represented in following equation: Y = -18.01 ln(x) +75.82; 0.8023, Y = -19.29 ln(x) +80.55; 0.8264 and Y = -19.81 ln(x) + 81.52; 0.8453. However, the fitted logarithmic curves of SF vs. CR for red, green and blue component and their R-square values are represented in following equation: Y = -

20.81 ln(x) + 90.99; 0.755, Y = -19.93 ln(x) + 88.84; 0.748 and Y = -21.13 ln(x) + 92.75; 0.7712.

The study of correlation coefficient and fitted logarithmic equation with the R-square evaluation indicates there are strong correlations between IAM and SF of three colour (red, green and blue) component against PSNR and CR. The initial result on IAM an SF correlation will be investigated using statistical test to get confidence conclusion in causality effect.

4.5 Statistical Test for Causality Effect Provident

Previous study [9] indicated image gradient (IAM) and spatial frequency (SF) as image features that have strong correlation to wavelet based codec. The peak signal to noise ratio (PSNR), compression ratio (CR) and bits-per-pixel (bpp) are evaluated, and then coefficient correlation between them and IAM and SF are evaluated. Statistical test based on Friedman's test are conducted even though the correlations are strong to receive conclusion of causality effect.

The IAM and SF values of red green and blue component from 450 images are scat plotted against the PSNR, CR and bpp value. Figure 4.6(a) shows the scatter plot of 450 images using symlet wavelet; Figure 4.7(a) shows the scatter plot of 450 images using db 4 wavelet and Figure 4.8(a) shows the scatter plot of 450 images using `bior 6.8` wavelet.

The 450 random selected images have different IAM and SF values. For statistical testing, same number of images on each colour IAM and SF interval are needed. In this research, 45 images represent the population from each interval. Figure 4.6(b) shows the scatter plot of 225 images using symlet wavelet; Figure 4.7(b) shows the scatter plot of 225 images using db 4 wavelet and Figure 4.8(b) shows the scatter plot of 225 images using `bior 6.8` wavelet. All of them have been categorized in five intervals with 45 images in each interval. Forty-five images are chosen because it is enough for statistical study. As mentioned earlier, for each colour component, IAM

and SF are taken into five intervals. Each interval is represented by forty-five images. Therefore, only 225 images are taken per test. Every test depends on the IAM or SF colour component interval, so the images of one test are not as same as other test.

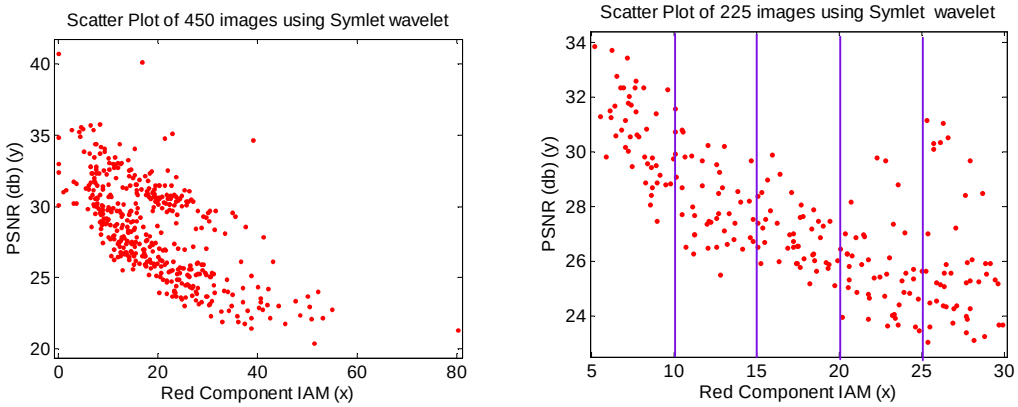

(a) (b)

Figure 4.6 Scatter plots of PSNR (using `Symlet 4`) vs. red component IAM from 450 and 225 images

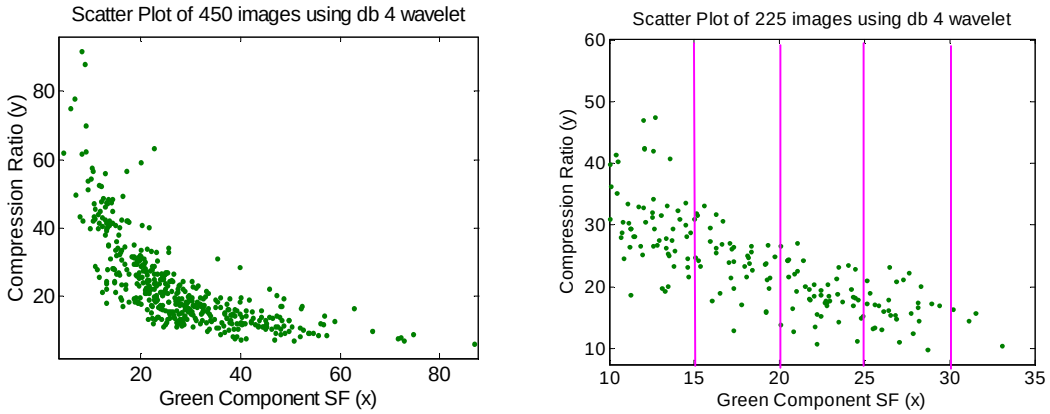

(a) (b)

Figure 4.7 Scatter plots of CR (using `db 4`) vs. green component SF from 450 and 225 images

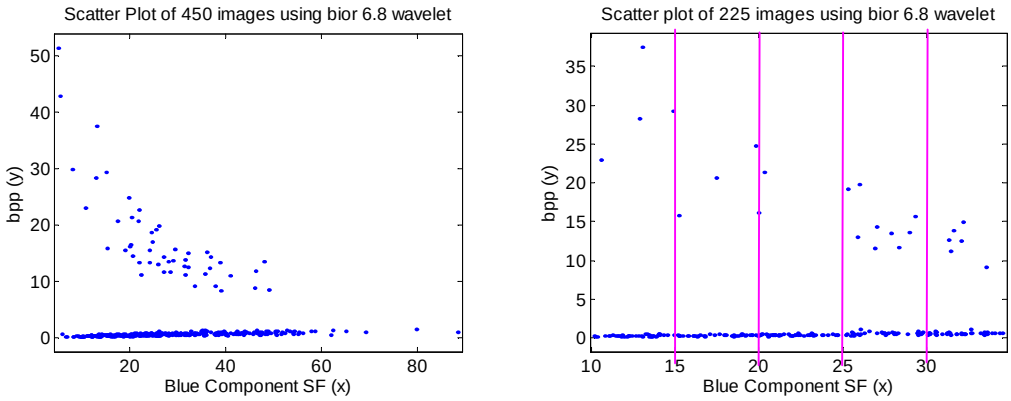

(a) (b)

Figure 4.8 Scatter plots of bpp (using `bior 6.8`) vs. blue component SF from 450 and 225 images

IAM intervals are 5-10, 10-15, 15-20, 20-25 and 25-30, while SF intervals are 10-15, 15-20, 20-25, 25-30 and 30-35. To satisfy every interval has same number of images (45), we evaluated IAM and SF values. Taking 225 from 450 images is done for every colour component on IAM and SF recursively. After selecting, the scatter plots of codec performance vs. IAM or SF are seen in Figure 4.6(b), 4.7(b) and 4.8(b).

Matrix modeling is applied to various 225-images. Figure 4.9 is a matrix evaluation example where each column represents five intervals of red component IAM, the PSNR using `bior 6.8` wavelet values for Kruskal-Wallis test. The matrix model for this evaluation is shown in Figure 4.10. Other matrixes that are evaluated in this study are matrix for PSNR values for red component IAM using `Haar, db2, db4, bior 4.4, bior 6.8, Coif 4` and `Sym 4` wavelets. The matrixes of CR values for green component SF using `haar, db2, db4, bior 4.4, bior 6.8, Coif 4` and `Sym 4` wavelets are also evaluated. Finally, the matrixes of bpp values for blue component SF using `haar, db2, db4, bior 4.4, bior 6.8, Coif 4` and `Sym 4` wavelets are evaluated as well.

Figure 4.11 shows matrix model for Friedman's test. The first-45 rows are PSNR evaluated using bior 6.8, while second-45 rows are PSNR evaluated using sym 4. This matrix has size 90 x 5; a quite large of matrix size, so limited space doesn't allow

researchers to put up whole data. Various others matrixes developed are matrix for PSNR values for red component IAM of 225 images selected using `haar-db2`, `haar-db4`, `haar-bior 4.4`, `db2-db4`, `db2-bior 4.4`, `db2-bior 6.8`, `db4-bior 4.4`, `db4-bior 6.8`, `db4-coif 4`, `bior 4.4-bior 6.8`, `bior 4.4-coif 4` and `bior 4.4-sym 4`. Matrix for CR values of green component SF of 225 images selected using same wavelet couples. Furthermore, matrixes for bpp values for blue component of 225 images are also selected using the same wavelet couples.

	Red IAM Interval				
	5-10	10-15	15-20	20-25	25-30
	29.759	30.316	30.2	31.39	32.128
	31.434	28.183	28.36	29.521	30.017
	27.712	27.233	27.004	28.355	26.913
	25.661	25.132	25.395	28.994	25.611
	23.491	25.659	25.649	24.246	30.352
	29.519	31.322	30.699	32.478	32.577
	29.196	28.151	30.464	29.129	30.657
	26.773	28.39	29.512	28.14	28.331
	25.418	24.514	26.265	25.686	27.554
	24.787	24.27	23.117	25.637	29.821
	30.435	29.579	32.642	32.461	32.774
	27.157	29.762	27.272	28.537	29.949
	26.899	26.046	25.583	26.388	26.509
	25.197	26.935	26.879	29.722	27.159
	24.136	26.359	24.482	25.069	27.188
	29.265	33.049	34.362	32.69	31.027
	27.464	28.271	27.078	27.622	30.232
	26.39	26.608	28.894	29.241	26.261
	24.559	27.111	25.049	24.249	24.409
	27.233	25.547	26.148	24.291	25.96
	31.382	29.704	31.295	30.833	29.309
`bior 6.8`	26.692	27.879	27.56	27.965	27.727
	27.379	28.359	28.221	28.672	28.33
	26.008	25.736	25.481	27.24	25.847
	24.683	25.522	23.558	25.499	26.032
	29.912	33.182	30.869	33.946	30.483
	29.641	27.097	27.56	30.507	31.6
	28.05	27.265	27.868	26.648	27.081
	25.821	24.125	26.119	26.155	25.914
	24.833	24.823	26.263	25.438	30.318
	30.434	29.064	31.328	32.995	32.159
	28.541	26.072	27.456	30.28	28.763
	26.502	26.168	28.504	26.847	27.239
	25.299	25.757	25.985	26.654	24.393
	25.806	26.009	26.277	28.378	31.107
	30.303	29.612	31.88	31.03	32.125
	28.514	27.146	28.989	31.01	30.908
	26.792	27.728	30.05	27.789	27.169
	24.514	26.82	26.448	27.585	24.42
	26.212	24.403	26.189	30.558	31.312
	31.97	28.242	33.478	31.663	29.526
	28.045	28.364	26.983	30.133	29.513
	28.114	26.74	26.526	27.867	27.518
	28.755	26.82	27.309	24.383	30.065
	25.925	27.212	23.863	30.181	28.683

Figure 4.9 Evaluation matrix of PSNR values using `bior 6.8` in red IAM interval for Kruskal-Wallis test.

	Red IAM Interval				
	5-10	10-15	15-20	20-25	25-30
	29.759	30.316	30.2	31.39	32.128
	31.434	28.183	28.36	29.521	30.017
	27.712	27.233	27.004	28.355	26.913
bior 6.8	.				.
	.				.
	28.114	26.74	26.526	27.867	27.518
	28.755	26.82	27.309	24.383	30.065
	25.925	27.212	23.863	30.181	28.683

Figure 4.10 Matrix modeling for of PSNR values using `bior 6.8` in red IAM interval for Kruskal-Wallis test.

	Red IAM Interval				
	5-10	10-15	15-20	20-25	25-30
	29.759	30.316	30.2	31.39	32.128
	31.434	28.183	28.36	29.521	30.017
	27.712	27.233	27.004	28.355	26.913
bior	.				.
6.8	.				.
	28.114	26.74	26.526	27.867	27.518
	28.755	26.82	27.309	24.383	30.065
	25.925	27.212	23.863	30.181	28.683
	29.273	28.689	28.489	32.422	31.659
	29.486	26.455	26.592	27.456	28.898
	25.891	26.62	26.559	28.193	26.38
sym 4	.				.
	.				.
	26.315	26.416	28.712	27.584	26.515
	27.368	26.147	26.679	24.919	28.532
	24.746	26.689	23.849	30.901	27.948

Figure 4.11 Matrix modeling of PSNR values using `bior 6.8` and `Symlet 4` in red IAM interval for Friedman's test.

The evaluation using Kruskal-Wallis test produces p-values from 0.000166 to 0.17421. Table 4.11 illustrates some results of the test, where PSNR, CR and bpp in seven different wavelets are evaluated for red component IAM, green component SF and blue component SF interval. 0.001824 to 0.015528 is the range of p-values for measured PSNR in red component IAM interval. P-values range for measured CR in green component SF interval is from 0.090185 to 0.17421, when for measured bpp in blue component SF interval is from 0.000166 to 0.00539.

Table 4.12 Result summary of Kruskal-Wallis's test for PSNR, CR and bpp in different intervals and wavelets.

Interval	Measured Values	p value
Red Comp IAM	PNSR for `haar`	0.001949
Red Comp IAM	PSNR for `db2`	0.002448
Red Comp IAM	PSNR for `db4`	0.001824
Red Comp IAM	PSNR for `bior 4.4`	0.012534
Red Comp IAM	PSNR for `bior 6.8`	0.015528
Red Comp IAM	PSNR for `coif 4`	0.007314
Red Comp IAM	PSNR for `Sym 4`	0.003219
Green Comp SF	CR for `haar`	0.090185
Green Comp SF	CR for `db2`	0.106435
Green Comp SF	CR for `db4`	0.09605
Green Comp SF	CR for `bior 4.4`	0.103881
Green Comp SF	CR for `bior 6.8`	0.14178
Green Comp SF	CR for `coif 4`	0.17421
Green Comp SF	CR for `Sym 4`	0.097815
Blue Comp SF	bpp for `haar`	0.000166
Blue Comp SF	bpp for `db2`	0.000221
Blue Comp SF	bpp for `db4`	0.0002
Blue Comp SF	bpp for `bior 4.4`	0.000357
Blue Comp SF	bpp for `bior 6.8`	0.001496
Blue Comp SF	bpp for `coif 4`	0.00539
Blue Comp SF	bpp for `Sym 4`	0.000243

Table 4.13 Result summary of Friedman's test for PSNR, CR and bpp in different intervals and wavelets.

Interval	Measured Values	p-value
Red Comp. IAM	PSNR in haar and db2	1.12E-06
Red Comp. IAM	PSNR in Haar and db4	9.35E-07
Red Comp. IAM	PSNR in Haar and bior 4.4	7.29E-06
Red Comp. IAM	PSNR in db2 and db4	1.01E-06
Red Comp. IAM	PSNR in db2 and bior 4.4	8.11E-06
Red Comp. IAM	PSNR in db2 and bior 6.8	1.06E-05
Red Comp. IAM	PSNR in db4 and bior 4.4	5.58E-06
Red Comp. IAM	PSNR in db4 and bior 6.8	7.34E-06
Red Comp. IAM	PSNR in db4 and coif 4	3.24E-06
Red Comp. IAM	PSNR in bior 4.4 and bior 6.8	5.07E-05
Red Comp. IAM	PSNR in bior 4.4 and coif 4	2.36E-05
Red Comp. IAM	PSNR in bior 4.4 and sym 4	9.83E-06
Green Comp. SF	CR in Haar and db2	0.0035316
Green Comp. SF	CR in Haar and db4	0.0032687
Green Comp. SF	CR in Haar and bior 4.4	0.0036167
Green Comp. SF	CR in db2 and db4	0.0038428
Green Comp. SF	CR in db2 and bior 4.4	0.004226
Green Comp. SF	CR in db2 and bior 6.8	0.0059327
Green Comp. SF	CR in db4 and bior 4.4	0.0036751
Green Comp. SF	CR in db4 and bior 6.8	0.0053337
Green Comp. SF	CR in db4 and coif 4	0.007283
Green Comp. SF	CR in bior 4.4 and bior 6.8	0.0057759
Green Comp. SF	CR in bior 4.4 and coif 4	0.0077721
Green Comp. SF	CR in bior 4.4 and sym 4	0.0037632
Blue Comp. SF	bpp in Haar and db2	5.91E-09
Blue Comp. SF	bpp in Haar and db4	5.40E-09
Blue Comp. SF	bpp in Haar and bior 4.4	1.00E-08
Blue Comp. SF	bpp in db2 and db4	7.16E-09
Blue Comp. SF	bpp in db2 and bior 4.4	1.32E-08
Blue Comp. SF	bpp in db2 and bior 6.8	6.41E-08
Blue Comp. SF	bpp in db4 and bior 4.4	1.18E-08
Blue Comp. SF	bpp in db4 and bior 6.8	5.68E-08
Blue Comp. SF	bpp in db4 and coif 4	2.62E-07
Blue Comp. SF	bpp in bior 4.4 and bior 6.8	1.01E-07
Blue Comp. SF	bpp in bior 4.4 and coif 4	4.55E-07
Blue Comp. SF	bpp in bior 4.4 and sym 4	1.44E-08

Friedman's test produces various p-values for many composition matrixes, with minimum amount of 5.4E-09 and maximum amount in 0.0077721 as shown at Table 6.12. For more detail, in red component IAM interval, the p-value to PSNR is about 9.35E-07 to 5.07E-05. 0.0032687 to 0.0077721 is the p-value belongs to CR in green component SF interval. Finally, p-value is between 5.4E-09 to 4.55E-07 when bpp evaluated in blue component SF interval.

These p-values that come from using both methods are close to 0, it means this casts doubt on the null hypothesis that the images from different IAM/SF interval values have same mean PSNR, CR and bpp values. The small p-value that close to 0 indicates the IAM and SF interval affects the value of PSNR, CR and bpp.

4.6 Determine the Most Optimum Wavelet for Colour Image Codec

Various wavelets give different PSNR, CR and bpp values as shown at Figure 4.4 till Figure 4.6. Selection of the most optimum wavelet from various wavelet families for image compression is a challenging problem. There are many wavelets that can be used to transform an image in a wavelet-based codec. However, it is necessary to use only 'one' wavelet to compress an image. An appropriate choice of wavelet significantly improves coding performance, fidelity and image perceptual quality. The most appropriate wavelet will give a good compressed image; otherwise the inappropriate selection will produce a low quality image.

Figure 4.12 illustrates an example of choosing a wavelet in colour image codec, Figure 4.12(a) shows the compressed image result of "Red and Yellow.bmp" using the suitable wavelet and Figure 4.12(b) shows the compressed image of same image using inappropriate wavelet. The resultant image looks blurred.

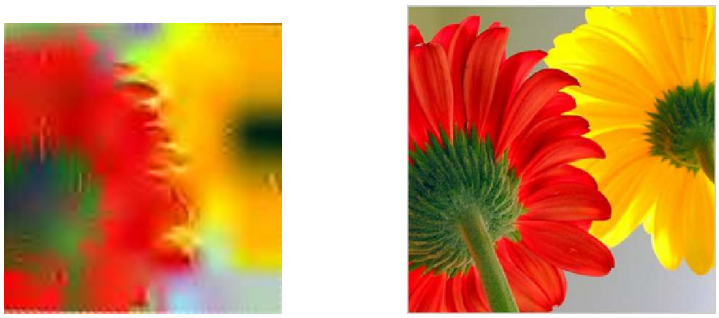

(a) (b)

Figure 4.12 Compressed images of "Red and Yellow.bmp" using two different wavelet.

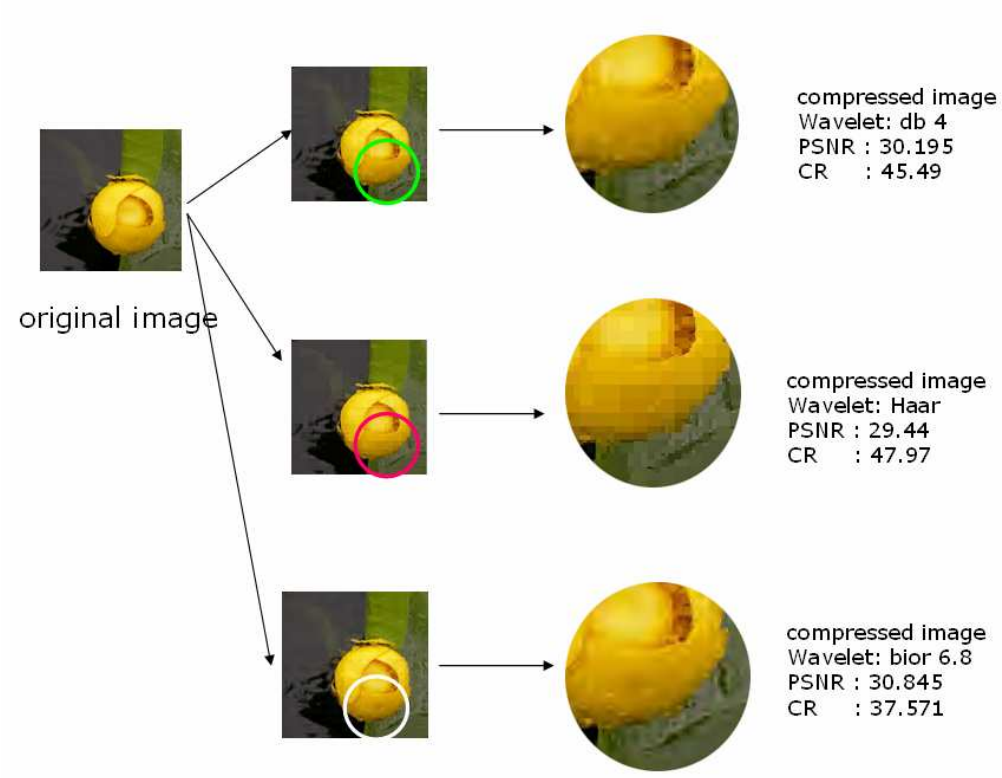

Figure 4.13 Original and compressed image of "liliwater.bmp" using db4, haar and bior 6.8 wavelets.

Figure 4.13 represents the original image, and three compressed images of "liliwater.bmp" using db4, haar and bior 6.8 wavelets. The compressed image using db4 wavelet visually looks better than the compressed image using haar wavelet, but using db4 and bior 6.8 the compressed images look similar. The blocking artifacts are shown at compressed image produced by Haar wavelet. It is

correspondence the high compression ratio or the low bit rate. The PSNR value using db4 is 30.195, using `haar` wavelet is 29.44 and 30.845 is the PSNR value using `bior 6.8.`

It is difficult to consider all of the highest PSNR, CR and bpp values together. Human vision subjectively evaluates measure the digital image quality. Human eyes are sensitive to a small different PSNR value, but not for CR. Based on this reason, this research chooses the wavelet that gives the highest PSNR as the most appropriate filter. CR and bpp as other measurements in image compression are ignored, because this research focuses in the eye catching quality, assuming that the CR and bpp values are acceptable.

Table 4.14 Result summary of Friedman's test for PSNR, CR and bpp in different intervals and wavelets

	PSNR	CR
`haar`	29.273	33.374
`db2`	29.684	36.355
`db4`	29.306	34.11
`bior 4.4`	30.053	34.934
`bior 6.8`	29.759	27.021
`coif4`	29.548	19.635
`sym4`	29.509	35.134

Table 4.13 is a list for PSNR and CR value of compressed from `"A SHARP.bmp"` image using various wavelets. Therefore the couple values are drawn in a scatter plotting graphic.

Figure 4.14 illustrates the `"A SHARP.bmp`" image and it's CR vs. PSNR value scatter plotting. It is an example of seven variation compressed image results of `"A SHARP.bmp"`. As mentioned before, the highest PSNR value is the concern of this research. For this example, the selected wavelet is `bior 4.4` that give highest PSNR of 30.053 even thought the 34.934 of CR is not the highest value. In Figure 4.14 the point is circled in red.

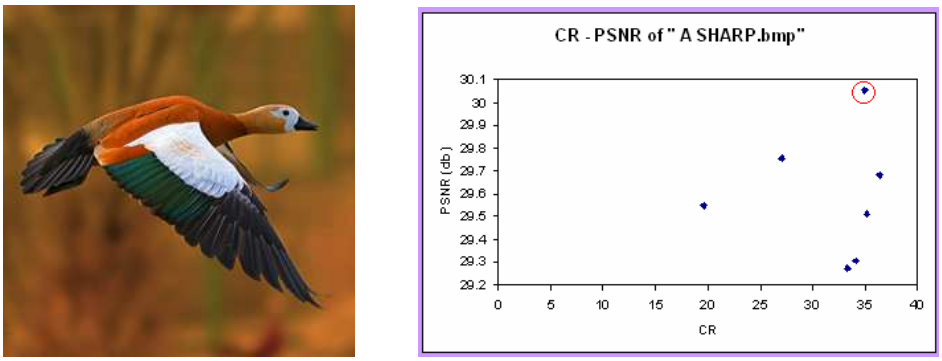

Figure 4.14 "A SHARP.bmp" image and its CR vs. PSNR value scatter plotting.

The most appropriate wavelets for the other images are also determined by choosing the wavelet that gives the highest PSNR value.

Due to limited space, the whole list of image and the wavelet for each image will not be shown here. Table 4.14 shows the result example for the choosing wavelet evaluation. Several images, that is, "bear", "bird", "cow", "foxx", "goat", "abi", "ali", "boy", and "clown" are compressed using different wavelets. The chosen wavelet is the wavelet that results the higest PSNR, Therefore, a numerical code is used to each wavelet type. The numerical code for haar, db2, db4, bior4.4, bior6.8, coif4, and sym4 are 1, 2, 3, 4, 5, 6 and 7 respectively. If these codes will be evaluated for eight outputs MLP topology, the numerical codes for wavelets are changed into 8 digit number (using number 1 and 0). The 8 digit wavelet codes are shown in Table 3.1.

Table 4.15 The example for the choosing wavelet evaluation.

	bear	bird	cow	foxx	goat	abi	ali	boy	clown
haar	25.752	34.282	27.235	23.568	25.570	23.521	27.498	26.056	26.416
db2	26.509	35.142	26.990	24.095	26.155	23.909	28.628	25.876	26.005
db4	26.551	35.038	26.560	24.025	25.858	24.327	27.941	25.670	26.248
bior 4.4	26.563	35.819	27.097	24.791	26.749	25.320	29.524	26.190	26.591
bior 6.8	26.773	35.694	27.379	24.787	26.792	25.132	29.579	26.168	26.740
coif4	26.449	35.007	27.177	24.318	26.288	24.080	28.739	25.921	26.786
sym4	26.286	35.584	26.881	24.297	26.023	24.807	28.815	25.920	25.973
highest PSNR	26.773	35.819	27.379	24.791	26.792	25.320	29.579	26.190	26.786
chosen wavelet	bior 6.8	bior 4.4	bior 6.8	bior 4.4	bior 6.8	bior 4.4	bior 6.8	bior 4.4	coif 4
numerical code for chosen wavelet	5	4	5	4	5	4	5	4	6

4.7 Neural Network Implementation on Adaptive Wavelet Selection

Data used in the neural network consist of input and output. For each image, there are six input involving IAM values from red, green and blue colour component, also SF values from the same three colour component, as well. As the output is a code for chosen wavelet. In multilayer perceptron term, there are six input nodes and one output node.

In the neural network implementation the images used are separated into two sets of images. The first set, consisting of 80% of the total images are used as training data and the remaining 20% are used as the testing data. The training data consists of 360 images and the testing data consists of 90 images.

Many MLP topologies are investigated to get the weights of the network. Several topologies, one hidden layer and two hidden layers are used in this study. The systems are developed using the TRAIN (training data set) to generate a network design. Therefore, the created networks are also simulated using TEST (testing data set) to understand the generalization ability of the designs. The accuracy of each topology can be evaluated.

The training and testing accuracies (in percent %) of several MLP topologies are represented in Table 4.15. Table 4.15 lists four types of MLP topologies: single-output one-hidden-layer, single-output two-hidden-layer, eight-output one-hidden-layer and eight-output two-hidden-layer MLPs. For example, when written the topology is 6-4-1, that means the number of hidden layer is one and there are six nodes in input, four nodes in hidden layer, and one node in output layer. Other example is 6-13-21-8, which means the number of hidden layer is two and the topology six nodes in input, 13 nodes in the first hidden layer, 21 nodes in the second hidden layer and eight nodes in output layer.

Table 4.16 MLP topologies and the accuracy of training and testing (in %).

MLP Topology	Number of hidden layer	Training accuracy	Testing accuracy
6-4-8	1	61.389	51.111
6-5-8	1	67.778	58.889
6-6-8	1	69.722	57.778
6-10-8	1	75.000	70.000
6-12-8	1	76.389	71.111
6-13-8	1	84.167	74.444
6-15-8	1	83.333	81.111
6-16-8	1	82.222	78.889
6-18-8	1	85.278	78.889
6-20-8	1	85.278	78.889
6-23-8	1	91.111	83.333
6-35-8	1	92.222	78.889
6-13-15-8	2	92.500	86.667
6-13-18-8	2	94.444	84.444
6-13-21-8	2	93.611	86.667

Eight output nodes represent the output, which is the wavelet type. The eight nodes output used digital codes as listed in Table 3.3.

In neural network, the input and output values are assigned to -1 to 1 or 0 to 1, depend on the sigmoid function. In the output, this study uses log-sigmoid transfer function. The eight output values can be assigned to 0 and 1. The output can represent wavelet types that have coded from 10000000 to 00000001. However, in eight nodes output topology, the log-sigmoid transfer function is implemented.

This research experiments various topologies to establish the most appropriate network design. To estimate generalization ability of each topology, the testing data set is applied and the accuracy is calculated.
Figure 4.15 represents the graph of training and testing accuracy from 'eight-output' topologies.

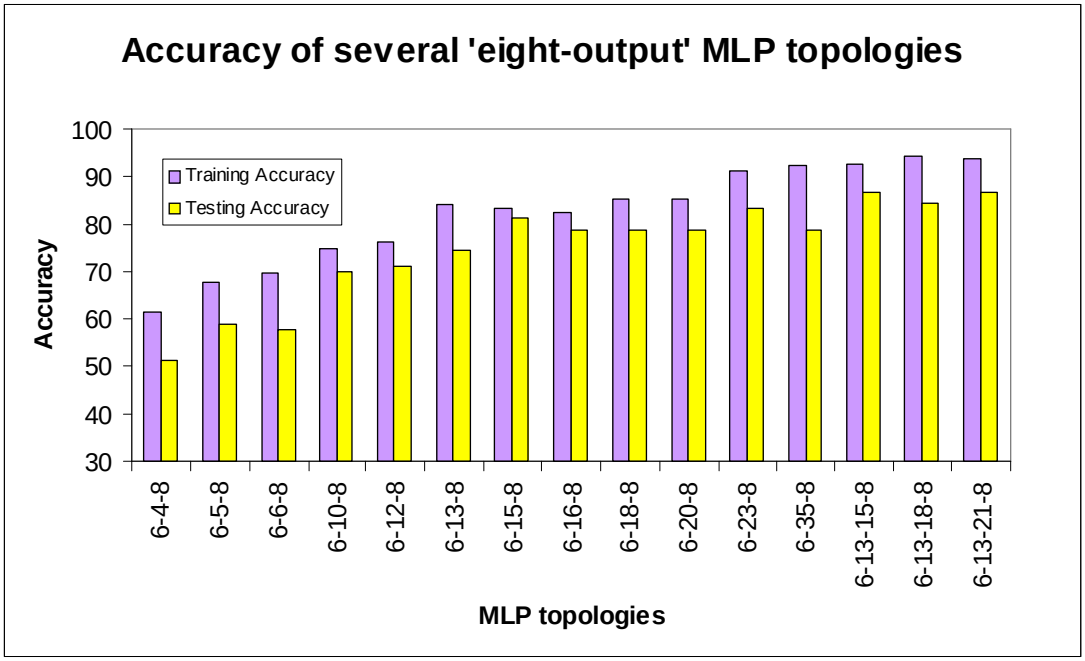

Figure 4.15 Graph of training and testing accuracy from 'one-output' topologies.

In the neural network development, all images are used without considering the image categories, because the system will be used to identify all images. A large number of

data will help to identify the best network topology, however it spend more time to converge.

From the Table 4.15, the highest testing accuracy is 86.667 % when the network uses 6-13-15-8 and 6-13-21-8 MLP. It indicates that the MLP topology can be used in the system to solve the wavelet selection problem.

4.8 Summary

This chapter described in details the relationship between certain image features (namely IAM and SF) and the wavelet based codec performance measures. These features are used as the input into the neural network designed. The cause-effect is an important factor in this research and therefore a detail study is conducted and reported in this chapter.

Overall, the experimental results presented in this chapter have shown the utility of MLP neural network based on the IAM and SF to select the most appropriate wavelet in colour image codec base on the image feature. IAM and SF values are used as the input into the network; furthermore the wavelet type chosen is used as the output/target. The training process is used to design the network and the testing process is used to evaluate the accuracy and generalization.

Several topologies are investigated and the best topology is MLP which is used to select the wavelet to compress an image. Adaptive wavelet based colour image codec has been designed in this research. This approach can give optimum colour image compression, using the most appropriate wavelet chosen by neural network. The system developed has been tested with different type of image. The results show that is broadly successful in achieving visually satisfactory compressed images.

CHAPTER 5

CONCLUSION

5.1 Introduction

In the introduction to this thesis the problems associated with selecting an appropriate wavelet to compress colour images were discussed in detail. The discussions pointed out that there is not any wavelet that would compress all types of images efficiently. The thesis argued that the image features could be used to help select an appropriate wavelet to compress for a given image.

This chapter will first review the cause-effect study in relationship with image features. The results of the cause-effect is used to help select an appropriate wavelet is also discussed. This chapter will draw some conclusions from the research work completed and make some recommendation for future work.

5.2 Image Feature and Cause-Effect

This study shows that various image features have no strong correlation to the wavelet based colour image compression. However, these indicate that there is a strong negative correlation between the image gradient and spatial frequency versus PSNR and CR. The results also indicate that there is a strong positive correlation between IAM and SF versus bpp.

The study of fitted logarithmic equation with the R-square evaluation indicates there are strong correlations between IAM and SF of three colour (red, green and blue)

component against PSNR and CR. The initial result on IAM an SF correlation will be investigated using statistical test to get confidence conclusion in causality effect.

The results of nonparametric hypothesis test using Kruskal-Wallis and Friedman test yield p-values that are close to 0, which rejects the null hypothesis that the images from different IAM/SF interval values have same mean PSNR, CR and bpp. The small p-value that close to 0 indicates the IAM and SF interval affects the value of PSNR, CR and bpp.

5.3 Choosing Wavelet Filters

Numerous of wavelet filters are available under different families. Also, filters with different characteristics are evolving at regular intervals. This thesis show that in wavelet based image compression techniques, the selection of filters has considerable impact the compression performance. The filter suitable for one image may not be the best for another.

Compression performance can be measured based on PSNR, CR and bpp values. It is difficult to consider all of the highest PSNR, CR and bpp values together. Human vision subjectively evaluates the digital image quality. Human eyes are sensitive to a small different PSNR value, but not for CR. Based on this reason, the wavelet that gives the highest PSNR as the most appropriate filter. CR and bpp as other measurements in image compression are ignored, because this research focuses in the image quality, assuming that the CR and bpp values are acceptable.

5.4 Neural Network Structure

The use of MLP neural network based on the IAM and SF is to select the most appropriate wavelet in colour image codec base on the image features. IAM and SF values are used as the input into the network; furthermore the wavelet type chosen is

used as the output/target. The training process is used to design the network and the testing process is used to evaluate the accuracy and generalization.

In the experiment, several topologies are investigated using MLP which is used to select the wavelet to compress an image. Adaptive wavelet based colour image codec has been designed in this research. This approach can give optimum colour image compression, using the most appropriate wavelet chosen by neural network. The system developed has been tested with different type of image. The results show that is broadly successful in achieving visually satisfactory compressed images.

5.5 Thesis Contributions

The following summarize the major contributions.

i. This research developed an image compression-decompression system for various image classes, both natural or synthetic image, so it is can be used without considering the image type.

ii. The results of statistical test using Kruskal-Wallis and Friedman test have given proof that two image features, namely IAM and SF have causality effect relation to the wavelet based colour image codec measurement (PSNR, CR and bpp values). This is the main contribution of this research.

iii. The adaptive wavelet selection is developed as a tool in the wavelet based colour image codec. The training evaluation used the MLP network, with the IAM and SF as the input and the chosen wavelet as the output/target.

iv. An adaptive system is designed in this work to compress colour image using the most appropriate wavelet for each image, ignore the image categories/classes. That means it is useful for many application.

5.6 Recommendations

The following recommendations are suggested in order to improve the in this thesis.

i. Applying more wavelet types. It is possible that other wavelets with varying coefficient will have better compression performance.

ii. Investigating other MLP topologies to reduce the number of neuron and node in this work.

iii. Optimization of artificial neural network parameters may improve the accuracy of the system.

In conclusion, this thesis has shown that is feasible to utilize a neural-network approach to select the appropriate wavelet to compress any given image efficiently.

REFERENCES

[1] Masud, S. and J.V. McCanny. *Finding a suitable wavelet for image compression applications*. in *Acoustics, Speech and Signal Processing, 1998. Proceedings of the 1998 IEEE International Conference on*. 1998.

[2] Mallat, S., *A Theory for Multiresolution Signal Decomposition: The Wavelet Representation.* IEEE Transactions on Pattern Analysis and Machine Intelligence, 1989. Vol. 11No.7: pp. 674-693.

[3] Daubechies, I., *Ten Lectures on Wavelets*, ed. CBMS. 1992, Philadelphia: SIAM.

[4] Rioul, O. *On the choice of wavelet filters for still image compression*. in *IEEE International Conference on Acoustics, Speech and Signal Processing (ICASSP '93)*. 1993. Minneapolis, Minn, USA.

[5] Buschgens, T. and F. Hartenstein. *Finding the right wavelet for image compression: on the relevance of criteria*. in *Digital Signal Processing Workshop Proceedings, 1996., IEEE*. 1996.

[6] Villasenor, J., B. Belzer, and J. Liao, *Wavelet Filter Evaluation for Image Compression.* IEEE Transactions on Image Processing, 1995. Vol. 2: pp. 1053-1060.

[7] Irijanti, E., V.V. Yap, and M.Y. Nayan. *Neural network for the best wavelet selection on colour image compression*. in *Information Technology, 2008. ITSim 2008. International Symposium on*. 2008.

[8] Saha, S. and R. Vemuri. *An Analysis on the Effect of Image Activity on Lossy Coding Performance*. in *EEE International Symposium on Circuits and Systems (ISCAS 2000), May 2000*. 2000. Geneva, Switzerland.

[9] Saha, S. and R. Vemuri. *How Do Image Statistics Impact Lossy Coding Performance?* in *International Conference on Information Technology: Coding and Computing (ITCC)*. 2000. Las Vegas.

[10] Saha, S. and R. Vemuri. *Effect of Image Activity on Lossy and Lossless Coding Performance*. in *IEEE Data Compression Converence (DCC 2000)*. 2000. Snow Bird, Utah.

[11] Saha, S. and R. Vemuri, *An analysis on the effect of image features on lossy coding performance.* Signal Processing Letters, IEEE, 2000. Vol. 75: pp. 104-107.

[12] Eskicioglu, A.M. and P.S. Fisher, *Image quality measures and their performance.* Communications, IEEE Transactions on, 1995. Vol. 4312: pp. 2959-2965.

[13] Sprljan, N., S. Grgic, and M. Grgic. *ImAn - educational tool for image analysis*. in *EUROCON 2003. Computer as a Tool. The IEEE Region 8*. 2003.

[14] Umbaugh, S.E., *Computer Imaging, Digital Image Analysis and Processing*. 2005: CRC Press Book. 659.

[15] Dunn, S. *Digital Color*. 1999 2/17/1999 [cited; Available from: http://davis.wpi.edu/~matt/courses/color/.

[16] Burdick, H.E., *Color Space*. 2000] [Microsoft, *Cube RGB color space*. 2009.

[17] Umbaugh, S.E., *Computer Vision and Image Processing, a practical approach using CVIPtools*. 1998: Prentice-Hall International, Inc. 504.

[18] Sayood, K., *Introduction to Data Compression*. second edition ed. 2000: Morgan Kaufmann Publishers.

[19] Topiwala, P.N., *Wavelet Image and Video Compression*. 1998: Kluwer Academic Publishers. 438.

[20] Xiao, P., *Image Compression by Wavelet Transform*, in *Departement of Computer and Information Sciences*. 2001, East Tennessee State University. p. 69.

[21] Acharya, T. and A.K. Ray, *Image Processing, Principles and Applications*. 2005: Wiley-Interscience. 428.

[22] Sarkar, T.K., M. Salazar-Palma, and M.C. Wicks, *Wavelet, Applications in Engineering Electromagnetics*. 2002, Boston, London: Artech House.

[23] Saha, S., *Image compression; from DCT to wavelets: a review*. Crossroads, 2000. Vol. 63: pp. 12-21.

[24] Said, A. and W.A. Pearlman, *A new, fast, and efficient image codec based on set partitioning in hierarchical trees.* Circuits and Systems for Video Technology, IEEE Transactions on, 1996. Vol. 63: pp. 243-250.

[25] Salomon, D., *Data Compression: The Complete Reference*. 2nd ed. 2000: Springer.

[26] Raj. SG, R.K., Raju. G, *Study on the Choice ofWavelet Filters for Image Compression using Neural and k-Nearest Neighbor Classifiers.* Journal of Wavelet Theory and Applications, 2008. Vol. 2Number 1 (2008): pp. 15–30.

[27] Haykin, S., *Neural Network, A Comprehensive Foundation*. second ed. 1999, New Delhi: Prentice-Hall. 842.

[28] Ripley, B.D., *Pattern Recognition and Neural Networks*. 1996: Cambridge University Press.

[29] Durai, S.A. and E.A. Saro, *Image Compression with Back-Propagation Neural Network using Cumulative Distribution Function.* Proceedings Of World Academy Of Science, Engineering And Technology, 2006, 2006. Vol. 17 December 2006

[30] Dony, R.D. and S. Haykin, *Neural network approaches to image compression.* Proceedings of the IEEE, 1995. Vol. 832: pp. 288-303.

[31] Saha, S. and R. Vemuri. *On Lossy Image Compression Using Adaptive Wavelet Filter*. in *European Signal Processing Conference (EUSIPCO 2000).* 2000. Tampere, Finland.

[32] Saha, S. and R. Vemuri. *Adaptive Wavelet Filters in Image Coders - How Important are They?* in *IEEE IECON '99*. 1999. San Jose, California, .

[33] Burdick, H.E., *Digital Imaging: theory and applications*. 1997: McGraw-Hill.

[34] Parker, J.R., *Algorithms For Image Processing and Computer Vision*. 1997: Wiley Computer Publishing, John Wiley & Sons, Inc. 417. pp. 120-122, 153.

[35] Sprljan, N., S. Grgic, and M. Grgic, *ImAn - Educational Tool for Image Analysis.* IEEE Transactions on Communications,, 2003. Vol. 43, No. 12.

[36] Taubman, D.S. and M.W. Marcellin, *JPEG2000: Image Compression fundamentals, standards and Practice*. 2002: Kluwer Academic Publishers. 753.

[37] Terki, N.D., N. Baarir, Z. Ouafi, A. *Study of filter effects in wavelet image compression*. in *IEEE, Information and Communication Technologies: From Theory to Applications*. 2004. Damas.

[38] Keinert, F., *Wavelets and Multiwavelets*. 2004: Chapman & Hall/CRC.

[39] Mallat, S., *A Wavelet Tour of Signal Processing*. second ed. 1999, London: Academic Press.

[40] Walter, G.G. and X. Shen, *Wavelets and Other Orthogonal Systems*. 2001, CRC Press. p. 372.

[41] Irijanti, E., V.V. Yap, and M.Y. Nayan. *The effects of colour image features on the performance of a wavelet-based codec*. in *International Conference on Intelligent and Advanced System (ICIAS 2007)*. 2007. Kuala Lumpur, Malaysia.

[42] Wadsworth, H.M., *Handbook of Statistical Methods for Engineers and Scientists*. second ed. 1997: Mc Graw Hill.

[43] Motulsky, H., *Intuitive Biostatistics*. 1995: Oxford University Press.

[44] Marques de S, J.P., *Applied Statistics Using SPSS, STATISTICA, MATLAB and R*. 2007: Springer-Verlag Berlin Heidelberg.

[45] StatSoft. *Elementary Concepts in Statistics*. 1984-2008 [cited 2009 30 June 2009]; Available from: http://www.statsoft.com/textbook/esc.html.

[46] Du, K.-L. and M.N.S. Swamy, *Neural Networks in a Softcomputing Framework*. 2006: Springer.

[47] Picton, P., *Neural Networks*. Second ed. Grassroots series. 2000: Palgrave.